Ergonomic-Centric Methods for Workplace Design in Industrialized Construction

by

Jingwen Wang

A thesis submitted in partial fulfillment of the requirements for the degree of

Doctor of Philosophy

in

Civil (Cross-disciplinary)

Department of Civil and Environmental Engineering
University of Alberta

ABSTRACT

As the leading cause of nonfatal occupational injuries, work-related musculoskeletal disorders account for approximately 33% of all occupational injuries and illnesses in the United States and approximately 44% of such injuries in Alberta, Canada. The risk of developing a work-related musculoskeletal disorder is closely related to the physical demands associated with awkward body postures and repetitive motions. In industrialized construction, poor workplace design may increase the probability of injury and work absenteeism, leading to schedule overruns and decreased production rates. Thus, this research investigates and develops ergonomic-centric methods to automatically evaluate the continuous motions in operational tasks for the purpose of workplace design and modification in industrialized construction.

To mitigate the risk of developing a work-related musculoskeletal disorder, various observational rule-based ergonomic posture assessment methods have been developed and widely used to facilitate ergonomic risk evaluation in various industrial sectors. However, the applicability and reliability of rule-based ergonomic posture assessments to automatically evaluate continuous motions have not yet been examined. The current practice of using these assessments for automated evaluation of continuous motions is challenged in three notable respects: (1) inaccuracy of the ergonomic risk assessment results, attributable to human perception errors and subjectivity during observations, as well as measurement errors and instrument limitations when using vision-based approaches to estimate body joint angles; (2) lack of consideration of the standard motion time feature when analyzing the ergonomic risks of continuous motions in operational tasks; and (3) overestimation (in existing methods for assessing ergonomic risk in continuous motions) due

to a failure to account for the effect of natural posture sway, as well as ambiguous posture categorization in the adjustment risk rating process in existing ergonomic risk assessment methods.

To overcome these challenges, a systematic and objective framework is proposed by which to automatically assess the risks of continuous motions in construction tasks and thereby achieve an ergonomic-centric workplace design method that overcomes human perception errors and measurement limitations, considers standard motion time features, and accounts for the effect of natural posture sway. The three main contributions of this research are that it (1) improves the accuracy of rule-based ergonomic risk assessment methods by incorporating fuzzy logic in order to better capture the gradual transitions characteristic of continuous human motion; (2) adjusts the motion time in ergonomic risk assessment of continuous motions by integrating the predetermined motion time system; and (3) eliminates the detrimental effect of natural posture sway on continuous motion assessments by identifying and adapting the acceptable posture sway magnitudes of body joints in the motion capture experiments. A series of laboratory experiments are presented that demonstrate the feasibility and effectiveness of the proposed framework for assessing ergonomic risks of continuous motions in workplace design and modification to facilitate occupational health and safety in industrialized construction.

PREFACE

This thesis is an original work by Jingwen Wang and follows a monograph format. Three journal papers and two conference papers related to this thesis have been published or submitted as listed below.

- **Wang, J.,** Han, S., and Li, X. (2021). 3D fuzzy ergonomic analysis for rapid workplace design and modification in construction. *Automation in Construction*, 123, 103521. Dr. Han and Dr. Li were the supervisory authority and were involved with concept formation and manuscript composition.

- **Wang, J.,** Li, X., Han, S., and Al-Hussein, M. 3D standard motion time-based ergonomic risk analysis for workplace design in modular construction. *Automation in Construction* (Under review). Dr. Al-Hussein was the supervisory authority and was involved with concept formation. Dr. Li and Dr. Han were the supervisory authority and were involved with concept formation and manuscript composition.

- **Wang, J.,** Mohamed, Y., Han, S., Li, X., and Al-Hussein, M. 3D ergonomics-based motion-level productivity analysis for intelligent manufacturing in industrialized construction. *Canadian Journal of Civil Engineering* (Under review). Dr. Al-Hussein was the supervisory authority and was involved with concept formation. Dr. Li and Dr. Han were the supervisory authority and were involved with concept formation and manuscript composition. Ms. Yomna Mohamed was an undergraduate research student involved in the model development.

- **Wang, J.**, Li, X., Han, S., and Al-Hussein, M. (2020). Construction workers' behaviors assessment using 3D visualization and fuzzy logic method. *Proceedings, ICCREM 2020: Intelligent Construction and Sustainable Buildings*, Stockholm, Sweden, Jun. 4–5, pp. 48–54. Dr. Al-Hussein was the supervisory authority and was involved with concept formation. Dr. Li and Dr. Han were the supervisory authority and were involved with concept formation and manuscript composition.

- **Wang, J.,** Mohamed, Y., Han, S., Li, X, and Al-Hussein, M. (2021). Automated ergonomics-based productivity analysis for intelligent manufacturing in industrialized construction. *Proceedings, CSCE Construction Specialty Conference*, Niagara Falls, ON, Canada (virtual conference), May 26–29. This paper received the Best Student Paper Award at the 2021 CSCE Construction Specialty Conference. Dr. Al-Hussein was the supervisory authority and was involved with concept formation. Dr. Li and Dr. Han were the supervisory authority and were involved with concept formation and manuscript composition. Ms. Yomna Mohamed was an undergraduate research student involved in the model development.

The research project of which this thesis is a part received research ethics approval from the University of Alberta Research Ethics Board, Project Name "Ergonomics and workplace design for industrialized construction", No. Pro 00091270, approved on October 1, 2018.

ACKNOWLEDGEMENTS

First and foremost, I would like to express my sincere gratitude to my supervisors, Dr. Mohamed Al-Hussein, Dr. Xinming Li, and Dr. SangHyeok Han, for their immense support, inspiration, visionary guidance, and consistent encouragement during my studies. I am also grateful to my supervisory and examining committee, Dr. Yasser Mohamed, Dr. Lindsey Westover, and Dr. Zoubeir Lafhaj, for their valuable insights. Without their support, I would never have completed this degree.

I would also like to express my gratitude to Jonathan Tomalty and Kristin Berg for their generous support in editing my thesis and publications. Many thanks to all my colleagues from our great lab for their continuous support. Special appreciation goes to Dr. Bin Zheng and colleagues from the Department of Surgery at the University of Alberta for their support and for sharing their many years of knowledge and experience.

Especially, I offer my deepest gratitude to my family and friends for their encouragement and never-ending support at every stage of my academic and personal life. Without their great support behind me, I could not have completed this long journey. Most importantly, my deepest gratitude is given to my dearest mother, Ms. Lijie Wang, for her unconditional support and love.

Last, but not least, I would like to express my deepest gratitude to my beloved husband for his boundless patience, kindness, and love. Your energy and support motivated every step I took along this journey. Thanks for making my life so beautiful!

TABLE OF CONTENTS

LIST OF FIGURES

LIST OF TABLES

LIST OF ABBREVIATIONS

3D	Three Dimensional
3DSSPP	3D Static Strength Prediction Program
ANOVA	Analysis of Variance
BVH	Biovision Hierarchy
fps	Frames per Second
IMU	Inertial Measurement Unit
JRPDS	Job Requirements and Physical Demands Survey
NIOSH	National Institute for Occupational Safety and Health
OCRA	Occupational Repetitive Actions
OWAS	Ovako Working Posture Analysing System
PiG	Plug-In Gait
QEC	Quick Exposure Check
REBA	Rapid Entire Body Assessment
RMSE	Root Mean Square Error
RULA	Rapid Upper Limb Assessment
SD	Standard Deviation
WCB	Workers' Compensation Board
WMSD	Work-related Musculoskeletal Disorder

CHAPTER 1: INTRODUCTION

1.1 Background and Motivation

As one of Canada's largest industrial sectors, the construction industry employs approximately 1.5 million workers and contributes approximately $140 billion (CAD) to the economy annually, accounting for about 7.5% of Canada's gross domestic product in 2020 (Statistics Canada 2021; Build Force Canada 2021). Despite being a significant employer and economic driver, though, the construction industry has an unsatisfactory occupational health and safety record (Umer et al. 2018). Work-related musculoskeletal disorders (WMSDs) are among the leading causes of nonfatal occupational injuries in construction. According to the Bureau of Labor Statistics, the incidence rate of WMSDs in construction was 31.2 for every 10,000 full-time workers, accounting for approximately 9% higher than the average rate for all industries in 2017 in the United States (CPWR 2019). Workers are commonly exposed to the risks of WMSDs due to the high physical demands and repetitive nature of construction tasks (Boschman et al. 2012; Fung et al. 2008; Merlino et al. 2003; Schneider 2001). WMSDs account for approximately 33% of all occupational injuries and illnesses in the United States (Bureau of Labor Statistics 2016) and approximately 44% of such injuries in Alberta, Canada (Labour and Immigration 2019). Thus, improving workplace safety practice to mitigate the risks of WMSDs is crucial for the construction industry.

Industrialized construction has been increasingly popular in North America due to its many benefits to project stakeholders, such as increased productivity, improved product quality, reduced construction waste, and decreased environmental risks for construction workers (Yin et al. 2019; Kamali and Hewage 2016). As distinct from conventional construction, industrialized construction provides a controlled factory environment with the support of automated machinery at workstations, thereby reducing the motions required of workers to complete operational tasks (Li et al. 2019a). However, considerable physical demands are still imposed on workers in industrialized construction, leading to a high risk of developing WMSDs. The nature of these physically demanding operations is highly influenced by the workplace design characteristics. An ergonomic-centric workplace design that takes ergonomics into consideration can help to uphold the health and safety of workers while enhancing product quality and productivity, whereas with poor ergonomic design of the workplace results in an elevated risk of workers developing WMSDs, leading to an increase in workers' compensation costs (Inyang et al. 2012) and schedule overruns due to work absenteeism (Bureau of Labor Statistics 2016; Rinder et al. 2008). As such, ergonomic-centric workplace design is essential not only as a means of proactively mitigating the risk of developing a WMSD, but also as a way to improve productivity in industrialized construction.

Working postures and motions involved in the completion of tasks are closely related to WMSD risks (Wang et al. 2015; NIOSH 2014; Kivi and Mattila 1991; Punnett and Wegman 2004). In construction, WMSDs are usually the result of forceful exertion, awkward postures, and repetitive motions (Wang et al. 2015). To mitigate these risks, various observation-based ergonomic posture assessment methods have been developed and widely used to facilitate workplace safety practices. In current practice, the working postures described by body joint angles are used as the primary inputs in assessment methods used to address WMSDs risks. However, these assessment methods are heavily reliant on manual observation of working postures, which is error-prone and time-consuming (Taneja et al. 2011). With the recent advances with respect to motion capture and imitation technologies, working postures and continuous motions can be accurately obtained for the purpose of ergonomic risk assessment. However, the applicability and reliability of rule-based assessment methods to automatically evaluate the continuous motions have not yet been examined.

In current practice, ergonomic posture assessment methods are challenged to efficiently generate accurate and reliable risk ratings of continuous motions to support ergonomic-centric workplace design. To evaluate ergonomic risks, body joint angles describing the working postures are required, and these joint angles can be obtained either from visual estimations and human judgment (McAtamney and Corlett 1993; Hignett and McAtamney 2000; Golabchi et al. 2016b), or by using sensing devices and vision-based technologies (Yu et al. 2019; Seo et al. 2015; Han et al. 2013). A great deal of variance is encountered in the estimations of body joint angles, however, due to human perception errors and subjectivity during observations (McAtamney and Corlett 1993; Burdorf 2010), and due to instrument errors and limitations when using vision-based approaches (Yu et al. 2019; Li and Buckle 1999). This variance in joint angle estimations, in turn, leads to variations in the ergonomic risk assessment results themselves. As such, the first motivation underlying this research is to address the need for an automated method to eliminate the variations in ergonomic risk ratings resulting from human perception errors and measurement errors in estimating the joint angles.

Meanwhile, the use of advanced motion capture technologies has enabled the safety risk evaluation of continuous motions in construction tasks. However, studies in this area have tended to focus on the motion data collection process, with investigations of the suitability of ergonomic posture assessments with respect to continuous motions being more limited. Specifically, the risk assessment of continuous motions is typically conducted as risk assessments of a series of discrete working postures, with a standardized motion time feature not considered. To obtain consistent and quantitative risk assessments of continuous motions for the purpose of evaluating workplace design in a sound, ergonomic-centric manner, then, standard motion time durations within these continuous motions must be considered. Thus, the second motivation underlying this research is to develop an automated method that implements standard motion times in the ergonomic risk assessments in order to improve the reliability of risk assessment of continuous motions.

Finally, the results of ergonomic risk assessments of continuous motions are highly influenced by the natural posture sway in the completion of the operational tasks. In current practice, posture categorizations in the primary risk rating process of ergonomic risk assessments are strictly defined. For these posture categories, 0° is the boundary, meaning there is no threshold by which to determine whether a risk score of 1 is needed or not. In reality, though, workers cannot always maintain a joint angle with 0° due to the body structure and the natural posture sway typical of continuous motions performed by humans. In spite of this reality, an objective definition of posture categorizations that accounts for the minor movements of body joints due to posture sway has not yet been incorporated into the adjustment risk rating process in existing assessment tools. Moreover, to address this deficiency, assumptions are made that differ depending on the study, resulting in inconsistencies (Li et al. 2018; 2019b; Ryu et al. 2020; Wang et al. 2021a). Due to the posture sway and the discrete boundaries between posture categories in existing ergonomic risk assessments, overestimations and fluctuations in risk ratings are observed with respect to the risk assessment of continuous motions. Thus, the third motivation underlying this research is to carry out an experimental study to identify the minor movements of body joints that naturally occur in the completion of operational tasks and use them as criteria for the posture categorizations in the risk assessment.

To summarize, the novelty of the proposed research lies in the automated assessment of continuous motions to address the aforementioned challenges in existing observation-based ergonomic posture assessment methods, including (1) variations in the assessed risk resulting from human perception errors and measurement errors in the body joint angle estimation, (2) variations in the assessed risk due to the lack of standard motion time durations, and (3) variations in the assessed risk caused by a failure to account for the natural posture sway in continuous motions. Indeed, although accurate and reliable ergonomic risk assessment of continuous motions in the completion of operational tasks is an essential component of ergonomic-centric workplace design in industrialized construction, as note above, existing ergonomic risk assessment methods are not suitable for the evaluation of continuous motions. This research thus proposes a systematic and objective framework to automatically assess the ergonomic risks of continuous motions performed as part of operational tasks in industrialized construction for ergonomic-centric workplace design evaluation. The proposed framework can reduce the risk of WMSDs and potential injuries and improve productivity in industrialized construction.

1.2 Research Objectives

With this background and motivations, the following research questions are applied in this research to examine and answer the research problems.

1) How do we efficiently generate an accurate and reliable ergonomic-centric workplace design based on limited design information?
2) How do we accurately assess the risks of dynamic and continuous motions based on the postures and associated standard motion times in order to support the ergonomic-centric workplace design?
3) How do we effectively update this ergonomic-centric workplace design with respect to the natural minor movements of human body joints?

The overall goal of this research is to develop a systematic and objective framework to automatically assess the ergonomic risks of continuous motions in the construction tasks in order to identify and evaluate the ergonomic performance of workplace design in industrialized construction. This research seeks to achieve the following objectives:

Objective 1. Improve the accuracy of ergonomic risk ratings through the integration of fuzzy logic approach with ergonomic posture assessments in 3D visualization.

This objective addresses the variations in assessment results caused by the human perception and measurement errors in estimating body joint angles. The developed system can incorporate the rule-based fuzzy logic modelling process with ergonomic posture assessments for the evaluations at four different levels, including the joint-level, body segment-level, integrated body segment-level, and full body-level evaluation.

Objective 2. Develop an automated 3D standard motion time-based ergonomic risk analysis system, based on the predetermined motion time system, for assessing the risks of continuous motions in ergonomic-centric workplace design.

The developed system includes the automated rule-based motion recognition algorithm, which is capable of detecting all the basic motions and updating the standard motion time durations with the ergonomic risks to enhance the assessment results of continuous motions.

Objective 3. Develop an automated rule-based ergonomic risk assessment for the continuous motions that updating the posture categories to incorporate the posture sway effect on the body joints.

In current practice, no tolerance is applied in the postural judgment of ergonomic risk assessment methods. However, due to the lack of joint allowance settings, ergonomic risk tends to be overestimated. The predefined posture categories in the secondary adjustment risk rating process are described with ambiguous words, which should be quantitatively defined to eliminate the overestimations and fluctuations in ergonomic risk ratings resulted from posture sway. Thus, the focus herein is on the use of posture sway experiments to identify the minor movements of body joints that naturally occur during continuous motions in the completion of operational tasks in industrialized construction.

1.3 Thesis Organization

This thesis is composed of seven chapters.

Chapter 1: Introduction. This chapter presents the research background, motivations, and objectives of the proposed research.

Chapter 2: Literature review. This chapter provides a critical review of the previous studies related to this research, including the ergonomic risk assessment techniques, fuzzy logic approaches in ergonomics, motion time analysis techniques, and previous studies on posture sway analysis in motion capture system.

Chapter 3: Research methods. This chapter introduces the main research methods applied in this thesis for the completion of the research objectives.

Chapter 4: 3D fuzzy ergonomic analysis for rapid workplace design and modification in construction. This chapter introduces an automated 3D fuzzy logic-based ergonomic analysis method developed using fuzzy logic modelling process and rule-based ergonomic risk assessment methods in 3D visualization. The 3D fuzzy ergonomic analysis method is used to mitigate the human perception and measurement errors during the posture risk classification, which is to improve the accuracy and reliability of rule-based ergonomic risk assessment for continuous motions in the evaluation of rapid workplace design and modification.

Chapter 5: 3D standard motion time-based ergonomic risk analysis for workplace design in industrialized construction. This chapter introduces a systematic and objective methodology to automatically assess ergonomic risks of dynamic and continuous motions using predetermined motion time system in 3D visualization. The methodology for automatically recognizing 3D motions is presented, and the development of standard motion time integrated ergonomic risk analysis method is demonstrated to assess the ergonomic risks of continuous motions for workplace design.

Chapter 6: Postural sway analysis for the limits of automated ergonomic risk assessment of dynamic motions in modular construction. This chapter presents an analysis of posture sway to investigate the acceptable magnitudes regarding posture categorizations for the adjustment risk rating process in the rule-based ergonomic risk assessment methods. Furthermore, this chapter introduces a novel posture sway-incorporated ergonomic risk assessment system to evaluate the ergonomic risks of dynamic and continuous motions.

Chapter 7: Conclusions. This chapter provides a summary of the conclusions that are drawn from this research. The academic and industrial contributions of this research are provided. The limitations and future research directions are also outlined in this chapter.

CHAPTER 2: LITERATURE REVIEW

This chapter reviews existing studies in the following areas as presented in the literature: (1) ergonomic risk assessment methods; (2) automated ergonomic risk assessment methods; (3) fuzzy logic techniques in ergonomic risk assessment; (4) the methods of predetermined motion time system; and (5) previous studies of posture sway analysis. The objective of this literature review is to justify the research objectives and eventual contributions.

2.1 Ergonomic Risk Assessment Methods

Ergonomic risks are physical conditions that may pose risk of injury to the musculoskeletal system, resulting in the work-related musculoskeletal disorders (WMSDs) (Occupational Safety and Health Administration 2022). According to the Canadian Centre for Occupational Health and Safety, WMSDs are defined as "*a group of painful disorders of muscles, tendons, and nerves*", which commonly resulted from awkward working postures and repetitive movements in operational tasks (CCOHS 2022). In construction, workers are frequently exposed to various degrees of ergonomic risks that can lead to WMSDs due to the dynamic and physically demanding nature of operational tasks. Continued exposure to the ergonomic risks and WMSDs leads to occupational injuries and illnesses, loss of workdays and productivity, and an increase of workers' compensation costs (Inyang et al. 2012; Bureau of Labor Statistics 2016).

Ergonomic risk assessment methods are have been used effectively in a number of different industries to evaluate the ergonomic risks associated with the various working postures assumed in the performance of operational tasks in order to mitigate the risk of developing a WMSD. In construction, rule-based ergonomic posture assessment methods have been applied to improve the production rate and lower compensation costs by eliminating high-risk tasks, improving work comfortability, reducing work-related injuries, decreasing the probability of medical leaves, and ensuring that production is on schedule (Inyang et al. 2012; Li et al. 2019b; Golabchi et al. 2016b; 2018; Yu et al. 2019; Wang et al. 2021a). These assessment methods can be classified into three groups according to the measurement methods, including self-report assessment methods, observation-based assessment methods, and direct measurement-based methods (Li and Buckle 1999; David 2005).

2.1.1 Self-report Assessment

Self-report assessment methods are subjective and performance-based measurements usually through rating scales, checklists, diaries, interviews, and questionnaires. These methods are widely used to assess the physical loads, body discomfort, and work stress using the self-report tools such as the Borg Scale (Borg 1970; Li and Yu 2011), the Nordic Musculoskeletal Questionnaire (Kuorinka et al. 1987), and the Job Requirements and Physical Demands Survey (JRPDS) (Dane et al. 2002). The advantages of self-report assessment methods include simple to apply, cost-effective, and applicable to various occupations (Li and Buckle 1999; David 2005). However, these methods have several limitations, such as time-consuming, error-prone, subjective, and difficult to validate (Wang et al. 2015; Li et al. 2018; Li and Buckle 1999; David 2005). In addition, these methods cannot collect the accurate postures and motion data continuously. Thus, the self-report assessment method cannot be applied to the quantitative assessment of continuous motions.

2.1.2 Observation-based Ergonomic Posture Assessment

Observation-based ergonomic posture assessments are widely accepted as one of the most important tools available to assess exposures to risk factors for WMSDs. These methods are based on direct observations of working postures in operational tasks carried out by ergonomist (Li and

Buckle 1999). The wide applications of an observation-based assessment method in the context of workplace design are due to several reasons, such as their capability of providing accurate results based on simple input information (i.e., mainly joint angles), and their implementation is practical and affordable compared with other techniques (e.g., computer vision-based methods, direct measurement-based methods, etc.) (David 2005). However, the accuracy of these observation-based assessment methods may be compromised due to observer errors, subjective metrics, or inter-rater reliability issues (Wang et al. 2015; Valero et al. 2016; Li et al. 2018; Li and Buckle 1999; David 2005), since they only identify the primary postures or injury types associated with the highest ergonomic risk during the task operation.

Several observation-based assessment methods have been developed for systematically assess risk factors, including the Ovako Working Posture Analysis System (OWAS) (Karhu et al. 1977; 1981), the National Institute for Occupational Safety and Health (NIOSH) lifting equation (Waters et al. 1993), Occupational Repetitive Actions (OCRA) (Occhipiniti 1998), Quick Exposure Check (QEC) (Li and Buckle 1998), Rapid Upper Limb Assessment (RULA) (McAtamney and Corlett 1993), and Rapid Entire Body Assessment (REBA) (Hignett and McAtamney 2000; Janowitz et al. 2006). Among these observation-based methods, OWAS, RULA, and REBA have been most commonly used in construction (Mattila et al. 1993; Golabchi et al. 2016b; Li et al. 2018; 2019b; Yu et al. 2019; Ryu et al. 2020; Wang et al. 2021a). These methods are rule-based assessment methods, which provide the ergonomic risk scores based on the working posture, force load, and activity conditions. The risks of whole-body postures are generated by combining risk scores of specific body segments in these methods (David 2005). As shown in Figure 2-1, the whole body is divided into two sections in REBA and RULA, which are the section of neck, trunk and legs, and the section of the arms and wrists. Three sections are used in OWAS, which are back, arms, and legs sections. The predefined posture categories for ergonomic risks are used in each section, and then the sections are combined by the score tables to generate the final scores and the corresponding action levels. In REBA and RULA, the working postures are described as joint angles of body segments. However, the posture categories in OWAS are classified using ambiguous words. Thus, REBA and RULA are more suitable to quantitatively evaluate the ergonomic risks of continuous motions.

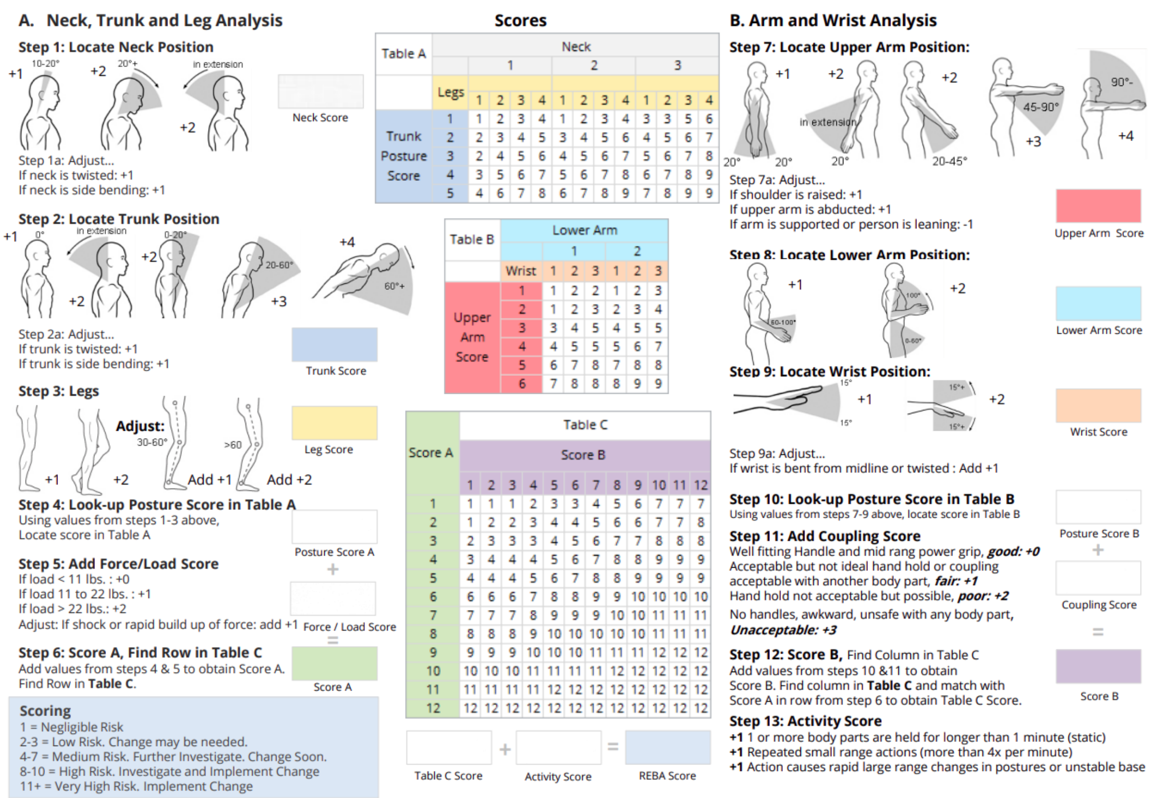

a)

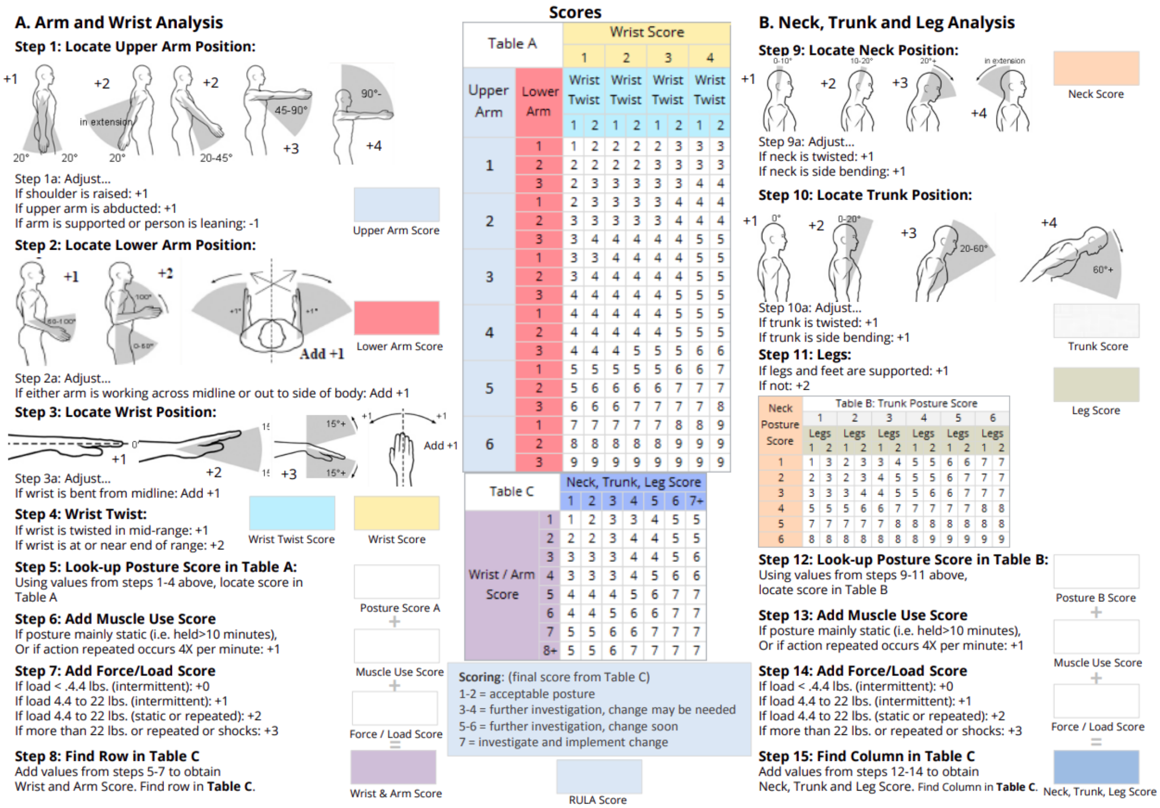

b)

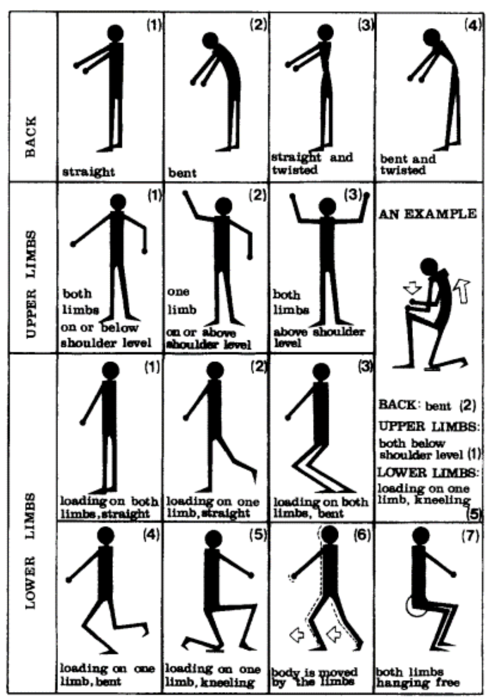

c)

Figure 2-1. Predefined posture categorizations in (a) REBA; (b) RULA; and (c) OWAS (Ergonomics Plus 2021a; 2021b; Karhu et al. 1977)

In current practice, the rule-based assessment methods are traditionally used to assess the static postures based on the manual observation of body joint angles. In REBA and RULA, the body joint angles are the main inputs, which are defined as the angles formed between the body segment and the extension of its connected body segment (θ = flexion/extension; β = rotation; γ = lateral bending; $\Delta\theta$ = difference between legs). For each joint angle, the posture categories and the associated risk scores are predefined in REBA and RULA, as summarized in Table 2-1. As the main concern, the quantitatively predefined posture categories for the individual joint risk scores are describing the postural conditions in the flexion and extension position in the sagittal plane of the posture. The joint angles in transverse and frontal planes are evaluated as adjustment risk factors to account for the postural conditions such as twisting, side bending, and abducting. It should be noted that the postures in the sagittal plane are the main concern in risk ratings, while the postures in the transverse and frontal planes are used to adjust the risk ratings for each body segment (McAtamney and Corlett 1993; Hignett and McAtamney 2000). However, only the ranges of joint angles in the sagittal plane are described in detail for the risk categorization.

Table 2-1. Posture categories and corresponding risks in REBA and RULA

	Sagittal plane		Transverse plane		Frontal plane	
Body segment	Posture category	Score	Posture category	Score	Posture category	Score
Neck (REBA)	$0° \leq \theta \leq 20°$	1	$\beta \neq 0°$	+1	$\gamma \neq 0°$	+1
	$\theta > 20°$ or $\theta < 0°$	2				
Neck (RULA)	$0° \leq \theta \leq 10°$	1	$\beta \neq 0°$	+1	$\gamma \neq 0°$	+1
	$10° < \theta \leq 20°$	2				
	$\theta > 20°$	3				
	$\theta < 0°$	4				

Trunk (REBA and RULA)	$\theta = 0°$	1	$\beta \neq 0°$	+1	$\gamma \neq 0°$	+1
	$0° < \theta \leq 20°$ [or $\theta < 0°$ (REBA only)]	2				
	$20° < \theta \leq 60°$	3				
	$\theta > 60°$	4				
Leg (REBA and RULA)	$\Delta\theta = 0°$	1	–	–	–	–
	$\Delta\theta \neq 0°$	2				
	$30° < \theta \leq 60°$	+1				
	$\theta > 60°$	+2				
Upper arm (REBA and RULA)	$-20° \leq \theta \leq 20°$	1	–	–	Shoulder raise	+1
	$20° < \theta \leq 45°$ or $\theta < -20°$	2			Abducted arm	+1
	$45° < \theta \leq 90°$	3			Support arm or leaning	-1
	$\theta > 90°$	4				
Lower arm (REBA and RULA)	$60° \leq \theta \leq 100°$	1	Across the midline (RULA only)	+1	–	–
	$0° \leq \theta \leq 60°$ or $\theta > 100°$	2			–	–
Wrist (REBA)	$-15° \leq \theta \leq 15°$	1	$\beta \neq 0°$	+1	$\gamma \neq 0°$	+1
	$\theta > 15°$ or $\theta < -15°$	2				
Wrist (RULA)	$\theta = 0°$	1	Twist in mid-range	+1	$\gamma \neq 0°$	+1
	$0° < \theta \leq 15°$ or $-15° \leq \theta < 0°$	2				
	$\theta > 15°$ or $\theta < -15°$	3	Twist at end of range	+2		

Note: θ = flexion/extension; β = rotation; γ = lateral bending; $\Delta\theta$ = difference between legs.

In the primary risk rating process of joint angles in the sagittal plane, the predefined posture categories are quantitatively classified using the joint angle ranges with no threshold on the boundaries, which is challenging for the observers to accurately distinguish the posture categories when the joint angle is around the boundaries (Golabchi et al. 2016b; Wang et al. 2020; 2021a). In the field observations, visually-estimated joint angles may differ depending on the observer, and may even differ for the same given observer through multiple iterations. Visually the same postures may be characterized differently in terms of ergonomic risk due to inherent subjectivity (McAtamney and Corlett 1993; Golabchi et al. 2016b). For instance, a 15-participant survey on joint angle estimations of trunk flexion as part of a prior study (see Figure 2-2) resulted in twelve estimations assigning a risk score of 3 and three estimations assigning a risk score of 4, with this variance in risk rating attributable to issues of human perception and inter-/intra-observer reliability. Thus, the human perception and inter-/intra-observer reliability can cause the variance in body joint estimations, which in turn affect the risk classifications in the ergonomic assessment, ultimately compromising the accuracy of the corresponding ergonomic risk results (Li et al. 2019b; Golabchi et al. 2016a; 2016b; 2017). In addition, the instrument errors and complicated working environment may lead to measurement errors, which in turn may result in inaccuracy of the assessed ergonomic risk (Yu et al. 2019; Golabchi et al. 2017).

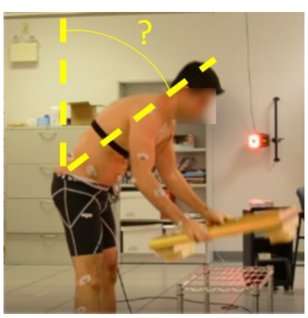

	+3	**+4**
Risk category	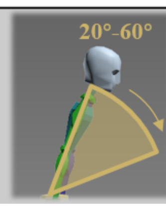	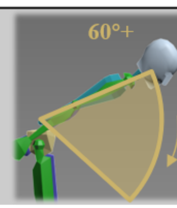
Survey result	12/15	3/15

Figure 2-2. Results of survey on joint angle estimations of trunk flexion (Wang et al. 2021a)

In the secondary risk rating process of joint angles in transverse and frontal planes, the predefined posture categories for adjustment risk scores are qualitatively described with the ambiguous words, such as twisting or not twisting, side bending or not side bending, and abducting or not abducting. Thus, the discrete boundary between posture categories is 0° for the adjustment risk factors, making it challenging for observers to clearly distinguish between posture categories (Golabchi et al. 2016b; Wang et al. 2021a). However, body sway naturally occurs during continuous motions, with the resulting minor movements of body joints generating additional risk scores. As a result, overestimations and fluctuations in risk ratings are identified, which is due to the body sway that naturally occurs during continuous motions. Thus, to automatic and quantitatively assess the ergonomic risks, acceptable minor movements of body joints due to the posture sway are required for the ergonomic risk assessment of the dynamic and continuous motions.

2.1.3 Direct Measurement-based Ergonomic Assessment

Direct measurement-based ergonomic assessment methods typically use electromyography (EMG), goniometers, inclinometers, force sensors, accelerometers, sonic sensors, and optical markers that are attached directly to the subject for objective measurement results to increase the accuracy of the ergonomic risk assessment (Wang et al. 2015; Li and Buckle 1999; David 2005). Physiological methods are direct measurement-based methods that use instrumentation to monitor the physical status of the human body in analyzing biomechanics and the loading to which tissue and joints are subjected. An example is EMG, which is used primarily in studying muscle exertion for the purpose of evaluating muscle fatigue (Wang et al. 2015).

The wearable motion capture system based on the inertial measurement units (IMU) is another direct measurement-based method, which has been proven as an effective method to collect the body joint angles data for the ergonomic risk assessment (Vignais et al. 2013; 2017; Valero et al.

2016; Rye et al. 2021). The IMU-based motion capture system can track the continuous motions through the measurement of segment accelerations and angular rates (Chen et al. 2017). As a wearable system, it allows the direct measurement of working postures and motions in the industrial environments without interrupting the ongoing production. However, the IMU sensors are required to firmly attached to the workers' body, which may lead to the worker discomfort and changes of the original working postures.

In the case of joint angle measurements, the optical marker-based motion capture method is a widely used direct measurement-based method, as it has been shown to be accurate, including for comparative purposes (Vena et al. 2011a; 2011b; Hebert and Lewicke 2012; Hebert et al. 2014; Schofield et al. 2014). The optical marker-based motion capture systems such as VICON system and OptiTrack system are commonly used in the laboratories for capturing the continuous motions by using high-speed cameras and reflective markers. Due to the high accuracy and reliability, the optical marker-based motion capture systems are considered as the ground truth for the kinematic data collection, which can be used as the basis for comparison in the laboratory studies (Kim and Nussbaum 2013; Eichelberger et al. 2016). Thus, VICON system has been selected in this research. Although these methods provide a high level of accuracy with respect to a range of exposure variables, they have some notable limitations, such as their time-intensiveness, the need for costly equipment and experts to conduct the assessment, and the possibility of worker discomfort, job modification, or interruption during the data collection phase (Inyang et al. 2012; Wang et al. 2015; Li et al. 2018; David 2005).

2.2 Advanced Ergonomic Risk Assessment

With the advanced motion data collection techniques, automated ergonomic posture assessments can be conducted based on the collected continuous motions and the observation-based ergonomic risk assessment methods. The motion data collections through computer vision and 3D visualization are used in construction for the ergonomic risk assessment of construction workers (Golabchi et al. 2015; Li et al. 2019b; Yu et al. 2019; Wang et al. 2021a).

2.2.1 Computer Vison-based Assessment

The computer vision-based assessment method has gained increasing interest and adoption within the construction industry in recent years because of its speed and because it does not interrupt the work. The working postures and motions are identified continuously by using pictures and videos from single or multiple cameras in the computer vision technologies. In construction, the computer vision-based method has been widely used to analyze the productivity and monitor the health and safety (Brilakis et al. 2011; Escorcia et al. 2012; Han et al. 2013; Yu et al. 2019). However, this method still needs improvement since it is difficult to acquire accurate positions of body segments in a complex construction environment, and due to viewpoint limitations, the impact of illumination changes and occlusions, and the amount of time required for algorithm development, testing, and data post-processing (Wang et al. 2015; Li et al. 2018; Seo et al. 2015). It should be noted that these methods are post-assessment methods, meaning that the workers under observation are performing tasks in an existing workplace.

2.2.2 3D Visualization-based Assessment

3D visualization-based assessment is proposed as an alternative to post-assessment. 3D visualization collects the body joint angles in the 3D human model of operational tasks and automatically evaluates the animated motions based on observation-based ergonomic risk assessment methods (Li et al. 2018; 2019b). Accurate 3D visualization of the operational tasks is essential and can be developed in two steps: (1) developing the 3D workplace in the form of 3D geometric models, including layouts, dimensions, equipment, tools, and materials; and (2) creating a 3D human model based on anthropometric data and imitating the motions of workers based on the task requirements and the associated workplace design. The working postures and motions are designed according to the collected images and videos based on the designer's experience. Once the 3D models are obtained, the body joint angles are extracted from the 3D visualization of the worker's motions and post-processed to obtain the REBA and RULA ergonomic risk ratings. The accuracy and reliability of the 3D visualization-based assessment has been validated by Li et al. (2018) through a repetitive lifting experiment as part of a past study.

As a proactive method, 3D visualization seeks to provide ergonomic risk evaluation for workplace design at the design stage, offering the following benefits: (1) it is capable of obtaining reasonably accurate human body continuous motion data (e.g., joint angles) in the 3D model; (2) it is capable of assessing ergonomic risks at the design stage prior to real-world implementation, leading to cost savings in the long run; (3) it can proactively analyze motions without needing a human subject to physically perform the task; and (4) it can visualize and analyze the modified work intuitively (Li et al. 2018; 2019b). However, there are also several limitations that must be overcome in order to achieve reliable ergonomic-centric workplace design.

As mentioned above, the 3D visualization of the operational task is created based on the designer's experience. Subjective judgments concerning the positions of key postures are involved in the development of 3D visualization. In the case of 3D visualization, up to 25° in variation in the main joint angle estimations throughout the repetitive lifting motions and variances in the corresponding risk ratings up to 1 risk score interval have been observed in the comparison between motion capture experiments and 3D modelling, for instance (Li et al. 2018). In addition, the discrete boundaries between the posture categories in REBA and RULA entail that a small change in joint angle input can result in a marked change in the risk assessment results. Thus, human perception and inter-/intra-observer reliability contribute to significant variability of the assessment results. To address this issue, artificial intelligence-based methods, such as fuzzy logic, can result in more accurate assessments and thereby reduce the impact of human perception errors and measurement errors. With the integration of fuzzy logic, the 3D visualization-based ergonomic risk assessments carried out can better capture the gradual transitions characteristic of continuous human motions, thereby preventing abrupt changes in risk ratings.

The reliability of 3D visualization-based assessment is also highly dependent upon the level of accuracy of the joint angles in the working postures and motions. In this respect, both the positions of body segments in the posture and the time feature during continuous motions both play an essential role in ensuring the accuracy of ergonomic risk assessment. In current practice, the standard movements in the 3D model are generally built using 24 to 30 frames per second (fps) for normal motions (Autodesk 2021). Although designers follow these standard movements when developing 3D models, the animated motion time (i.e., the time spent in a given motion in the 3D model) may not be the same as the standard motion time (i.e., the standard time spent in which a worker should complete that motion) in reality.

In addition, muscle use and activity scores are used to evaluate motion repetitiveness in RULA and REBA, respectively, but these scores are subjectively adjusted by the analyst based on their knowledge and experience. Thus, the methods underlying the predetermined motion time system can be applied to the ergonomic risk assessment of continuous motions in order to automatically and objectively generate a standard motion time-based ergonomic assessment, ultimately resulting in an ergonomic-centric workplace design.

2.3 Fuzzy Logic Techniques in Ergonomic Risk Assessment

In recent years, rapid advancements in computing have led to the emergence of fuzzy logic techniques. Fuzzy logic is a powerful approach for capturing intrinsic vagueness and challenging complex systems developed with the formulation of fuzzy set theory, first provided and further developed by Zadeh (1965; 1975a; 1975b; 1975c). Fuzzy logic can assist in capturing and adapting expert knowledge and experience for risk evaluations, since it permits the inclusion of human creativity and intuition (de Ru and Eloff 1996). According to the literature, fuzzy logic techniques have been developed by researchers for the evaluation of WMSDs with a focus on manual lifting tasks (Karwowski et al. 1987; 2006; Yeung et al. 2002; Chen et al. 1994). Fuzzy expert systems were designed to quantify the ergonomic risks to the upper limbs (Moynihan et al. 1995; McCauley-Bell and Badiru 1996).

With a focus on workstation analysis, a fuzzy multi-criterion decision-making model and a fuzzy expert system tool were developed for evaluating WMSDs (Nunes 2006; 2009). An ergonomic expert system was developed using one rule-based and six knowledge-based modules for WMSD risk assessment in a wide variety of applications (Pavlovic-Veselinovic et al. 2016). These studies have mainly focused on experts' linguistic explication of risk factors. However, in practice, the most important factor is the body joint. In this regard, Golabchi et al. (2016b) proposed using a fuzzy logic method in conjunction with RULA for field observation-based ergonomic risk assessment in construction. However, the details of how membership values were assigned to the variables, which is a crucial but also challenging step in the development of a fuzzy expert system, are not given in their study. Moreover, only 29 randomly generated static postures are investigated and analyzed, and the developed model can only be used to analyze ergonomic risk in a field setting. Therefore, more efforts are needed to develop the fuzzy logic method in conjunction with ergonomic posture assessments for automated evaluation of continuous motions to eliminate risk rating variations caused by human perception errors and measurement errors.

2.4 Predetermined Motion Time System

The motion analysis technique is commonly used for collecting motion times during manual operations. Predetermined motion time systems (PMTSs) provide standard cycle times for physical operations by characterizing the working methods and procedures. PMTSs are widely used in various industries for setting production standards, together with time studies, work sampling, and standard data (Freivalds and Niebel 2013). PMTSs are based on an engineered work measurement, which is essential for cost estimation, work planning and scheduling, and decision making (Genaidy et al. 1989). They are capable of providing process times in the planning phase, and of facilitating the design of work systems in a targeted manner. In current practice, time studies are commonly used in the construction industries due to its simplicity and effectiveness. However, the time study is a traditional technique relied on personal judgment which leads to highly subjective and unreliable results. In addition, it is time-consuming and error-prone when employed in a complex working environment. Thus, PMTS is a systematic and objective method to obtain the standard motion time durations, which can be used in the ergonomic risk assessment of continuous motions.

The commonly used PMTSs in current practice include Methods-Time Measurement (MTM) (Maynard et al. 1948), the Maynard Operation Sequence Technique (MOST) (Zandin 1980), and the Modular Arrangement of Predetermined Time Standards (MODAPTS) technique (Heyde 1983). In the MTM family, the original MTM system is commonly referred to as MTM-1, which is the most detailed MTM system. These methods can be distinguished with respect to the level of precision, the scope of data application, the classification of motion, and the unit of time used (Genaidy et al. 1989). The majority of PMTSs, though, do not sufficiently address the impacts of time standards, including various task variables, worker variables, and environmental variables (Genaidy et al. 1989). In addition to these deficiencies, PMTSs are time-consuming and difficult to apply, necessitating specialized training (Genaidy et al. 1989).

PMTSs have been employed in various manufacturing contexts to predict assembly task cycle times. The use of PMTSs has brought considerable benefits in the field of automobile manufacturing (Razmi and Shakhs-Niyaee 2008; Tuan et al. 2014). The time and motion analysis originated in industrial engineering, where production occurs in a steady-state environment (Thomas et al. 1990). Despite the wide and successful applications of PMTSs in other industries, though, these methods have seldom been applied in the construction manufacturing industry due to the dynamic nature of the industrialized construction facility. An industrialized construction setting in which intelligent manufacturing methods are employed offers a stable working environment and, hence, the opportunity to apply PMTSs for a motion time analysis in industrialized construction. In construction manufacturing, MODAPTS has been successfully integrated with discrete-event simulation modelling yielding reliable estimates of manual task durations (Golabchi et al. 2016a). However, this integrated method is not fully automated and requires specialized knowledge of simulation modelling.

2.5 Posture Sway Analysis

Posture sway, or body sway, is defined as the slight postural movements made by an individual to maintain a balanced position of the body segment. In previous studies, body sway has been assessed for static and dynamic conditions, such as standing and walking (Spirduso 1995). These studies have tended to focus on the development of various balance tests and measurements to provide information on balance capabilities during a static standing condition (Berg et al. 1989; Wing et al. 1995; Chang and Krebs 1999). For example, posture sway can be measured using a swaymeter (Lord et al. 1991), which measures the displacement of the body at the waist level. It can also be measured using Wright's ataxiameter (Nayak 1987), which measures the angular movement of the body around the ankle joint. As a more recent development, with the emergence of motion capture technology, accurate body sway information can be obtained by tracking human motion over a period of time. For example, researchers have demonstrated the effective use of a single camera to measure clinical statistics related to standing postural sway (Allin et al. 2008). Moreover, body sway measurement using inexpensive webcams has been validated in the case of a Vicon motion capture experiment (Wang et al. 2010). In another study, a markerless image processing algorithm was developed to estimate the anterior–posterior trajectory of the center of mass (Goffredo et al. 2006).

In the case of automated ergonomic risk assessments of continuous motions, the natural posture sway that occurs during the continuous motions involved in completing an operational task can result in overestimations and fluctuations in the ergonomic risk assessment results (Li et al. 2019b; Wang et al. 2021a). If we take, for instance, the posture categories in REBA and RULA, there is no threshold to determine whether a risk score of 1 is needed or not. For example, while the posture judgments for neck twisting position, neck lateral bending position, trunk twisting position, and trunk lateral bending position are all 0°, the worker cannot in reality maintain a joint angle with 0° due to the body structure and the minor movements of other body segments. Thus, for posture judgments, thresholds that account for the minor movements of body joints are required in order to ensure the accuracy of the automated ergonomic risk assessment of continuous motions. However, the human posture sway that naturally occurs during dynamic and continuous motions is not accounted for in existing ergonomic risk assessment methods. Thus, a laboratory investigation to determine the acceptable magnitude of minor body joint movements naturally occurring due to posture sway is needed in order to eliminate risk estimation errors and risk rating fluctuations in ergonomic risk assessments of continuous motions.

2.6 Research Gaps

This chapter reviewed the ergonomic risk assessment methods used in current practice. These assessment methods are rule-based methods for evaluating working postures. Based on a review of the relevant literature, there is no suitable assessment method for the ergonomic risk evaluation of dynamic and continuous motions. The use of existing methods for the automated assessment of dynamic and continuous motions is challenged in three notable respects, including (1) variance in ergonomic risk resulting from the discrete boundaries between the predefined posture categories in existing ergonomic risk assessment methods; (2) inaccuracy of the ergonomic risk assessment results due to the lack of consideration of continuity and standard motion time feature in dynamic and continuous motions; and (3) overestimation issues in the ergonomic risk assessment caused by the natural minor movements of human body joints in natural posture sway and the ambiguity in distinguishing between posture categories during the adjustment risk rating process in existing ergonomic risk assessment methods (i.e., REBA and RULA). Thus, this study seeks to fill the research gaps with respect to these three challenges in the automated ergonomic risk assessment of continuous motions.

According to the identified research gaps, fuzzy logic, PMTS, and posture sway analysis are reviewed. The findings underscore the need for a systematic and objective framework that integrates these methods (i.e., fuzzy logic, PMTS, and posture sway analysis) in order to automatically evaluate the ergonomic risks of continuous motions. Specifically, fuzzy logic can be deployed to eliminate the variations in risk ratings caused by human perception and measurement errors in body joint estimation. PMTS, meanwhile, can be applied to overcome the inherent limitations of subjective estimation of motion time durations. Posture sway analysis, finally, can be employed to identify the minor movements of body joints associated with natural posture sway in the determination of posture categories as part of ergonomic risk assessments. The following chapter describes in detail how these methods are integrated and used in the ergonomic risk assessment of continuous motions.

CHAPTER 3: RESEARCH FRAMEWORK

3.1 Background

This chapter introduces the overall research framework implemented in this thesis. As reviewed in the previous chapter, rule-based ergonomic risk assessment methods are crucial for the evaluation of ergonomic-centric workplace design in industrialized construction, and many research studies have been conducted in this domain. However, one of the key challenges of existing ergonomic risk assessment methods is the lack of an accurate and objective evaluation method for automatically assessing continuous motions that associated with the workplace design. In this chapter, a novel research framework for automated ergonomic risk assessment of continuous motions is outlined. The proposed framework can be divided into three main sections—3D fuzzy-based assessment, 3D standard motion time-based assessment, and posture sway-incorporated assessment for continuous motions—each of which is described briefly in this chapter. More details on analysis methods are included in subsequent chapters.

3.2 Proposed Framework

An overview of the proposed framework for automated ergonomic risk assessment of continuous motions is presented in Figure 3-1, which include three sections: (1) 3D fuzzy-based assessment; (2) standard motion time-based assessment; and (3) posture sway-incorporated assessment. In the present research, the 3D visualization-based ergonomic risk assessment method is used as the basis and as an example to illustrate the proposed framework and the implemented results. In order to design the ergonomic-centric workplace using the proposed framework, the 3D visualization of the workplace is required to develop and the 3D human model of the continuous motions in the tasks is required to create according to the workplace design. Then, the 3D human model is decomposed frame by frame to obtain the postures at each time frame in the continuous motion. The body joint angles are extracted from the postures at each time frame and formatted for the ergonomic risk assessments. The rule-based fuzzy expert system is developed and integrated with the rule-based ergonomic risk assessment methods to generate the risk rating scores of all postures for all the time frames in the continuous motion. Moreover, an experimental study in the motion capture system is proposed to identify the accepted posture sway magnitude to modify the posture categorization of adjustment risks in the current ergonomic risk assessments. Since the time feature of the continuous motions is necessary, the proposed framework integrates the standard motion time durations with ergonomic posture risk ratings. Thus, the research also involves the development of an automated rule-based motion recognition and automated PMTS interpretation algorithms to generate basic motion series and the corresponding standard motion time durations. Meanwhile, a mapping method of risk rating and standard motion time is proposed to generate the standard motion time-based ergonomic risk rating of continuous motions for the decision support of ergonomic-centric workplace design.

The decision support module is developed in the proposed framework. The average risk ratings of continuous motions based on the standard motion time is used to check the ergonomic performance of the workplace design. If the risk level is not satisfied, the modification recommendations are provided for the workplace design and the associated 3D human motions. Otherwise, the risk rating visualization of continuous motions is generated. Finally, the valuable information of the workplace design is outputted, including the fuzzy-based ergonomic risk ratings, standard motion time durations, visualization of continuous motions and the workplace design, and recommendations for work modification (if any). In this research, 3ds Max software is used to design workplaces, simulate detailed human motions, and develop work modifications intuitively. Python (version 3.7), a free programming language for statistical computing and graphics, allows users to effectively generate, modify, and structure data. Thus, Python is used to develop and drive all components of the entire framework.

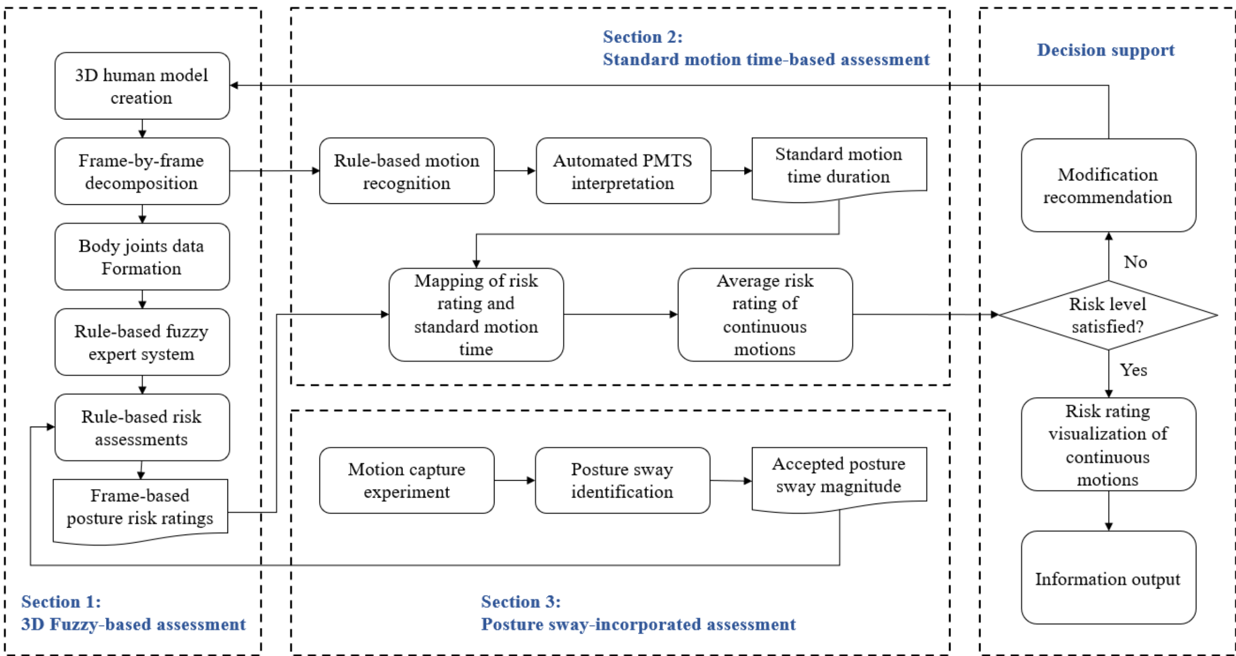

Figure 3-1. Overview of the proposed framework

As illustrated in Figure 3-1, the proposed framework can be divided into three main sections as follows:

1. **3D fuzzy-based assessment:** The development of an automated 3D fuzzy-based ergonomic analysis method serves the research objective 1, where the main tasks are to develop the specialized rule-based fuzzy expert system to integrate with the ergonomic posture assessment methods for the evaluation of continuous motions. The performance of the fuzzy logic integrated assessment method is also investigated and validated through a

repetitive lifting experiment. The methodology development is described in greater detail in Chapter 4.

2. **Standard motion time-based assessment:** The development of an automated method to integrate the predetermined motion time system with ergonomic risk assessment methods for identifying the standard motion time-based ergonomic risks of continuous motions is to fulfill the research objective 2. A rule-based motion recognition algorithm is proposed in this section to automatically detect motions and their parameters for the standard motion time determination. The MTM-1 system, one of the most detailed PMTSs, is incorporated into the proposed methodology for the purpose of producing standard time durations of continuous motions. The details of the proposed methodology and implementation cases are provided in Chapter 5.
3. **Posture sway-incorporated assessment:** The development of a posture sway-incorporated method serves the research objective 3, where the method modifies the posture categorization of adjustment risks in the ergonomic posture assessment methods. The motion capture experiments are conducted to identify the minor movements of body joints naturally occurring in the completion of tasks due to the posture sway. The identified minor movements of body joints are used for the determination of the associated posture categories. The posture sway-incorporated ergonomic analysis method is described in greater detail in Chapter 6.

CHAPTER 4: 3D FUZZY ERGONOMIC ANALYSIS FOR RAPID WORKPLACE DESIGN AND MODIFICATION IN CONSTRUCTION[1]

Accurate ergonomic risk assessment is a key to effective workplace design and modification in construction. However, conventional ergonomic risk assessment methods are time-consuming, error-prone, require human subjects, and are hindered by inter- and intra-observer reliability issues. This chapter discusses an automated proactive 3D fuzzy ergonomic risk analysis method that accurately quantifies ergonomic risks of continuous motions for rapid workplace design and modification, addressing all of the aforementioned limitations. A specialized rule-based fuzzy inference algorithm is integrated with 3D automated posture-based ergonomic risk assessments to better capture the gradual transitions characteristic of continuous human motion without abrupt changes in risk ratings. This method is tested in a repetitive lifting experiment, which proves its improved accuracy and reliability for ergonomic risk assessment. The results of the analysis are expected to facilitate the enhancement of safety performance, production performance, and market competitiveness in industrialized construction.

4.1 Methodology for 3D Fuzzy-based Assessment

The overview of the proposed system is presented in Figure 4-1. The work sequence, process features, and workplace design information serve as the original data source from which worker movements and features of the workplace can be derived and imitated in a 3D model. REBA and RULA are used as two major criteria for defining different risk levels, since they are posture-based

---

[1] A version of this chapter has been published in *Automation in Construction*, as follows: Wang, J., Han, S., and Li, X. (2021). 3D fuzzy ergonomic analysis for rapid workplace design and modification in construction. *Automation in Construction*, 123, 103521. https://doi.org/10.1016/j.autcon.2020.103521. It also has been reprinted with permission from the publisher.

methods commonly used in the area of ergonomic risk assessment. In the proposed methodology, REBA and RULA are integrated to provide greater flexibility by focusing on the entire body's postures, emphasizing the upper limb postures, and their combination. Some user-defined parameters are also required, especially for the purpose of extracting body movement data. Considering its many advantages, such as accuracy and processing speed, the fuzzy logic algorithm is the specialized rule-based fuzzy expert inference mechanism employed in this research. The main process includes 3D modelling, fuzzy processing, and interpretation of results. The outputs of the system are fuzzy-based REBA/RULA risk ratings, 3D ergonomic-centric design visualization, and recommendations for work modification (if any). The Python (version 3.7) programming language for statistical computing and graphics is used to develop and implement the proposed algorithm. Python is selected, it should be noted, due to its breadth and ease of use and its ability to effectively generate, modify, and structure data.

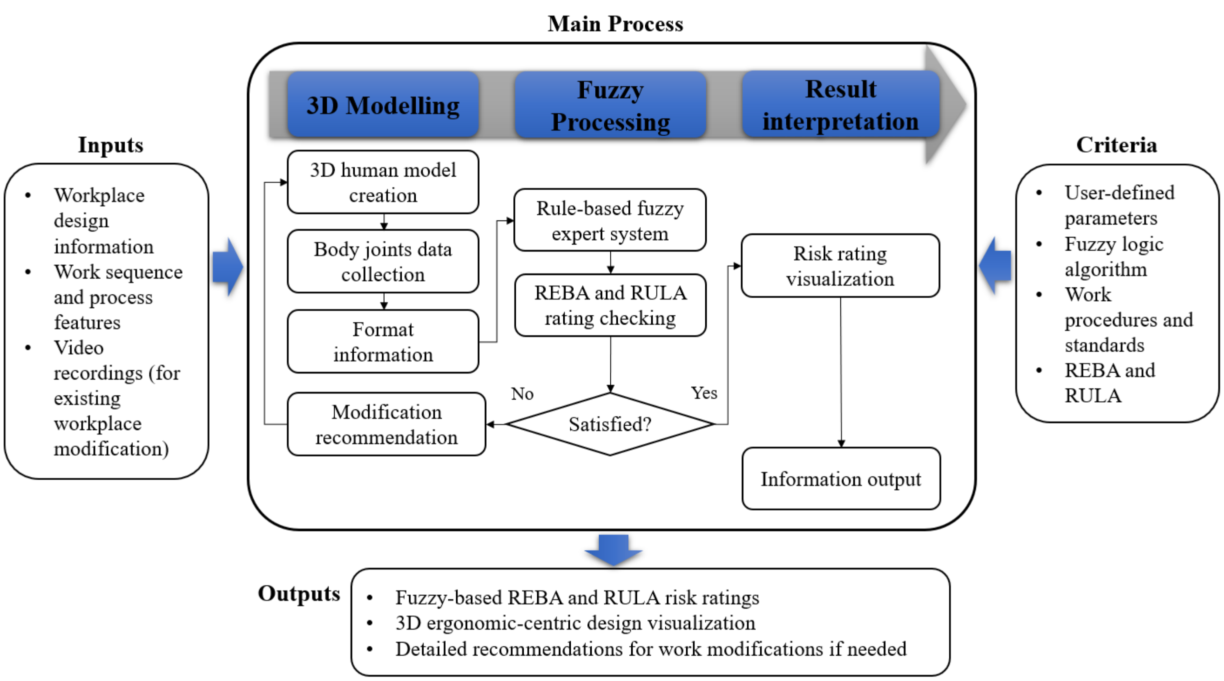

Figure 4-1. Overview of the 3D fuzzy ergonomic risk assessment system

4.1.1 Input Data Preparation

The input data is collected from the work sequence, process features, and workplace design information. (Video recordings are recommended if the assessment is for the purpose of assessing and modifying an existing workplace.) In order to capture the features of body movements for the convenience of later-stage processing, front-facing and profile videos are recorded. Workers' anthropometric data and repetitive information are also collected for the acquisition of user demands. Workstation dimensions and workplace layout are gathered from engineering drawings in order to obtain detailed information for the purpose of generating the 3D model. Other information, such as the weight and dimensions of module (e.g., walls and floors), task procedures and requirements, and tool specifications, is collected to support the subsequent processes.

4.1.2 Implementation Process

The implementation process is divided into three sequential phases—3D modelling; fuzzy processing; and interpretation of results—as shown in Figure 4-1. Based on the input data collected, an accurate 3D model is created frame-by-frame in 3ds Max software, which allows users to design workplaces, simulate detailed human motions, and develop work modifications intuitively. Body joint angles are required by REBA and RULA as input variables for the ergonomic risk assessment.

For automation and reliability purposes, a total of 41 joint angles covering the sagittal plane, frontal plane, transverse plane, and axial rotation are extracted and stored in a database for 3D modelling. Table 4-1 lists the detailed joint angle information, which is sufficient for the data formatting process and, ultimately, generating the required body segments' positions. The joint angle data in the time series format is transformed into a compatible and interpretable format for subsequent fuzzy logic algorithm processes. The hierarchical bone structure adopted in the 3D human model is the Biovision Hierarchy (BVH) format (Meredith et al. 2001), which is a compact and concise format for body configurations and rotational joint data representation in motion capture systems. As mentioned above, a total of 41 joint angles of the 3D human model are defined corresponding to the required angles of each body segment in the biomechanical analysis software, 3D Static Strength Prediction Program (*3D SSPP*) (University of Michigan 2017). The respective ergonomic risk rating methods integrated in the proposed system, it should be noted, each define a given body segment's position in terms of the joint angle between the body segment and the extension of its connected body segment. The joint angle conversion between the 3D biomechanical model and the REBA/RULA methods is described in detail in a prior study by authors of the present study (Li et al. 2019b).

To fit the requirements of the ergonomic risk rating methods in the fuzzy processing stage, a data formatting process is developed in Python to perform the joint angle conversion for subsequent ergonomic risk rating processes. The completed dataset is transformed into a table format in which each variable is saved in a column and each time frame is saved in a row. All the joint angles keep four decimal places as the float format to ensure precise computations in subsequent procedures.

Table 4-1. List of 41 joint angles extracted from the 3D human model

Body segment	Sagittal plane	Frontal plane	Transverse plane	Axial rotation
Head	1 Head_Flexion	2 Head_Lateral_Bending	–	3 Head_Rotation
Neck	4 Neck_Flexion	5 Neck_Lateral_Bending	–	6 Neck_Rotation

Shoulder	Clavicle_Vertical (7L/8R)	–	Clavicle_Horizontal (9L/10R)	–
Upper arm	UpperArm_Vertical (11L/12R)	–	UpperArm_Horizontal (13L/14R)	–
Lower arm	ForeArm_Vertical (15L/16R)	–	ForeArm_Horizontal (17L/18R)	–
Trunk	19 Trunk_Flexion	20 Trunk_Lateral _Bending	–	21 Trunk_Rotation
Pelvis	–	22 Pelvis_Lateral _Bending	–	23 Pelvis_Rotation
Upper leg	UpperLeg_Vertical (24L/25R)	–	UpperLeg_Horizontal (26L/27R)	–
Lower leg	LowerLeg_Vertical (28L/29R)	–	LowerLeg_Horizontal (30L/31R)	–
Foot	Foot_Vertical (32L/33R)	–	Foot_Horizontal (34L/35R)	–
Hand	Hand_Vertical (36L/37R)	–	Hand_Horizontal (38L/39R)	Hand_Rotation (40L/41R)

Note: Naming of 41 joint angles in the table above follows the conventions of the database, where “L” and “R” refer to the left and right sides of the body.

The proposed system employs a rule-based fuzzy expert system to eliminate discrepancies in ergonomic risk ratings and thereby improve the accuracy and reliability of the ergonomic risk assessment. Figure 4-2 shows the mechanism by which the rule-based fuzzy inference algorithm operates. The algorithm consists of three sequential components: input encoding, rule-based inference, and output decoding. It is a fuzzy logic-based method for modelling the subjective uncertainty first described by Zadeh (1965).

As traditional ergonomic risk assessment methods, REBA and RULA can only assess postures at a specific moment and provide an integer risk score, resulting in a stepped shape graphical representation of continuous postures. These predefined, discrete boundaries between risk categories entail that a small change in joint angle input can result in a sudden jump or drop in the assessment results. In other words, REBA and RULA are incapable of representing gradual transitions between different risk rating levels or incorporating human perception during identification of body segment positions, particularly for postures that involve body segment positions close to the predefined borders between risk categories.

With the introduction of 3D modelling, its highly precise quantitative body movement measurements only increase the demand for accurate assessment at the boundaries between risk categories. In REBA and RULA, changes in body joint angle as small as 1° or even 0.0001° can result in a sudden change in integer risk score, and fluctuations in risk scores when assessing continuous motions have been identified in the literature (Li et al. 2018). To achieve transitional risk scores that more accurately represent continuous motions, a fuzzy logic algorithm is integrated with REBA and RULA to address human perception issues and prevent these abrupt changes in risk scores.

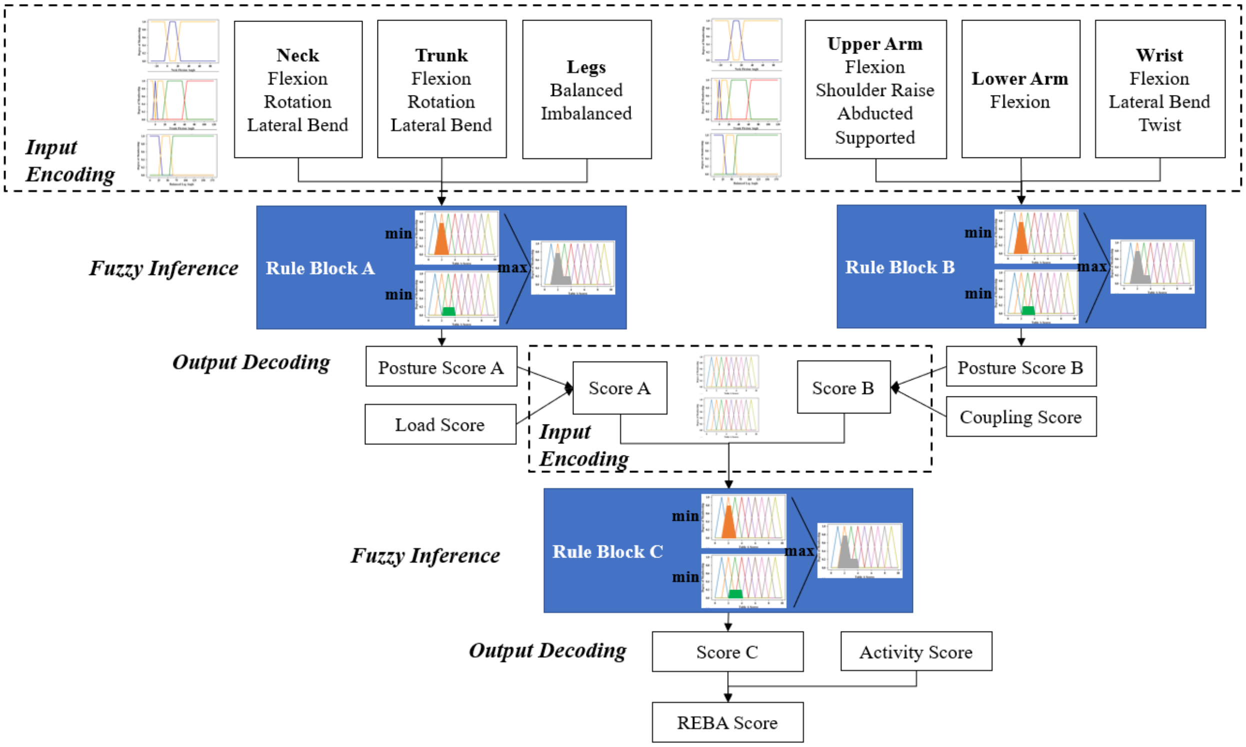

Figure 4-2. Rule-based fuzzy inference algorithm in REBA

The input encoding component involves membership function development of all model variables. The fuzzy membership function maps a universal set of objects, X, to the unit interval of 0 and 1, thereby enabling quantitative calculations in the subsequent fuzzy inference process. In a real environment, with inherent uncertainties and vagueness, there is always a lack of useful information to assist in making an appropriate decision for all joint angles. As such, deterministic values are incapable of accurately representing the postural performance.

Fuzzification in the input encoding component converts the numerical input values to the appropriate fuzzy sets through the use of various types of curves, including Gaussian, triangular, and trapezoidal membership functions (Klir and Yuan 1995). In the interest of simplicity and efficiency of the fuzzy logic computation, simplicity of the application, and to facilitate understanding for participants (Poveda and Fayek 2009), trapezoidal and triangular shapes are used to construct fuzzy membership functions for joint angles and risk scores to capture the uncertainty at the close-to-border positions in REBA and RULA. In the present research, threshold (I) is introduced to construct the membership functions. It is defined as the level at which the ergonomic effect begins to be produced, representing the smoothness of the effect in the risk transition. Thus, the gradual transition, considering both sides of the predefined border position, is from (border − I) to (border + I).

The threshold setting is the main criterion in the membership function development. Although the threshold is set as a user-defined parameter for better flexibility, it is capable of up to 5° to fulfill the trapezoidal or triangular shape of all possible membership functions. In this study, the maximum value of 5° is used for demonstration purposes. A transition range of 10° is also applied. This threshold setting ensures the membership value of 0.5 at the crossover points between adjacent membership functions, gradual transitions between risk categories, simple and uniform settings of the gradual transitions, and triangular or trapezoidal shapes of the membership functions in the fuzzy logic model. The points of intersection are set as the predefined borders in REBA and RULA for all body segments (except the trunk at the straight standing position in REBA and RULA and the wrist position at 0° in RULA) that obtain full degrees of membership.

The graphical representation of the threshold is the distance between the border of the risk category and the root of the membership function obtaining 0 degrees of membership, as shown in Figure 4-3. The trapezoidal membership function is constructed as per Equation 4-1, where μ_A is the membership value, α is the number of degrees at the lower border, and β is the number of degrees at the higher border predefined in REBA and RULA. The input variables of REBA/RULA in discrete form are transformed into trapezoidal membership functions that can be processed in the fuzzy inference system. Although the lateral bending angles in the frontal plane and axial rotation angles of body segments are simply defined as adjustments to supplement the flexion/extension angles in the sagittal plane in REBA and RULA, these angles are still assigned respective membership functions to facilitate the full coverage of the body postures in the proposed methodology.

$$\mu_A(\theta) = \begin{cases} 1 & \alpha + I \le \theta \le \beta - I \\ (I - \alpha + \theta)/2I & \alpha - I \le \theta \le \alpha + I \\ (I + \alpha - \theta)/2I & \beta - I \le \theta \le \beta + I \\ 0 & other \end{cases} \qquad \text{Equation 4-1}$$

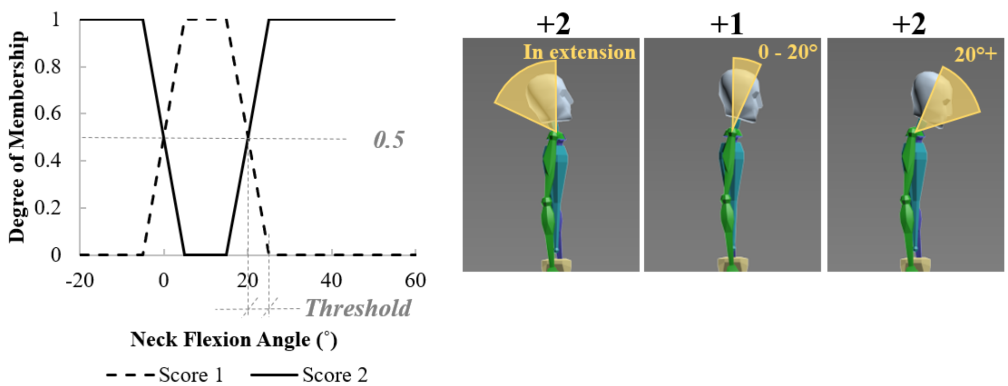

Figure 4-3. Graphical representation of Threshold (*I*) for neck flexion in REBA

Rule-based fuzzy inference processes examine the risks to which each body segment might be subjected and determine the level of risk based on REBA and RULA. Three sets of if-then rules are developed based on the three scoring tables in REBA and RULA, respectively. These if-then rules represent relationships among fuzzy variables and provide a fuzzy reasoning mechanism linking the input variables with the output or intermediate variables (Rey et al. 2017). The form of condition and conclusion statements captures qualitative concepts and represents the links between risks at the joint-level, body-segment-level, integrated-body-segments-level, and grand-level. A total of 240 and 272 if-then rules are developed for REBA and RULA, respectively. An example of an if-then rule derived from Table A in RULA (McAtamney and Corlett 1993) is shown in Figure 4-4.

Table A	**Wrist**	**1**		**2**		**3**		**4**	
Upper Arm	Lower Arm	Wrist Twist		Wrist Twist		Wrist Twist		Wrist Twist	
		1	2	1	2	1	2	1	2
1	1	1	2	2	2	2	3	3	3
	2	2	2	2	2	3	3	3	3
	3	2	3	3	3	3	3	4	4
2	1	2	3	3	3	3	4	4	4
	2	3	3	3	3	3	4	4	4
	3	3	4	4	4	4	4	5	5

If
UpperArmScore is 2 and
LowerArmScore is 1 and
WristScore is 3 and
WristTwistScore is 2
Then
Score A is 4

Figure 4-4. Example of an if-then rule derived from Table A in RULA (McAtamney and Corlett 1993)

The triangular norm (t-norm) and triangular conorm (t-conorm or s-norm) are indispensable fuzzy operators used to combine the if-then rules. They generalize the logical conjunction and disjunction to fuzzy logic, and, subsequently, correspond to the fuzzy intersection and union, respectively (Klir and Yuan 1995). For the inference process, the minimum t-norm operator that corresponds with the logical AND in the if-then rules is used to combine the input variables with the output for each rule, while the maximum s-norm operator is used for the aggregation of the rules (Klir and Yuan 1995). The fuzzy inference system establishes the links between the four levels for ergonomic risk assessment. With the implementation of the rule-based fuzzy inference algorithm, gradual and uniform transitions between risk rating levels are generated for all the joints and body segments.

The output decoding process is applied to obtain the deterministic values of the rule-based fuzzy inference system through the application of defuzzification techniques. Defuzzification is an inverse process of fuzzification, which is the final stage in the fuzzy logic system to generate the most accurate quantifiable representation of the aggregated fuzzy sets produced by the inference mechanism. This representation is achieved by assigning numerical values using defuzzification methods such as the centroid, bisector, and maxima methods (Klir and Yuan 1995). The most commonly used method is the center of area (*CoA)* method, also referred as the centroid method, which computes the geometric center of the fuzzy set. As an alternative method, the bisector method determines the half-area position of the fuzzy set, while maxima methods only consider values with maximum membership (Klir and Yuan 1995). The advantages of the *CoA* method are its consideration of all the information contained in the membership functions, as well as its consistency, simplicity, intuitive supportability, and computational efficiency (Runkler 1996). In light of these advantages, the *CoA* method is adopted in the methodology described herein. The calculation used here can be mathematically expressed as Equation 4-2 (Klir and Yuan 1995), where x is the ergonomic risk score, $\mu_A(x)$ is the corresponding membership values, and the x_{min} and x_{max} define the range of the ergonomic risk scores.

$$CoA(A) = \frac{\sum_{x_{min}}^{x_{max}} \mu_A(x) \times x}{\sum_{x_{min}}^{x_{max}} \mu_A(x)} \qquad \text{Equation 4-2}$$

In summary, the methodology is developed using trapezoidal and triangular membership function shapes, a minimum t-norm operator (for linking the input variables to the output in each rule), a maximum s-norm operator (for the aggregation of the rules), and *CoA* defuzzification (for generating the output in deterministic form). It should be noted that the workplace design can be modified using these outputs, whereby the user gains a more quantitative and determinate understanding of a worker's ergonomic performance.

An ergonomic risk rating check is conducted after carrying out the fuzzy inference. If the rating is satisfactory to the user, the workplace design and imitated movements are fixed, and we proceed to the next stage, which is the results interpretation stage. If the rating is not satisfactory to the user, the workplace parameters and the movements involved in performing a given task must be modified in the 3D model to address the identified high-risk motions. The results interpretation stage includes risk rating visualization of both the grand rating and the detailed ratings of body segments in the intuitionistic graphs. The information output is a concise and comprehensive summary that serves as a useful point of reference for any workplace redesign or work modification that may be required.

4.1.3 Output of Methodology

The outputs of the methodology include numerical ratings, visualized illustrations, statistical supports, and detailed information regarding any work modifications that may be required. To visually represent and compare the ergonomic risk ratings for entire dynamic motions, the risk ratings obtained from the aforementioned processes are plotted at four different levels: the joint-level, body-segment-level, integrated-body-segments-level, and grand-level. Statistics such as mean, maximum, and minimum of risk scores, corresponding risk levels, and frame percentage change can be obtained from the generated series of ergonomic risk ratings for continuous motions. Python is used to calculate any statistical summaries of interest, as well as to generate plots. Data visualization is used to serve the objective of easily and quickly retrieving ergonomic-centric workplace design information through implementation of the proposed system. 3D ergonomic-centric design can be visualized for demonstration and employee training purposes as well. If work modification is needed, detailed recommendations are provided.

In addition, to support decision making, the system can provide a statistical summary and quantitative comparison of ergonomic performance according to different workplace designs and task procedures visualized in the developed interface. The visual comparison of a worker's ergonomic performance in different workplace designs, meanwhile, helps to determine the direction of workplace design changes and work modifications based on the risk level and the motion ranges that pose high ergonomic risk. This leads to corrective or preventive solutions to ensure acceptable risk rating results. All the warnings, errors, origins, and possible solutions and corrections are presented in the proposed system's user interface as a point of reference for workplace and work design. The validation process for the methodology is discussed in the following section.

4.1.4 Validation Method

The proposed 3D fuzzy ergonomic risk assessment methodology is compared with the validated 3D visualization-based ergonomic risk assessment using the experimental data collected in the optical marker-based motion capture system and 3D modelling for validation. The purpose of integrating the experimental data with the 3D modelling data is to provide a validation process for the proposed methodology, thereby augmenting the accuracy and reliability of ergonomic-centric workplace design. A three-step validation is implemented encompassing joint allowance settings, frame-by-frame four-level risk rating comparisons, and correlation analysis.

The first step in the validation examines the joint allowance settings. The minor movements of joints and human body sway that occur naturally during the performance of tasks can result in uncertainty with respect to ergonomic risk rating. With the threshold setting in the fuzzification process, the transitions between different risk scores are formed. The optimal threshold value of each body joint can be validated through the experiments.

As the second phase in the validation process, frame-by-frame validation at four different levels is conducted to prove the accuracy and reliability of the 3D fuzzy methodology. The ergonomic risk ratings of experimental data, 3D extracted data, and 3D extracted data with the 3D fuzzy method at each time frame are compared at the joint-level, body-segment-level, integrated-body-segments-level, and grand-level. According to the architecture of REBA and RULA, the performance of each joint along three different planes and the axial rotations are validated, respectively, with subsequent validation of the overall performance. The risk rating at each time frame is compared using average error ($\overline{Error}$) and root mean square error (RMSE), as per Equation 4-3 and Equation 4-4.

$$\overline{Error} = \frac{1}{n}\sum_{i=1}^{n}(E_i - X_i) \qquad \text{Equation 4-3}$$

$$RMSE = \sqrt{\frac{\sum_{i=1}^{n}(X_i - E_i)^2}{n}} \qquad \text{Equation 4-4}$$

where E_i = risk ratings from experiment without joint allowance settings at time i;

X_i = risk ratings from experiment with joint allowance assumption and fuzzy allowance settings at time i, respectively.

Statistical associations are compared in the third step of validation through two correlation analyses. To ensure that the proposed 3D fuzzy method is correlated well with the 3D method, the correlation coefficient of the grand scores is compared between the 3D and 3D fuzzy methods (i.e., "3D vs. 3D-F"). Moreover, to validate that the proposed 3D fuzzy methodology provides a more accurate representation of the ergonomic performance of movements than does the 3D method, the risk ratings results from the experimental data are compared with the risk rating results of the

3D model extracted data, while the risk rating results from the experimental data are compared with those of the proposed 3D fuzzy model extracted data (i.e., "E vs. 3D" and "E vs. 3D-F", respectively). The statistical associations are represented using the Pearson correlation coefficient (*PCC*), which is determined as per Equation 4-5 (Rodgers and Nicewander 1988).

$$PCC = \frac{\sum_{i=1}^{n}(E_i - \bar{E})(X_i - \bar{X})}{\sqrt{\sum_{i=1}^{n}(E_i - \bar{E})^2}\sqrt{\sum_{i=1}^{n}(X_i - \bar{X})^2}} \qquad \text{Equation 4-5}$$

where E_i = risk ratings from experiment at time i;

$\bar{E}$ = mean risk ratings from experiment;

X_i = risk ratings from 3D and 3D fuzzy methods at time i, respectively;

$\bar{X}$ = mean risk ratings from 3D and 3D fuzzy methods, respectively.

4.2 Results

The implementation of the proposed system in a real construction task is described in this section. The experiment of a repetitive lifting task imitating a manual lifting task was conducted in an optical motion capture laboratory. The 3D model was created accordingly in 3ds Max software. The results obtained from the proposed methodology with various data input configurations are shown, focusing on the comparison of results between experimental and 3D fuzzy scenarios.

4.2.1 Experimental Setup

To mimic manual material lifting in a construction plant, an experiment of a repetitive lifting task performed in an optical marker-based motion capture system was conducted (Li et al. 2017). 41 joint angle data were extracted from the experiment to be compared with the corresponding 41 joint angle data from the 3D model. The experiment was performed at the Glenrose Rehabilitation Hospital's Syncrude Centre for Motion and Balance (Edmonton, Canada) by three male subjects ranging from 57.0 kg to 80.5 kg in body weight, from 173 cm to 180 cm in height, and from 27 to 31 years of age with no history of injury. In the experiment, 8 high-speed cameras were used to capture the body segments' kinematics with the configuration of 36 self-adhesive reflective markers attached to the specific joints on the skin. The object lifted was a 6.8 kg (15 lb), 45.7 cm × 61.0 cm (18 in × 24 in) rectangular window, initially positioned on a table whose center was positioned 50.8 cm (20 in) away from the knees. The entire dynamic motion of lifting the window, it should be noted, was divided into four sections: trunk flexion forward to reach for the window, trunk extension backward to move and lift the window close to the chest in an upright standing posture, trunk bending forward to return it to the table, and return to the natural standing posture. All four sections were repeated without bending of the legs or any twisting or lateral bending of the spine.

4.2.2 Implementation Results

The following implementation results illustrate the functionality of the fuzzy logic approach, as demonstrated in the subjective assumptions of joint allowance and in the high correlation between the 3D method and the proposed 3D fuzzy method. The results also illustrate the improved correlation of the proposed 3D fuzzy method comparing to the 3D method with respect to the baseline performance of the experimental data.

4.2.2.1 Joint Allowance

Detailed comparisons of joint angles between the lifting experiment and the corresponding 3D model as documented in a prior contribution by authors of the present work (Li et al. 2018) underscore the high accuracy and reliability of the 3D model developed based on the experiment. Experimental data are selected and processed as the basis for comparison, given the reliability of an optical marker-based motion capture data collection as described by Eichelberger et al. (2016). With the threshold settings in the fuzzification process in place, the gradual and uniform transitions between risk rating levels are generated for all joints and body segments. Figure 4-5 illustrates the transition performance using an example of the upper arm with a comparison between the initial risk scores obtained for upper arm flexion and the corresponding grand risk scores in both REBA and RULA, while other variables assigned with the lowest risk scores, respectively.

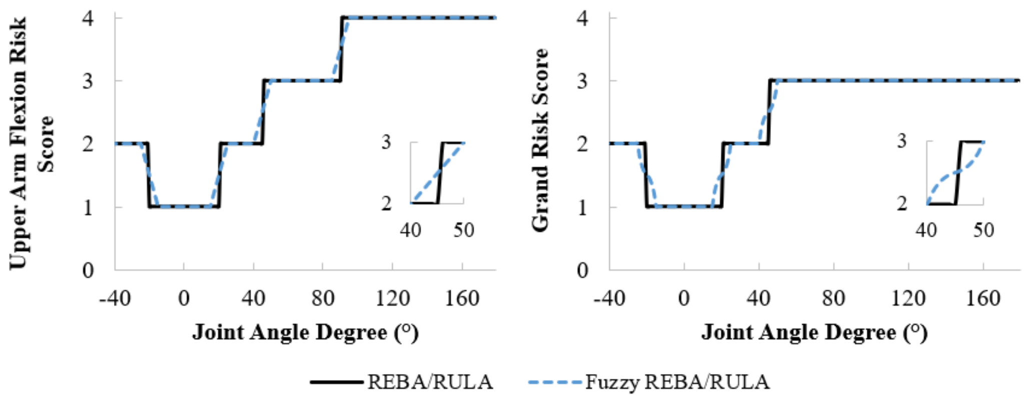

Figure 4-5. Gradual transition performance in REBA/RULA with the integration of rule-based fuzzy inference system: upper arm flexion as an example

In the experiment, the subjects are asked to conduct the movements with straight legs and without any twisting or lateral bending of the spine. However, in reality, it is inevitable that the trunk will be tilted slightly to the side and that the legs will be bent to a certain degree. As shown in Figure 4-6 (a), up to 4° of trunk lateral bending is observed among the three subjects. Thus, 4° is selected as the upper boundary for the lateral position in the judgment of trunk rating adjustment in REBA and RULA. In REBA, it should be noted, the risk ratings of legs are defined as either balanced or imbalanced, with this determination being made based on the difference in the angle formed between the two legs. Figure 4-6 (b) shows the angle difference between legs for all three subjects. As can be seen, the largest angle difference observed is in Subject 1, whose angle difference peaks at 13°. Thus, the upper boundary for balanced legs, derived from subject 2 and subject 3, is determined to be 5°. Assumptions related to joint allowance have also been employed in the previous study by Li et al. (2018) in order to achieve automated implementation of REBA and RULA in conjunction with 3D visualization. Although these assumptions are found to serve both the experimental data and the 3D modelling data satisfactorily, the subjective selection of these assumptions warrants further adjustment and validation by means of physical experimentation.

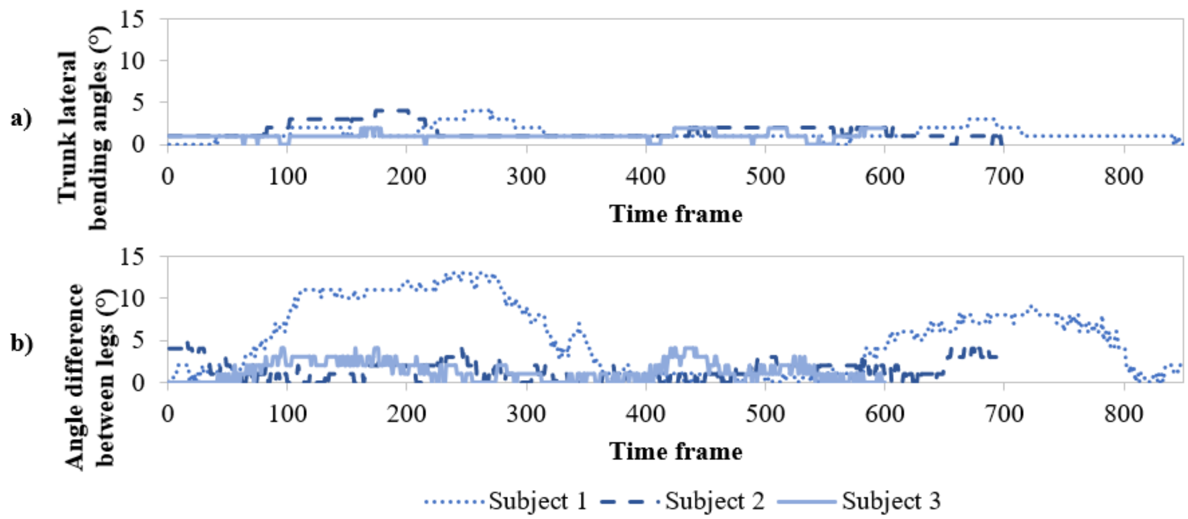

Figure 4-6. Trunk lateral bending angles (a) and the difference between left and right leg angles (b) observed during lifting experiment

Due to the limited joint angle data for the identification of the joint allowance settings, a fuzzy logic approach can be used to achieve gradual transitions around the boundaries when evaluating postures in REBA and RULA. In this manner, it can function as a gradual allowance setting in lieu of subjective joint allowance assumptions. Figure 4-7 illustrates the effect of the joint allowance settings on the balanced leg, trunk lateral bending, and the corresponding grand scores for Subject 2 as an example. The fluctuation in the leg risk ratings and in the grand-level risk ratings is attributable to the leg performance when no allowance is being applied, since, under this arrangement, the risk rating changes immediately when the legs are not balanced. The risk ratings for trunk lateral bending are between 0 and 1 when fuzzy logic is applied to the joint allowance settings. With respect to the grand scores, they are under-estimated when the joint allowance assumptions are not rigorous compared to the results when no joint allowance is applied. In other words, the gradual allowance settings assist in providing reasonable results at both the joint-level and the grand-level. Table 4-2 shows the average error and RSME for all three subjects. Considering the three subjects on average, the gradual allowance settings resulting from fuzzy logic integration provide 7.02% and 11.67% of reduced average errors and 7.41% and 6.22% of decreased RMSE in the grand risk ratings in REBA and RULA, respectively. As such, the fuzzy allowance is selected for use in the proposed 3D fuzzy method in order to improve the accuracy of the ergonomic risk ratings.

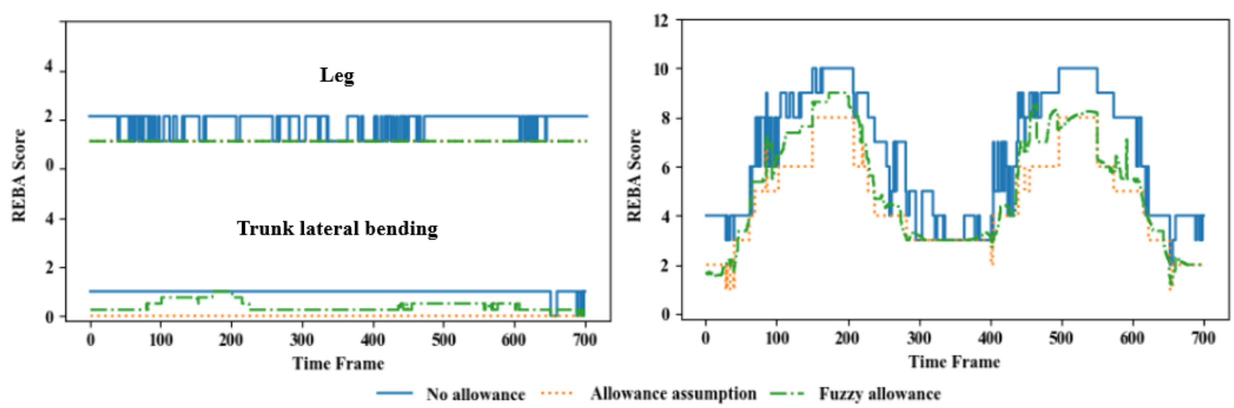

Figure 4-7. Risk ratings of leg and trunk lateral bending and the corresponding grand scores in REBA: Subject 2 as an example

Table 4-2. $\overline{Error}$ and RMSE comparison of grand ratings for all three subjects

		Subjects and methods								
		Subject 1			Subject 2			Subject 3		
Method	Factors	N	A	F-A	N	A	F-A	N	A	F-A
REBA	$\overline{Error}$	–	1.73	1.59	–	2.04	1.94	–	1.96	1.80
	RMSE	–	1.94	1.78	–	2.29	2.18	–	2.29	2.07
RULA	$\overline{Error}$	–	0.20	0.20	–	0.35	0.30	–	0.15	0.12
	RMSE	–	0.45	0.45	–	0.59	0.55	–	0.39	0.34

Note: N = no allowance; A = Allowance assumption; F-A = Fuzzy allowance.

4.2.2.2 Four-level Frame-by-frame Results

The risk ratings in REBA for trunk movement at the four different levels of assessment for Subject 2 are plotted in Figure 4-8 as an example. The risk ratings are integers appearing as stepped lines across the time series of continuous motion, while the risk ratings from the proposed 3D fuzzy methodology are decimals appearing as smooth curves across the times series due to the integration of fuzzy logic. In both the 3D and 3D fuzzy methods, the joint-level risk ratings of trunk lateral bending from the 3D model are not fully aligned with those from the experiment. This is due to the lack of reference in the transverse view and frontal view when building the 3D model. Furthermore, the horizontal joint angles are not as accurate as the vertical joint angles. Meanwhile, the risk ratings generated by the 3D and 3D fuzzy methods are found to be well aligned with one another with respect to joint-level trunk flexion/extension, body-segment-level trunk movement, integrated-body-segment-level trunk movement, and grand-level trunk movement.

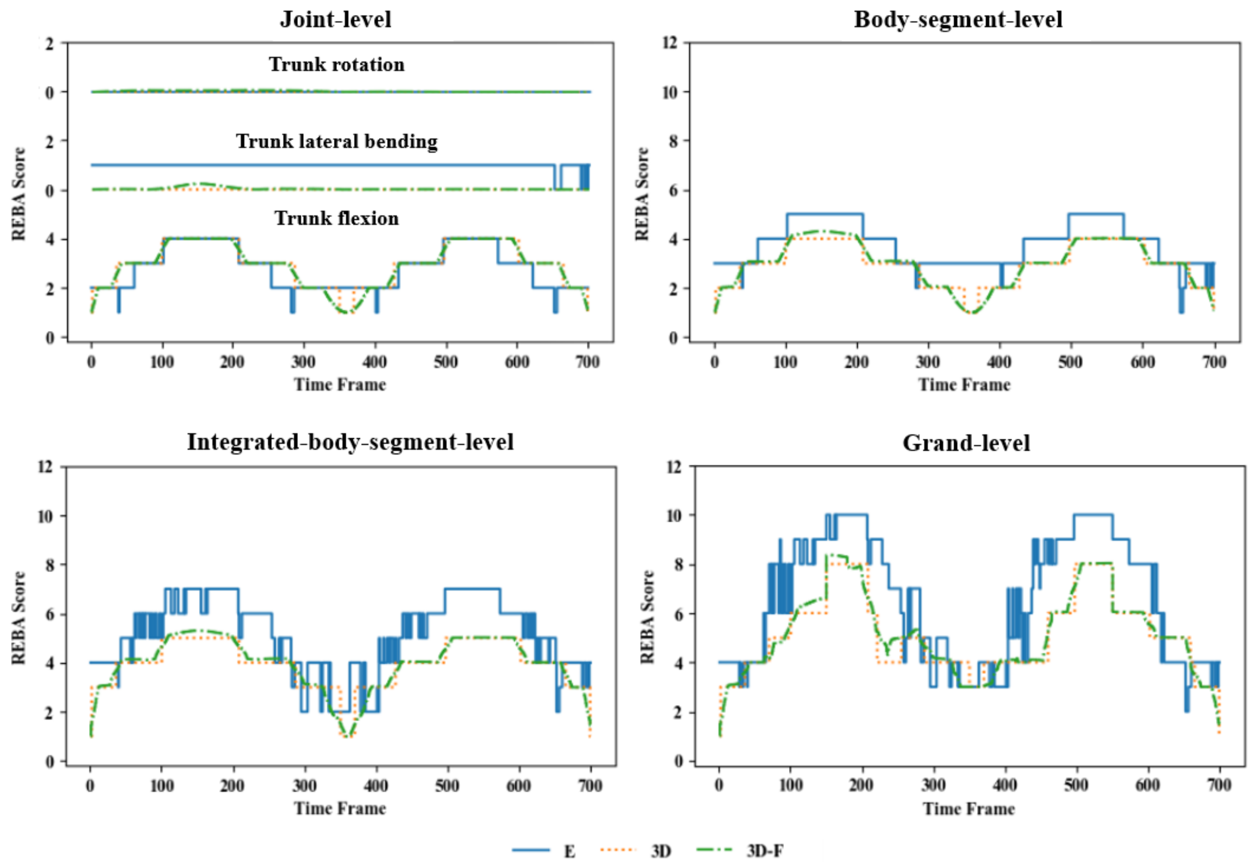

Figure 4-8. Four-level comparison of trunk risk rating in REBA: Subject 2 as an example

The grand scores are generated in consideration of force/load, coupling, and activity scores for REBA and in consideration of muscle use and force/load scores for RULA. The minimum coupling rating, activity rating, muscle use rating, and a load/force rating of 1 are applied in this study for both REBA and RULA. Figure 4-9 depicts the grand rating scores and risk levels of REBA and RULA for Subject 2 as an example. As can be seen in Figure 4-8 and Figure 4-9, the 3D fuzzy ergonomic analysis generally follows the same trend for both REBA and RULA. The three-step validation results indicate that the proposed 3D fuzzy approach is capable of improving the accuracy and reliability of the post-3D ergonomic analysis proposed by Li et al. (2019b). Considering the results of all subjects on average, the proposed 3D fuzzy ergonomic analysis provides improved accuracy of the estimation in REBA, with a 4.07% increase in $\overline{Error}$ and a 2.49% decrease in RSME on average, as well as of the estimation in RULA, with average decreases of 1.99% and 6.43% in $\overline{Error}$ and RSME, respectively.

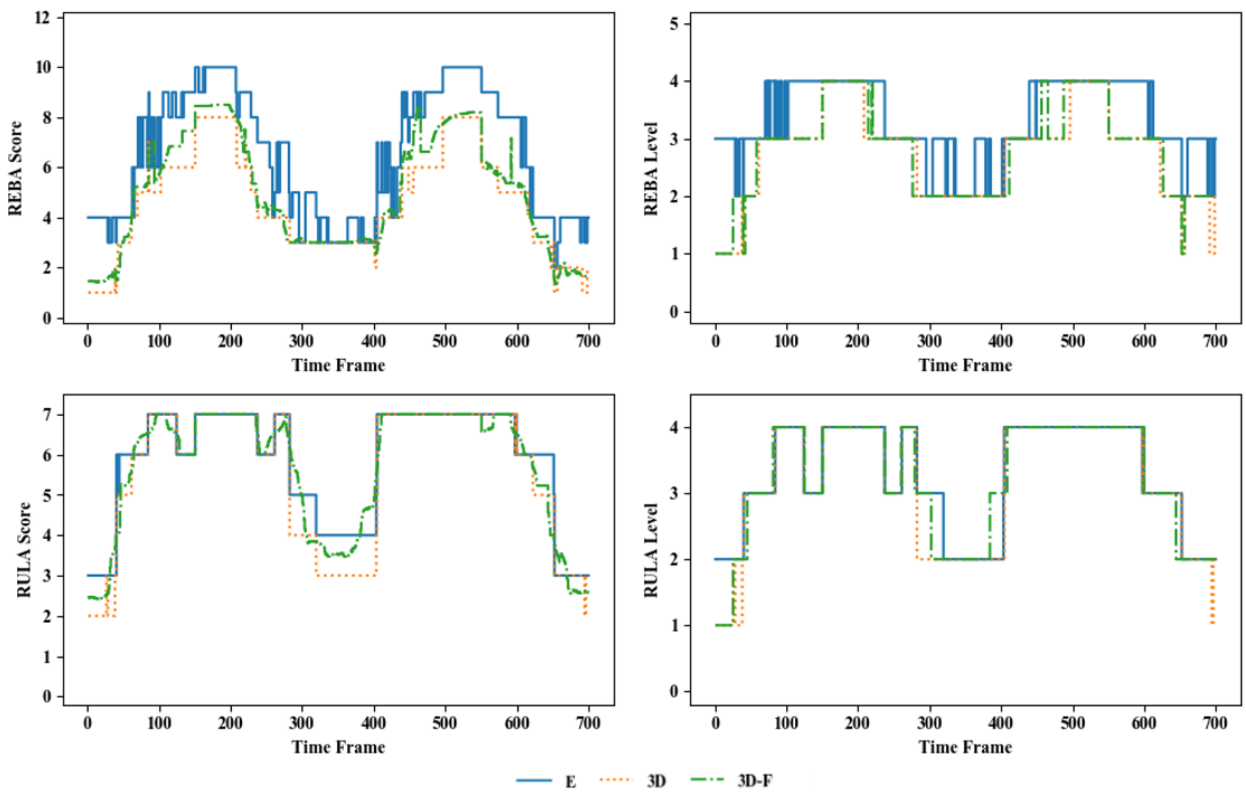

Figure 4-9. Grand-level comparison of risk scores and risk levels for the entire motion in REBA and RULA: Subject 2 as an example

4.2.2.3 Correlation Analysis

With respect to the grand-level risk rating comparison between the 3D method and the proposed 3D fuzzy method for all three subjects, average *PCCs* of 0.96 and 0.84 are obtained for REBA and RULA, respectively. This indicates a strong correlation between REBA/RULA and the proposed fuzzy-integrated REBA/RULA approach. Considering the experiment with REBA/RULA as the baseline performance, average *PCCs* of 0.81 and 0.84 for REBA and 0.56 and 0.67 for RULA are obtained in characterizing the relationships between experiment and 3D method and between experiment and 3D fuzzy method, respectively. The results indicate an improved correlation between REBA/RULA and the proposed fuzzy-integrated REBA/RULA according to the rule of thumb for interpreting the size of a correlation coefficient (Hinkle et al. 2003). Considering the results of all subjects on average, the 3D model data with the fuzzy-integrated REBA/RULA in the proposed system is found to represent a 3.29% average improvement in *PCC* for REBA and 18.93% for RULA compared with the 3D model data with REBA/RULA only. The results indicate that the proposed methodology is capable of providing gradual transitions between risk scores, and that the accuracy of the risk estimations is thereby improved. Table 4-3 summarizes the *PCCs* of the grand-level ratings for all three subjects.

Table 4-3. Correlation coefficient comparison of grand-level ratings for all three subjects

	Subjects and methods								
		Subject 1			Subject 2			Subject 3	
Method	3D vs. 3D-F	E vs. 3D	E vs. 3D-F	3D vs. 3D-F	E vs. 3D	E vs. 3D-F	3D vs. 3D-F	E vs. 3D	E vs. 3D-F
REBA	0.94	0.77	0.80	0.97	0.81	0.85	0.97	0.85	0.86
RULA	0.91	0.67	0.71	0.81	0.52	0.64	0.81	0.50	0.66

Note: E = experiment; 3D = 3D method; 3D-F = proposed 3D fuzzy method.

4.3 Discussion

The purpose of the proposed methodology is to accurately and efficiently quantify and compare the ergonomic risk ratings of workers in existing and proposed workplaces prior to implementation (i.e., before any critical or irreversible ergonomic hazards due to poor work design have occurred). The proposed methodology encompasses the following procedures: *(i)* it extracts and transforms motion-related features of the entire working process from 3D models into an interpretable dataset, thereby enabling the implementation of posture-based ergonomic risk assessment methods; *(ii)* it implements a fuzzy-based ergonomic assessment method to numerically evaluate ergonomic performance for rapid workplace design and modification, thereby improving the accuracy of the ergonomic risk assessment by incorporating more accurate information concerning body joint angles; *(iii)* it employs statistical analysis to quantitatively compute the ergonomic performance that can be expected to result from a proposed work modification, thereby reducing considerably the effort and cost incurred in workplace reconstruction (since a series of workplace designs can be evaluated and compared easily within the 3D environment); and *(iv)* it contemplates future applications that could comprehensively improve occupational health and production planning through the implementation of proactive ergonomic-centric workplace design.

It is also worth noting that the inputs and outputs, criteria, and principal processes in the proposed methodology are interpreted both mathematically and graphically. The present study expands upon a prior contribution by authors of the present work (Li et al. 2018; 2019b) through the implementation of a specialized rule-based fuzzy inference algorithm, accounting for minor movements of joints during task performance and thereby capturing the gradual transitions characteristic of continuous movement and achieving more realistic and accurate estimation. The integration in this methodology of the fuzzy logic algorithm addresses to some extent the limitations of REBA and RULA through the transitioning between risk ratings and the joint allowance settings. Moreover, the body movement evaluation process is automated for the entire continuous motions. The movement data from a repetitive lifting experiment in a laboratory environment imitating a real material lifting task in construction demonstrates the applicability and feasibility of the methodology.

The minor movements and human body sway, such as wrist lateral bending, wrist twisting, trunk lateral bending, and imbalanced leg posture, that occur naturally and are identified and quantified through physical experimentation, are not clearly accounted for in the key ratings in either REBA or RULA. Thus, joint allowance is investigated in order to validate judgment pertaining to posture in risk rating adjustments related to balance of the legs, raising of the shoulder, and lateral bending and rotation of the neck, trunk, and wrist. Other joint allowances are not addressed in the experiment, but will be further investigated in future research.

Considering the above ergonomic risk rating results for the three subjects, it can be concluded that the proposed 3D fuzzy method provides more accurate estimations of the grand ratings in REBA and a slight overestimation in RULA compared to the 3D method. In particular, implementing the experimental data in REBA and RULA without applying joint allowance settings is found to result in overestimation. The overestimation of the grand ratings in RULA is mainly attributable to the neck flexion and extension ratings. Possible explanations are that *(i)* the neck movements in the experiment have been underestimated due to only one marker having been placed on Cervical vertebra 7 (C7) during motion capture, and *(ii)* the grand ratings are more sensitive to the risk ratings for neck movements in RULA than they are in REBA, since there are four risk categories for neck position in RULA compared to only two risk categories in REBA.

Both REBA and RULA focus mainly on the risk ratings related to flexion and extension angles in the sagittal plane. The ratings associated with the axial rotation angles and the lateral bending angles in the frontal plane are considered adjustments to the risk ratings of the corresponding body segments. Accordingly, the experiment design described herein focuses on flexion and extension in the sagittal plane. The validity of this methodology can be greatly improved if more experimental configurations can be implemented and compared with the results from the proposed 3D fuzzy ergonomic analysis.

In the proposed system, both the risk scores and the corresponding risk levels based on REBA and RULA are automatically obtained for an entire continuous motion. There are five risk levels and four risk levels defined in REBA and RULA, respectively. The risk scores improved by the proposed method are considered to represent significant changes on the final ergonomic risk level judgments. Specifically, postures with a score of 11 in REBA or 7 in RULA are extremely risky postures (i.e., within the highest risk level) and therefore require immediate attention. Moreover, human perception errors and instrument limitations during experimentation may lead to high-risk postures going undetected, and this is a critical issue in ergonomic risk assessment that can be eliminated by the proposed method.

The research described herein is of practical value to the construction enterprises in that it provides an approach for assessing modified work to ensure improved performance and proactive mitigation of the risk of work-related injuries and accidents through: *(i)* providing holistic, efficient, rapid, and reliable ergonomic risk assessment without interrupting production; *(ii)* providing an operational-level analysis to identify opportunities for motion improvement prior to implementation of a proposed change to the existing workplace design; *(iii)* saving time, effort, and cost by avoiding the avoidable changes that result from inaccurate evaluation due to human perception errors; *(iv)* proactively reducing the potential injuries and claims associated with ergonomic risks; and *(v)* broadly improving productivity and quality while reducing workers' compensation costs through robust and accurate ergonomic analysis. The proposed system provides a more quantitative understanding of ergonomic performance in the context of ergonomic-centric workplace design and modification. Many practical challenges can be resolved through the use of the proposed system, which facilitates the enhancement of safety performance, production performance, and market competitiveness.

4.4 Summary

In this chapter, a specialized fuzzy expert system is designed and integrated with ergonomic posture risk assessment methods for improving the accuracy of assessment results. The proposed method can (1) generate gradual transitional boundaries to replace the discrete boundaries and integer-based risk scores in REBA and RULA; (2) eliminate the variance in ergonomic risk ratings caused human perception errors and instrument limitations when estimating body postures; (3) address the abrupt changes in risk ratings by better capturing the gradual transitions characteristic of continuous human motion; (4) reduce the fluctuations in risk ratings caused by the inevitable minor movements of body joints during human motion; and (5) improve the accuracy of risk scores for each body segment, and thereby increase the reliability of the resulting, as well as the depth of analysis they represent. As mentioned above, this system provides a more quantitative understanding of workers' ergonomic performance, and as such it can enhance construction enterprises' safety performance and, in turn, improve their productivity and market competitiveness.

CHAPTER 5: 3D STANDARD MOTION TIME-BASED ERGONOMIC RISK ANALYSIS FOR WORKPLACE DESIGN IN MODULAR CONSTRUCTION[2]

As construction workers are frequently exposed to ergonomic risks, accurate ergonomic risk analysis for workplace design is needed to mitigate risks and consequently improve productivity. Currently, ergonomic posture assessments of continuous motions in the 3D human model depend on the postures and the keyframe of the postures subjectively developed by designers. However, human perception errors and subjectivity on the decision of motion time can lead to variances in ergonomic risk ratings, which is not reliable to support workplace design with a constant standard of motion time. Thus, this chapter describes the development of 3D standard motion time-based ergonomic assessment by integrating the predetermined motion time system (PMTS). The proposed method seeks to improve the accuracy of ergonomic posture assessment of continuous motions by compiling the ergonomic risk ratings in terms of the standard motion time feature. PMTS is employed to determine the categorization rules in the rule-based motion recognition algorithm and the standard motion time durations of the motions identified in the proposed method. The effectiveness of the proposed method is validated in a case study of two workplace designs for manual assembly tasks in modular construction.

---

[2] A version of this chapter is under review for publication in *Automation in Construction*, as follows: Wang, J., Li, X., Han, S., and Al-Hussein, M. 3D standard motion time-based ergonomic risk analysis for workplace design in modular construction. *Automation in Construction*. (Under review).

5.1 Methodology for Standard Motion Time-based Assessment

In this chapter, a 3D standard motion time-based ergonomic risk analysis method is proposed for construction workers (herein referred to as “3D-MEC”) to provide automatic and detailed ergonomic posture analysis of dynamic and continuous motions for workplace design and modification in industrialized construction. An overview of the proposed methodology is presented in Figure 5-1. The inputs are the 3D model developed based on the standard operating procedure, measurements of workers (i.e., anthropometry) and the workstation (i.e., dimensions), and the recorded images and videos of the body motions (if any), shown as Part (a) of Figure 5-1. The outputs include the standard cycle time of the operational task, standard motion time-based ergonomic risk ratings of continuous motions, and modified work facilitation and workstation design evaluation.

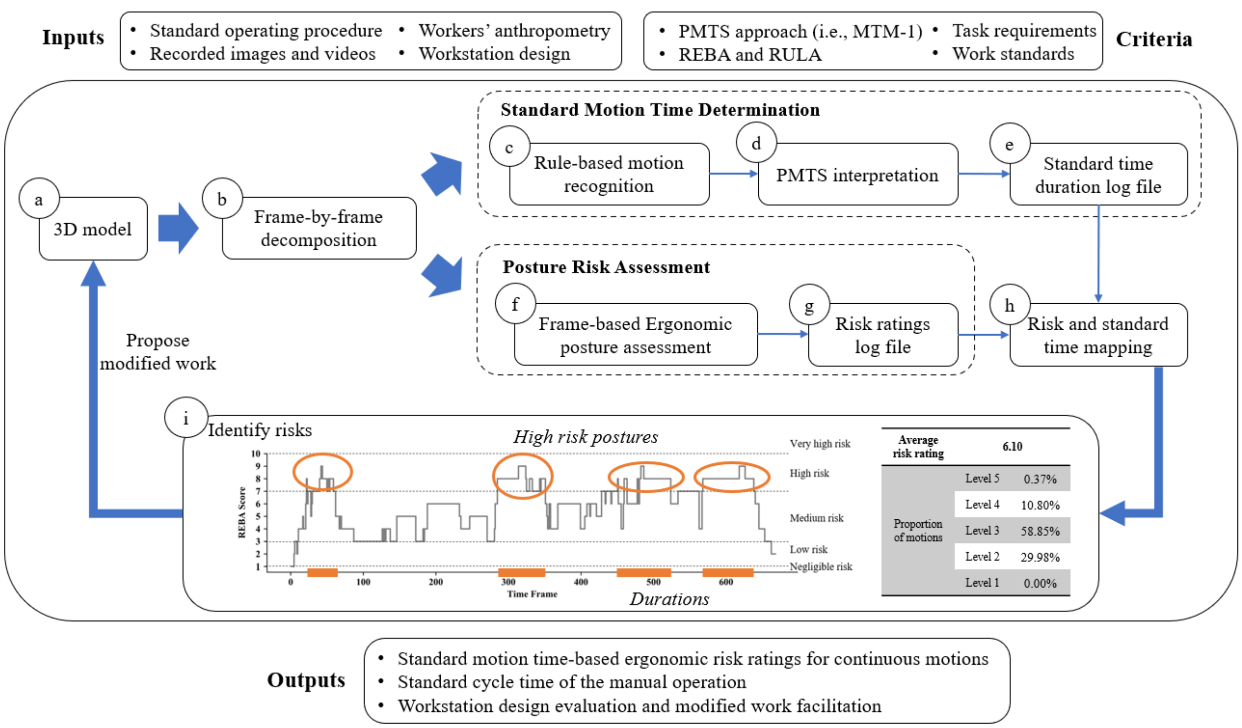

Figure 5-1. Overview of proposed methodology

The purpose of the proposed methodology is to: (1) obtain standard motion time data—in a Microsoft Excel format in this case, as shown in Part (e) of Figure 5-1—that records the standard cycle time of the manual operation in detail, and (2) generate standard motion time-based ergonomic risk ratings for continuous motions (as shown in Part (i) of Figure 5-1) to support the design of work modifications. For this purpose, several operations related to determining standard motion time and assessing posture risk—i.e., Part (b) to Part (h) of Figure 5-1—need to be conducted. The 3D model must be decomposed frame by frame, as shown in Part (b) of Figure 5-1, in order to extract the 3D coordinates of body joints and objects that appear at each frame of the 3D model. In the present research, MTM-1 is used as the criterion in the proposed rule-based motion recognition and PMTS interpretation algorithms, while REBA and RULA are applied as the main criteria in the frame-based ergonomic risk assessment process.

MTM-1 is a detailed PMTS method containing most of the basic motions seen in other PMTSs (Genaidy et al. 1989). The main input requirements of MTM-1 are motion types, influencing factors, and working conditions. For example, the standard motion time duration of the arm and hand motion "move" is determined by the moved distance of the hand or fingers, the weight of the object moved, and the working conditions (i.e., moving object to the other hand, to the approximate location, and to an exact location). The standard cycle times of basic motions, including arm and hand motions (e.g., reach, move, grasp, release, and turn, etc.), leg and foot motions, eye motions, and body motions (e.g., walk, bend, and sidesteps, etc.), are provided as the outputs of MTM-1, as summarized in Table 5-1 (Maynard et al. 1948; Freivalds and Niebel 2013; Groover 2013).

Table 5-1. Summary of 25 basic motions represented in MTM-1

MTM motions (Symbol)		Description	Factor	Standard time (TMU)	Animation time (Frame)
Arm and hand motions	Reach (R)	Movement of the hand or fingers	Motion length Motion case	1.6 – 26.7	2 – 29
	Move (M)	Relocating an object	Motion length Motion case Object weight	1.7 – 62.05	2 – 67
	Grasp (G)	Grasping an object	Motion case	0 – 12.9	0 – 14
	Position (P)	Align, orient, or engage an object to another	Class of fit Symmetry case Ease of handling	5.6 – 53.4	6 – 58
	Release (RL)	Surrendering control of an object	Motion case	0 – 2.0	0 – 2
	Turn (T)	Rotation of the hand and wrist	Degree of turn Object weight	2.8 – 28.2	3 – 30
	Apply pressure (AP)	Application of force	Motion case	10.6 / 16.2	11 / 17
	Disengage (D)	Separating two objects	Class of fit Ease of handling	4.0 – 34.7	4 – 37
Leg-foot motions	Leg motion (LM–)	Movement of leg	Motion length	7.1 + 1.2 × (length – 6 in) (TMU)	
	Foot motion (FM)	Movement of foot	Motion case	8.5 / 19.1	9 / 21
Eye motions	Eye focus (EF)	Visual attention on an object	–	7.3	8

	Eye travel (ET)	Eye movement with line-of-sight change	Motion length	15.2 × motion length / perpendicular distance (TMU)	
Body motions	Sit (SIT)	Act of sitting	–	34.7	37
	Stand (STD)	Act of standing	–	43.4	47
	Bend (B)	Act of bending	–	29.0	31
	Arise from bend (AB)	Act of arising from bent position	–	31.9	34
	Stoop (S)	Act of stooping	–	29.0	31
	Arise from stoop (AS)	Act of arising from stooped position	–	31.9	34
	Kneel on one knee (KOK)	Act of kneeling on one knee	–	29.0	31
	Arise from kneel on one knee (AKOK)	Act of arising from kneeling position on one knee	–	31.9	34
	Kneel on both knees (KBK)	Act of kneeling on both knees	–	69.4	75
	Arise from kneel on both knees (AKBK)	Act of arising from kneeling position on both knees	–	76.7	83
	Walk (W-FT/ W-P)	Act of walking	Number of feet/ Number of paces	5.3 × number of feet 15.0 × number of paces (TMU)	
	Sidestep (SS)	Act of sidestepping	Motion case	17.0+0.6× (length – 12 in) / 34.1+1.1× (length – 12 in) (TMU)	
	Turn body (TB)	Act of body turning 45° to 90°	Motion case	18.6 – 37.2	20 – 40

In MTM-1, all the basic motion times are tabulated in the time measurement unit (TMU), which is a base unit of measurement for precise and convenient calculations defined as 0.036 seconds (Maynard et al. 1948). It should be noted that is mainly the arm and hand motions that are of interest in this work, since most manual operational tasks in modular construction involve principally the arms and hands. Thus, in the present research, the rule-based motion recognition algorithm and PMTS interpretation algorithm are developed with a focus on arm and hand motions. (Full body motions will be further investigated in future research in order to mimic real-world construction operations in a more detailed and comprehensive manner.)

5.1.1 Standard Motion Time Determination

The purpose of the standard motion time determination is to automatically identify the basic motions and assign the standard motion time durations of continuous motions. It is composed of the rule-based motion recognition algorithm, PMTS interpretation, and standard motion duration logging process, as shown in Part (c) to Part (e) of Figure 5-1. The main process underlying the determination of standard motion time, meanwhile, is shown in Figure 5-2. After being processed in the frame-by-frame decomposition of the 3D visualization, the body postures within continuous motions are saved at each frame. Moreover, the dimensions of the biped bones are collected as the length, width, and height of cuboids, while the body joint data are extracted as the 3D coordinates of the pivot point of each bone at each frame. A total of 51 bones are used in the data processing; these include the head, clavicle, neck, spine, pelvis, thighs, calves, feet, toes, upper arms, forearms, hands, and finger bones. It should be noted that 5 fingers for each side of the body are set up in the 3D human model for precise animations and standard motion time determination. However, only one finger is required for the ergonomic risk assessment, since fingers are not considered in REBA and RULA. The dimensions and 3D coordinates of objects (i.e., work-related elements and tools) are exported from the 3D model at each frame. All these time-sequential data derived from the 3D model are stored for data processing in the subsequent phases of the rule-based motion recognition process in the formats expressed in Equation 5-1 (representing the 3D human model) and Equation 5-2 (representing the work-related elements and tools).

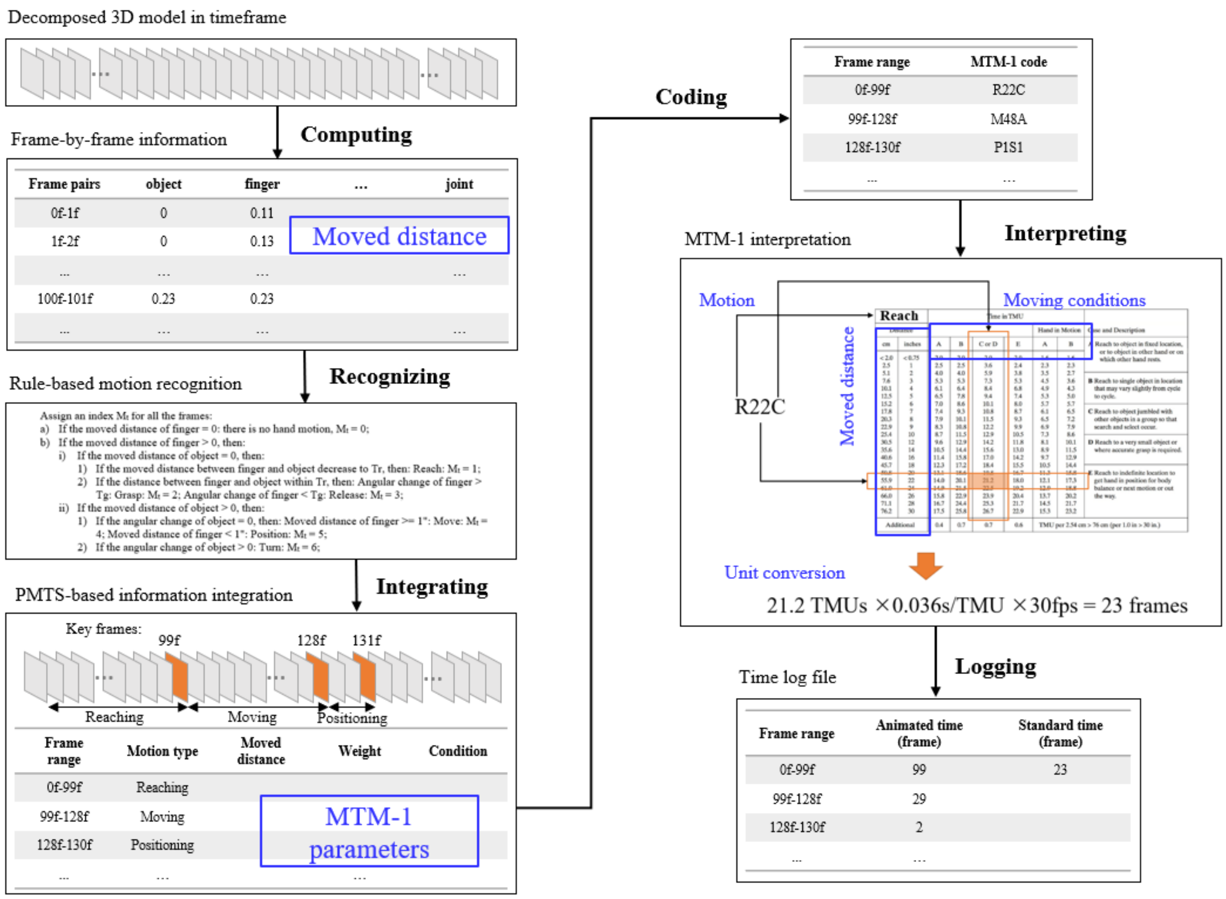

Figure 5-2. Processes for determining standard motion time

$$B_t = \begin{bmatrix} b_{1x} & b_{1y} & b_{1z} \\ b_{2x} & b_{2y} & b_{2z} \\ \vdots & \vdots & \vdots \\ b_{jx} & b_{jy} & b_{jz} \end{bmatrix}_t \qquad \text{Equation 5-1}$$

$$O_t = \begin{bmatrix} o_{1x} & o_{1y} & o_{1z} \\ o_{2x} & o_{2y} & o_{2z} \\ \vdots & \vdots & \vdots \\ o_{ix} & o_{iy} & o_{iz} \end{bmatrix}_t \qquad \text{Equation 5-2}$$

where, B_t and O_t are 3D coordinates of the biped bones and objects, respectively, at time frame t; b_{jx}, b_{jy}, and b_{jz} are the j^{th} bone's position at the x-, y-, and z-axes, respectively; and o_{ix}, o_{iy}, and o_{iz} are the i^{th} object's position at the x-, y-, and z-axes, respectively.

The rule-based motion recognition algorithm detects all the basic arm and hand motions in the continuous motion. Following the frame-by-frame decomposition of the 3D visualization, the distance moved by each body joint and object is computed between two adjacent frames based on their 3D coordinates and the Euclidean distance using Equation 5-3. As the smallest parts (in the case of arm and hand motions), fingers are used for rule-based motion recognition. The recognition rules are developed based on the positions and the MTM-1, and they include: (1) motion "reach" when the finger is approaching the object while the object is not moving; (2) motion "move" when the finger and object are close to one another and are moving at the same speed; (3) motion "grasp" when the fingers are closing to hold the object while the hand remains in the same position; (4) motion "release" when the fingers are opening to release the object while the hand remains in the same position; (5) motion "position" when the motion "move" is within 1 inch; and (6) motion "turn" when the object is turning while the positions of the hand and object remain the same.

$$d(p, q) = \sqrt{\sum_{t=1}^{n} (q_t - p_t)^2} \qquad \text{Equation 5-3}$$

where p and q are two points in Euclidean n-space, p_i and q_i are Euclidean vectors, starting from the origin of the space, and n represents n-space, which is 3D space in this case.

The pseudo-code for the proposed rule-based motion recognition algorithm is presented in Figure 5-3. The algorithm starts by defining tolerances for motions and loading all the 3D coordinates of the biped bones and objects at each frame into the 3D model. At this juncture, it should be noted that the variables of tolerance are predefined in such a way as to overlook minor movement in the 3D model when the animation is not developed in detail. For example, there may be some space between the object and hand when the object is held by the hand in the 3D model. The tolerance of reach (*Tr*) is used for determining whether the finger and the object are close enough when detecting the motion "reach". In other words, as long as the distance between finger and object is less than *Tr*, the motion "reach" is satisfied. In step 2, the distance moved by each biped bone and object between the t^{th} frame and the $t+1^{th}$ frame is calculated.

After step 2, values of the index M_t are assigned for all frames based on the distance moved by both the finger and the object as follows: $M_t = 0$ for the case of no arm or hand motion, $M_t = 1$ for "reach" motion, $M_t = 2$ for "grasp" motion, $M_t = 3$ for "release" motion, $M_t = 4$ for "move" motion, $M_t = 5$ for "position" motion, and $M_t = 6$ for "turn" motion. In step 3, the distance moved by the finger is first checked. If the distance moved by the finger is 0, then there is no arm or hand motion (i.e., $M_t = 0$). When the distance moved by the finger is greater than 0, the distance moved by the object is then checked. On the other hand, when the distance moved by the object is 0, the obtaining motions (i.e., motion "reach", "grasp", and "release") are identified with different rules. If the distance between finger and object decreases to within the threshold defined by *Tr*, the motion "reach" is identified for all these frames and a value of 1 is assigned to M_t. Moreover, if the distance between finger and object is within *Tr*, the angular change of the finger is then checked to distinguish between the motion "grasp" and the motion "release".

The angular change ($\Delta\theta$) between two frames, it should be noted, is calculated based on the dot product theory (Arfken and Weber 2000), as in Equation 5-4 and Equation 5-5. If the $\Delta\theta$ of finger is greater than 0, motion "grasp" is identified; otherwise, if $\Delta\theta$ of finger is less than 0, motion "release" is identified. For example, the given motion is categorized as grasping an object when $\Delta\theta$ is positive (i.e., closing fingers), while it is releasing an object if $\Delta\theta$ is negative (i.e., opening fingers). When the distance moved by the finger and that by the object are both greater than 0, the angular change of the object is checked to distinguish the rotate action (i.e., "turn" motion) and the locate actions (i.e., "move" and "position" motions). When the $\Delta\theta$ of the object is 0, the motion "move" is identified, provided that the distance moved by the finger and by the object are about the same and the total distance within these frames is greater than or equal to 1 inch; otherwise, the motion "position" is detected. The motion "turn", meanwhile, is identified when $\Delta\theta$ of the object is greater than 0. For example, the given motion is recognized as the motion "move" when both finger and object are moved from time frame t to $t + n$ and the total distance is greater than 1 inch. The M_t index having been assigned to all time frames with respect to one given object in Step 3, this procedure is then repeated for all objects with respect to a given side of the body in Step 4, and then Step 5 is to repeat Steps 3 and 4 for the other side of the body. Then, based on the degree of handling difficulty denoted in the simultaneous motion table in MTM-1, the simultaneous motion check between the left and right hands is performed in step 6 to generate the identified motions for the entire body in the time series. Based on the simultaneous motion check in MTM-1, only a longer time duration is considered when the motions are easy to perform simultaneously, while the time of arm and hand motion on the left side of the body and that on the right side of the body are both allowed when the motions are difficult to perform simultaneously (Maynard et al. 1948, Freivalds and Niebel 2013).

1. Start:
   a) Predefined variables: tolerance of reach (*Tr*)
   b) Read all the 3D coordinates of the biped bones and objects from the 3D model at each frame.
2. Calculate the moved distance of each biped bone and object between t^{th} frame and $t+1^{th}$ frame.
3. Assign an index M_t for all time frames with respect to one given object:
   a) If the moved distance of finger = 0: there is no hand motion, $M_t = 0$;
   b) If the moved distance of finger > 0, then:
      i) If the moved distance of object = 0, then:
         1) If the distance between finger and object decrease to *Tr*, then: Reach: $M_t = 1$;
         2) If the distance between finger and object is within *Tr*, then: Angular change of finger > 0: Grasp: $M_t = 2$; Angular change of finger < 0: Release: $M_t = 3$;
      ii) If the moved distance of object > 0, then:
         1) If the angular change of object = 0, then: Moved distance of finger >= 1": Move: $M_t = 4$; Moved distance of finger < 1": Position: $M_t = 5$;
         2) If the angular change of object > 0: Turn: $M_t = 6$;
4. Repeat step 3 for all objects with respect to a given side of the body;
5. Repeat step 3 and 4 for the other side of the body;
6. Simultaneous motion check between the left and right side of the body;
7. Generate recognized motions in time series;
8. End

Figure 5-3. Pseudo-code for rule-based motion recognition algorithm

$$\theta = \cos^{-1} A \cdot B/|A||B| \qquad \text{Equation 5-4}$$

$$\Delta\theta = \theta_t - \theta_{t+1} \qquad \text{Equation 5-5}$$

where A and B are vectors representing the body segments, and θ_t and θ_{t+1} are angles between vector A and B at frame t and $t+1$, respectively.

After all motions have been identified, these motions and their parameters are integrated to generate the PMTS-based information integration table (see Figure 5-2), which includes the frame range of each identified motion, motion type, and MTM-1 parameters such as distance moved, weight of object, and working conditions. The MTM-1 codes are then automatically generated (based on the MTM-1 parameters for interpreting the MTM-1 motion timetables) in order to extract the standard motion times for the identified motion series.

As shown in Figure 5-4, The MTM-1 code is constructed in 3 parts: (1) the MTM motion symbol (e.g., R for reach, M for move, G for grasp, etc.) for motion type, (2) the distance moved, and (3) the motion case type. For example, reaching out approximately 22 inches to retrieve screws from the screw box on the shelf can be coded as R22C, where C is included in the code because the screws may be jumbled together in the screw box. In the PMTS interpretation process, the MTM-1 code is used to extract the standard motion time from the MTM-1 system. As shown in the example in Figure 5-4, the given motion coded as R22C is assigned 21.2 TMUs using the MTM-1 table for motion "reach" with the parameters of 22 inches distance moved and motion case C. The standard motion time in TMUs is converted to 23 frames (i.e., about 0.8 s in the 30-fps model). The standard motion time durations are then logged in the time log file and compared with the animated time.

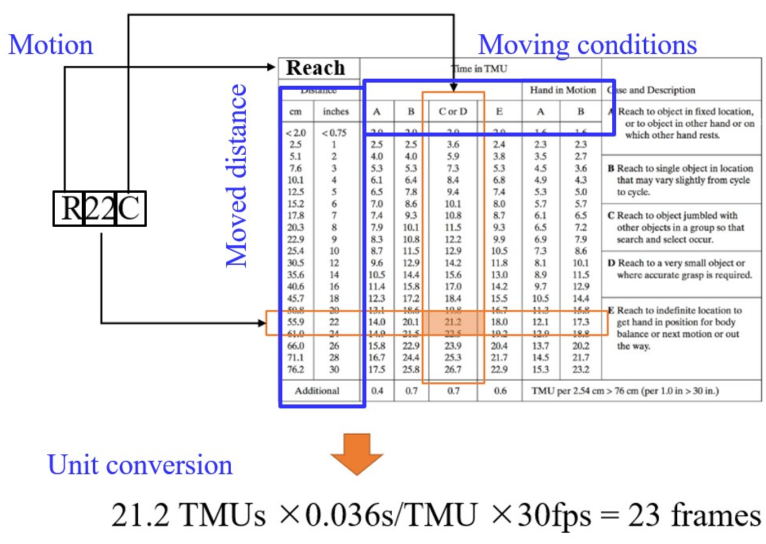

Figure 5-4. Example of MTM-1 Codes, interpretation, and unit conversion

5.1.2 Posture Risk Assessment

Posture risk assessment is another of the main processes; it seeks to identify the ergonomic risk of each body posture at each frame in the continuous motion. The frame-based ergonomic posture assessment and risk ratings are logged as part of this process. It should be noted that the ergonomic risk ratings at each frame are still assessed based on the static posture at the discrete timepoint. As shown in Figure 5-5, the degree of ergonomic risk depends on the posture, force load, and activity conditions. The postures are defined as joint angles of body segments, these being determined based on the positions of body segments in terms of the joint angle between the body segment and the extension of its connected body segment. The force load is considered from the perspectives of both magnitude and type of action (i.e., intermittent, static, repeated, and rapid). As with the risk rating adjustment, activity conditions are assessed based on the degree of motion repetitiveness (i.e., frequency per minute), corresponding to the activity score in REBA and the muscle use score in RULA. As a time-related factor, the activity score is mainly used to describe the dynamic feature and continuity of continuous motions. The output is presented in terms of the five risk levels in REBA and the four risk levels for RULA, as shown in Figure 5-5.

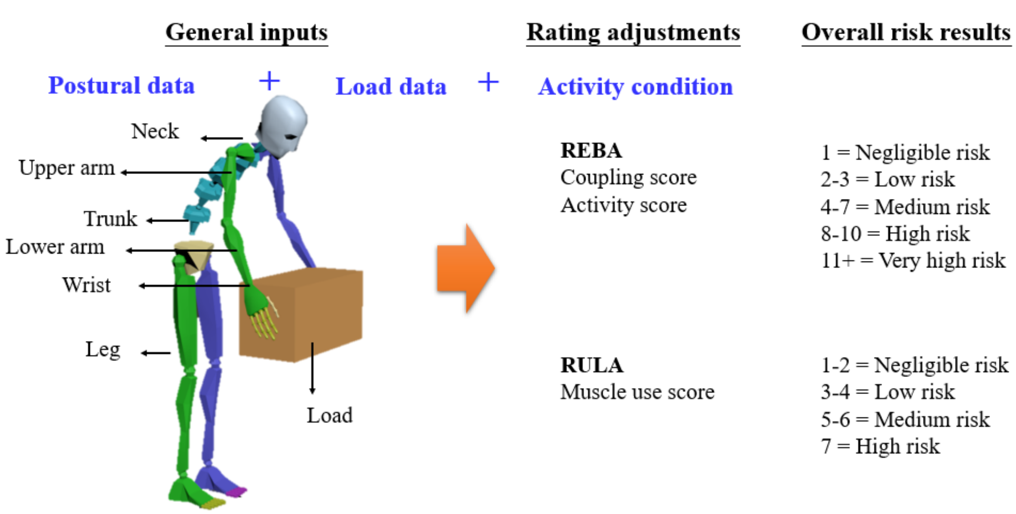

Figure 5-5. Inputs and outputs of REBA and RULA

In the present research, 3D coordinates of body joints are used to compute the required joint angle data in REBA and RULA at each frame. A total of 41 body joint angle data points covering the sagittal plane, frontal plane, transverse plane, and axial rotation are obtained from the 3D model, these being defined in terms of the required angles of each body segment in the biomechanical analysis software, 3D Static Strength Prediction Program (3D SSPP) (University of Michigan 2017). The joint angle conversion of the 41 joint angles computed among different frames in the 3D model must accommodate the REBA/RULA requirements, which is described in detail in a prior study co-authored by the author of the present work (Li et al. 2019b). In the present research, continuous motions are presented as a series of postures in a time sequence for the purpose of ergonomic risk assessment. Each posture obtains risk scores from both REBA and RULA. The output of the posture risk assessment process is the risk ratings log file for all the postures at each time frame in time series; this is subsequently used in the risk and standard motion time mapping process.

5.1.3 Risk and Standard Time Mapping

The ergonomic risk scores and standard motion time durations of the analyzed postures are mapped in order to generate accurate risk ratings for the continuous motions. According to the standard time and animated time range of the identified motion, the standard times of each time frame in the animated frame range are calculated using the linear interpolation method. As shown in Figure 5-6, the identified motion spans from the 1st frame to the 31st frame in the animation, corresponding to 15 frames in the standard motion time determination algorithm. Thus, the standard time range is scaled down from 31 frames to 15 frames using the linear interpolation method. Since the time frames are all integers, the standard frames are rounded up to the nearest integer. With regard to the REBA and RULA scores, the same frames are deduplicated to obtain the risk scores associated with the standard frames. It should be noted that the highest risk score is selected to represent the risk rating of the standard frame during the deduplication process. Figure 5-7 presents the graphic results of the risk and standard time mapping process. As can be seen, the risk ratings in REBA and RULA still follow the same trend after being mapped with the standard motion time.

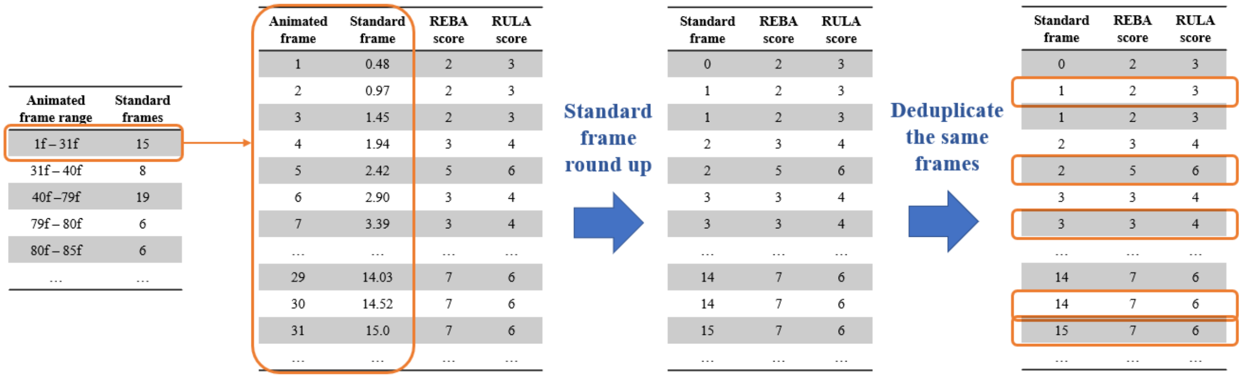

Animated frame range	Standard frames
1f – 31f	15
31f – 40f	8
40f –79f	19
79f – 80f	6
80f – 85f	6
...	...

Animated frame	Standard frame	REBA score	RULA score
1	0.48	2	3
2	0.97	2	3
3	1.45	2	3
4	1.94	3	4
5	2.42	5	6
6	2.90	3	4
7	3.39	3	4
...	...	...	...
29	14.03	7	6
30	14.52	7	6
31	15.0	7	6
...	...	...	...

Standard frame round up

Standard frame	REBA score	RULA score
0	2	3
1	2	3
1	2	3
2	3	4
2	5	6
3	3	4
3	3	4
...	...	...
14	7	6
14	7	6
15	7	6
...	...	...

Deduplicate the same frames

Standard frame	REBA score	RULA score
0	2	3
1	2	3
1	2	3
2	3	4
2	5	6
3	3	4
3	3	4
...	...	...
14	7	6
14	7	6
15	7	6
...	...	...

Figure 5-6. Risk and standard time mapping process

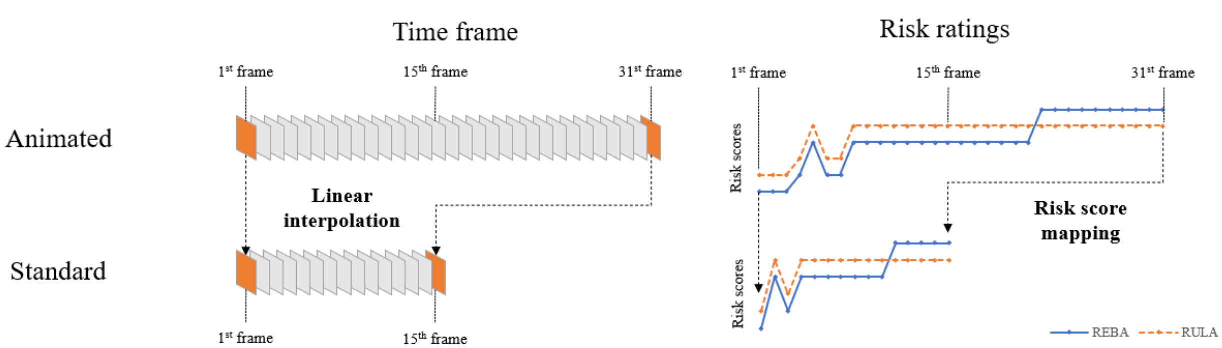

Figure 5-7. Graphic results of risk and standard time mapping

After the mapping process, the average risk ratings of manual operations are generated as the key indicators for workplace design. The common scenarios of standard motion time and average risk ratings in the 3D model are shown in Figure 5-8. If the animated time is longer than the standard motion time, the standard average risk rating is lower. Otherwise (i.e., when the animated time is shorter than the standard motion time of the motion), the standard average risk rating is higher. It should be noted that, with the exception of the average posture risk ratings, the activity condition is also time-related, meaning that standard motion time is required in order to ensure accurate ergonomic risk analysis.

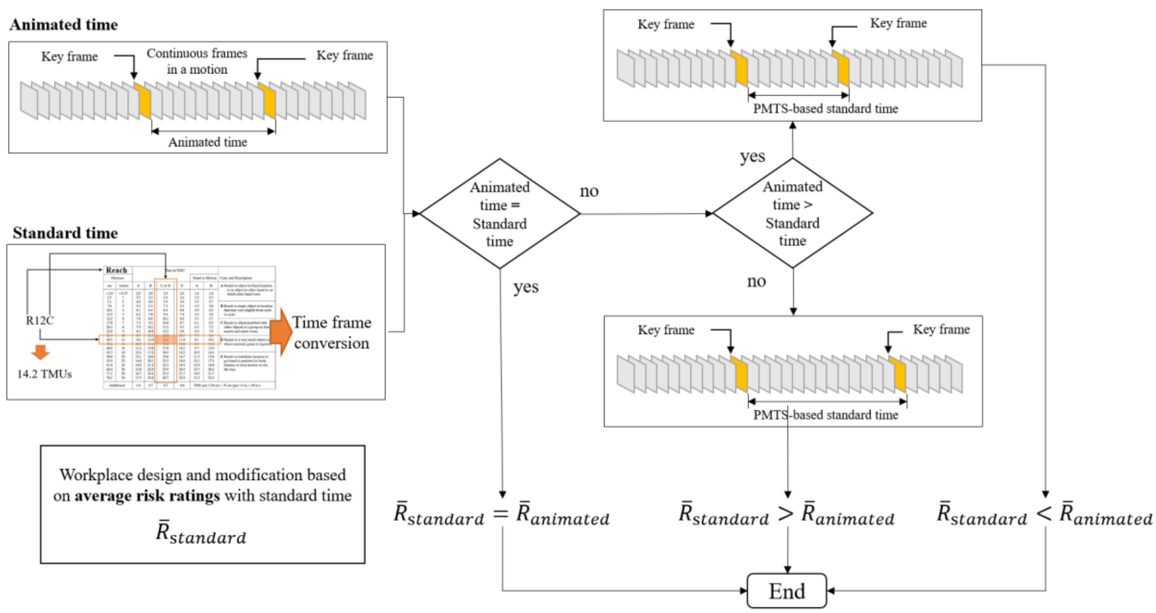

Figure 5-8. Common scenarios of standard motion time and average risk ratings in 3D model

5.2 Case Study

The proposed methodology in the present research is implemented in a case study to evaluate two proposed design alternatives for an existing workstation on a production line of window manufacturing in Edmonton, Canada. In current practice, a female worker works over years at a horizontal table with the toolboxes underneath the table, which makes the worker easily pick the hardware and screws for the hardware installation tasks. According to the self-report from the worker, the pains of the back, neck, and shoulders were noticed. Thus, the company requested an on-site investigation to design a new workstation for mitigating the WMSDs. To avoid the interruption of production and to save the cost of building prototypes, the new workstation designs and the corresponding human motions are created in the 3D model to evaluate the standard motion time-based ergonomic performance and support the final decision making on the workstation design. In this case, the installation of snubbers (i.e., hardware installed on the hinged side of the window frame to prevent bowing) is modelled for the evaluation of design alternatives. The case study focuses on the awkward body posture and standard motion time analysis rather than on heavy loads on the body since the handled materials are small and lightweight. Two aspects of the study are completed in this section: (1) comparison of the standard motion time and animated time for design alternatives; and (2) comparison of the standard motion time-based ergonomic risk rating results for design alternatives to support the design marking on the workstation design.

5.2.1 Workstation Design Alternatives

The workstation is used for hardware installation on window frames, including the installation of hinges, snubber, tie bar, handle, and operator. During the on-site investigation, ergonomic risk assessment resulted in a finding that the maximum risk resulted from the forward bending and twisting of the neck and trunk of the worker to fit the working surface. The identified issues of developing WMSDs include: (1) the worker tends to frequently adopt neck and trunk bending postures and twisted positions to fit the working surface at the inner side of window frames; (2) the worker tends to bend more for the trunk to reach the objects in the toolboxes underneath the table; and (3) the worker stands close to the edge of the table to leaning forward to support the window frame for hardware installation, which may create pressure pointing on the main body. To address the abovementioned identified issues, the modified work recommendations involve: (1) tilting the table to a certain degree to expose the working surface, which reduces the degree of bending and twisting of the body; and (2) fixing window frames on the workstation using fixed clips to reduce the possible pressure pointing on the main body when the worker uses the body to support the window frame. Two new workstation designs are proposed, as presented in Table 5-2.

Case 1 design is to provide a supportive table with a height of 85 cm to assist with the hardware installation task. The panel is tilted to 20° and the toolbox is located on top of the table due to the space limit. Case 2 design is tilted to 60° and the toolbox remains under the table.

Table 5-2. Summary of relevant workstation design specifications

Workstation design	Case 1	Case 2
Shop drawing	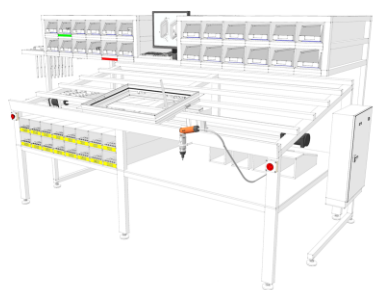	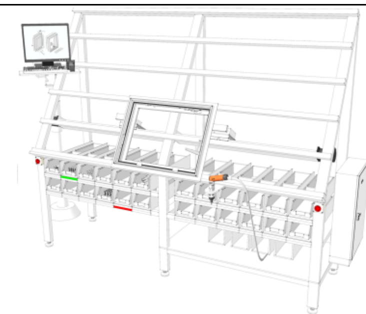
Table slope	20°	60°
Table dimensions	Length (x) = 2,800 mm Height (y) = 850 mm Width (z) = 1,500 mm	Length (x) = 2,800 mm Height (y) = 850 mm Width (z) = 800 mm
Shelf dimensions	Length (x) = 3,000 mm Height (y) = 1,800 mm Width (z) = 1,000 mm	Length (x) = 2,800 mm Height (y) = 1,000 mm Width (z) = 800 mm

According to the design specifications, human motions of completing the task are imitated in the 3D model, including: (1) picking up hardware from the shelves; (2) placing hardware in the target position on the window frame; (3) picking up screws from the box on the shelves; and (4) attaching hardware to the window frame using screws and an impact driver. The above processes are repeated until all types of hardware are installed. As shown in Figure 5-9, the height of the subject is set as 163 cm with the default setting for the size of body segments, according to the worker's height in current practice as well as the 50^{th} percentiles of female height in North America. Although the motions in current practice are used as a reference, the magnitudes of motions are adjusted according to design specifications. The speeds of motions are imitated based on the collected video of motions and the designer's experience and will be adjusted to the standard motion time durations based on the proposed method. As the smallest hardware, the installation of the snubber is modelled for the analysis in this case study.

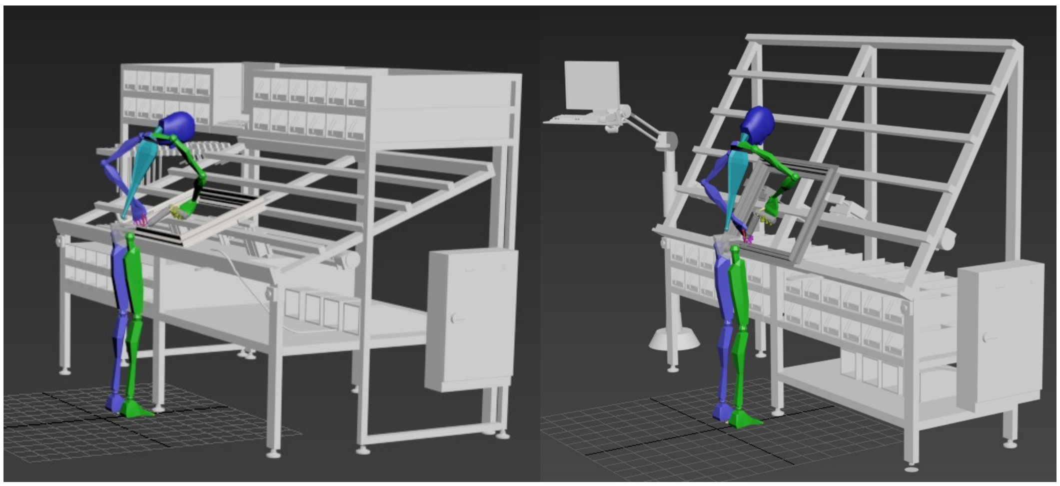

Figure 5-9. 3D human model simulation of Case 1 and Case 2 designs

5.2.2 Comparison of Standard Motion Time and Animated Time for Design Alternatives

After being processed by the standard motion time determination algorithm, all the motions in the continuous movement and their standard motion time durations are generated and saved in a log file. In this case, there are 6 subtasks in the task of snubber installation on a window frame, which is the installation of 2 snubbers and 4 screws. As shown in Figure 5-10, the installation of snubber includes the recognized motions of "reach", "grasp", "move", "position", and "release" using the left hand and "move" motion with the screwdriver using the right hand. The corresponding case types are generated based on working conditions to obtain the standard motion time durations. In this case, about 109 frames are animated for this subtask, which corresponds to 73 frames based on the standard motion time determination algorithm. Also, the standard motion time duration is generated for each recognized motion in the subtask, respectively.

Frames in 3D model	Recognized motions and objects				Case type		Standard motion-time (in frame)		
Frame	Left Motion	Right Motion	Left Object	Right Object	Left Case	Right Case	Left Frames	Right Frames	Final Frames
0f-39f	Reach	Move	-	screwdriver	A	B	23	26	26
39f-40f	Grasp	Move	-	screwdriver	1A	B	2	6	6
40f-99f	Move	Move	snubber001	screwdriver	B	B	29	15	29
99f-100f	Position	Move	-	screwdriver	1SE	B	6	6	6
100f-109f	Release	Move	-	screwdriver	1	B	2	6	6

Figure 5-10. Example of the log file with recognized motions and standard motion time information

In the case study, the task is animated with 575 frames and 554 frames for Case 1 and Case 2, respectively. With the proposed 3D-MEC method, the standard motion time durations are 537 frames and 425 frames for Case 1 and Case 2, respectively. As shown in Table 5-3, approximately 6.6% and 23.3% decreases in the standard motion time durations are identified for Case 1 and Case 2, respectively. Here the animated times of the operation are longer than the standard motion times resulting from the proposed method. The possible reasons include: (1) the detailed animations with a focus on both body postures and the motion speed; (2) the recorded video reference may not be at a normal speed in the operation due to the worker's real-time condition (e.g., fatigue and experience); and (3) the designer's experience and personal judgment of the motion speed for the adjusted motion magnitude according to the design alternatives. Thus, the workplace design can be more reliable based on the standard motion time information resulting from the proposed methodology.

Table 5-3. Comparison of standard motion time and animated time for design alternatives

	Case 1	Case 2
Animated time (frame)	575	554
Standard motion time (frame)	537	425
Difference (%)	6.6%	23.3%

5.2.3 Comparison of Standard Motion Time-Based Risk Results for Design Alternatives

The ergonomic posture risk ratings for design alternatives are evaluated at each frame for continuous motions and are further categorized into five risk levels for REBA and four risk levels for RULA. All the risk scores are generated and saved in the risk rating log file in the time series. According to the proposed 3D-MEC method, the standard motion time-based REBA and RULA risk scores are compared to risk scores from the 3D method (herein referred to as the baseline method), as presented in Figure 5-11 and Figure 5-12 for Case 1 and Case 2, respectively. The plotted risk rating curves from the proposed method are moving forward since the standard motion time durations are shorter than the animated times in both cases.

For Case 1, the shapes of risk rating curves are similar between the baseline method and the proposed method in REBA and RULA, respectively. The standard motion time durations are about the same, which are about 19 s for the baseline method and about 18 s for the proposed method. Thus, the standard motion time analysis slightly affects posture risk ratings in Case 1. However, the motion time duration decreases by about 4 seconds (from about 18 seconds to about 14 seconds) with the proposed method in Case 2. As mentioned above, the activity conditions are assessed by the degree of repetitiveness (i.e., 4 times repeat per minute) in REBA and RULA. The duration of 14 seconds is considered as a frequent repetition to add a score of 1 for the proposed method in Case 2. Thus, the shapes of risk rating curves are changed in Case 2. The posture risk ratings and standard motion time durations are mapped for the same motions using linear interpolation. In this case, the risk ratings of 6 subtasks are matched between the baseline method and the proposed method, as shown in Figure 5-11 and Figure 5-12. However, the proportions of each posture in the continuous motion are varied, which can lead to variations in the shapes of risk rating curves.

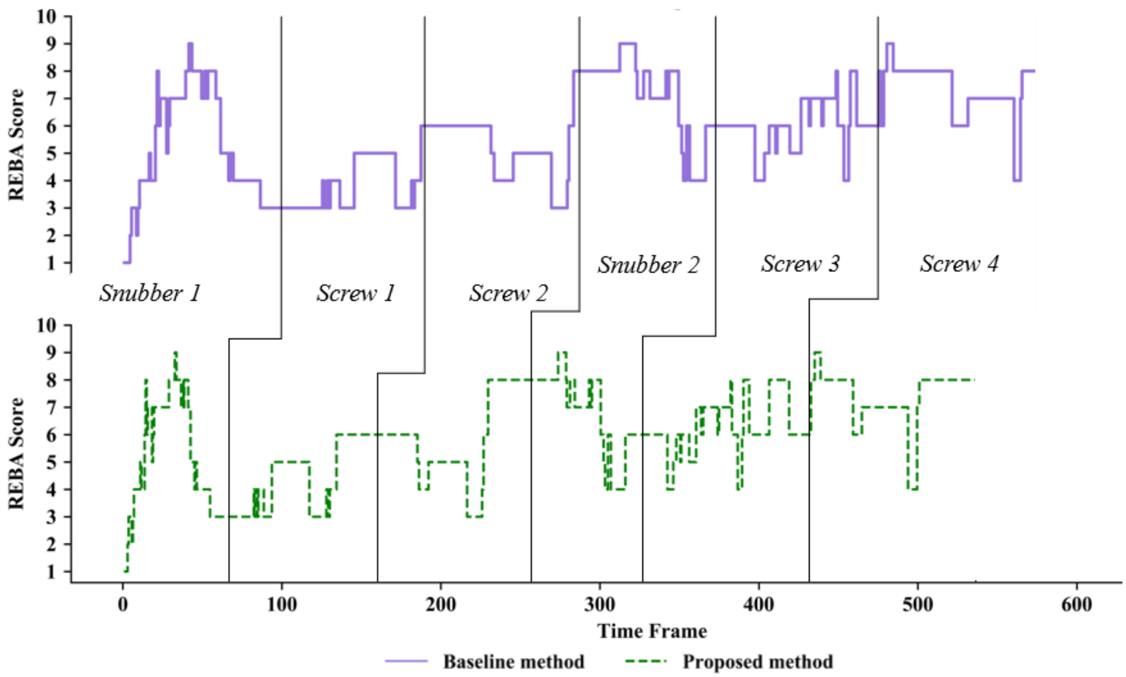

(a)

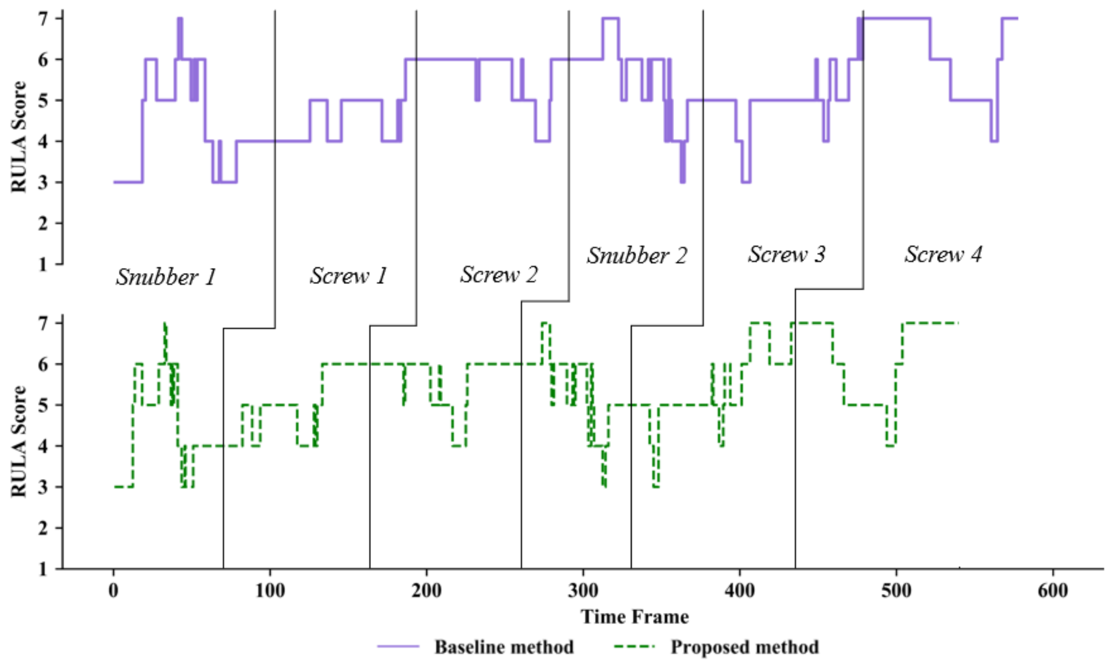

(b)

Figure 5-11. REBA and RULA total risk rating comparison for Case 1: (a) REBA score; (b) RULA score

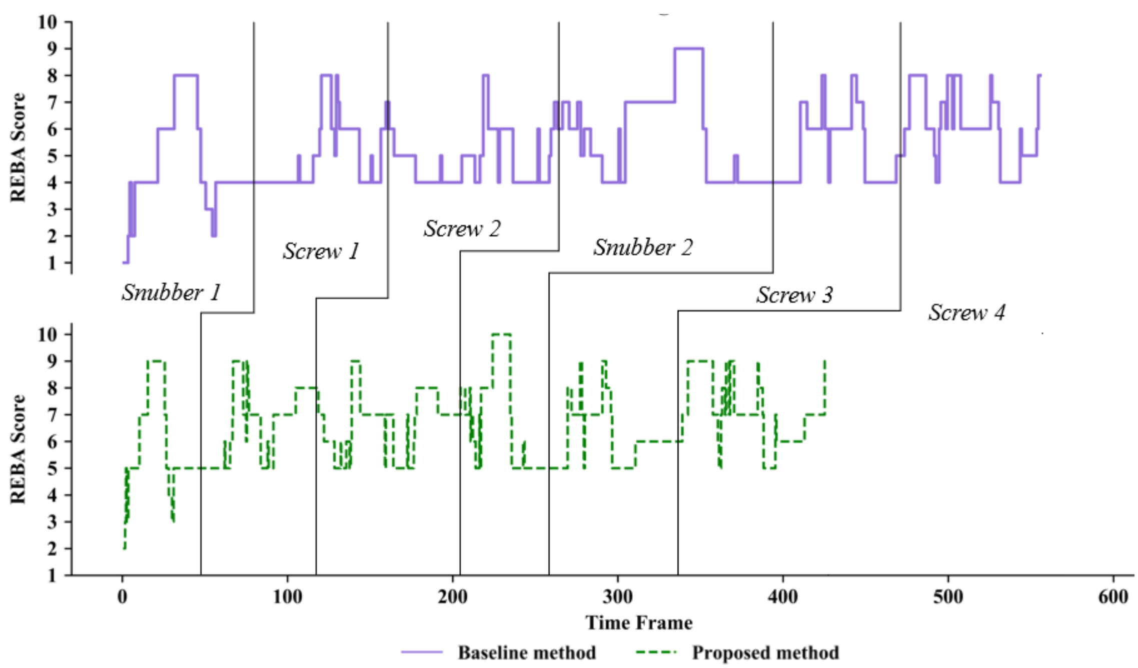

(a)

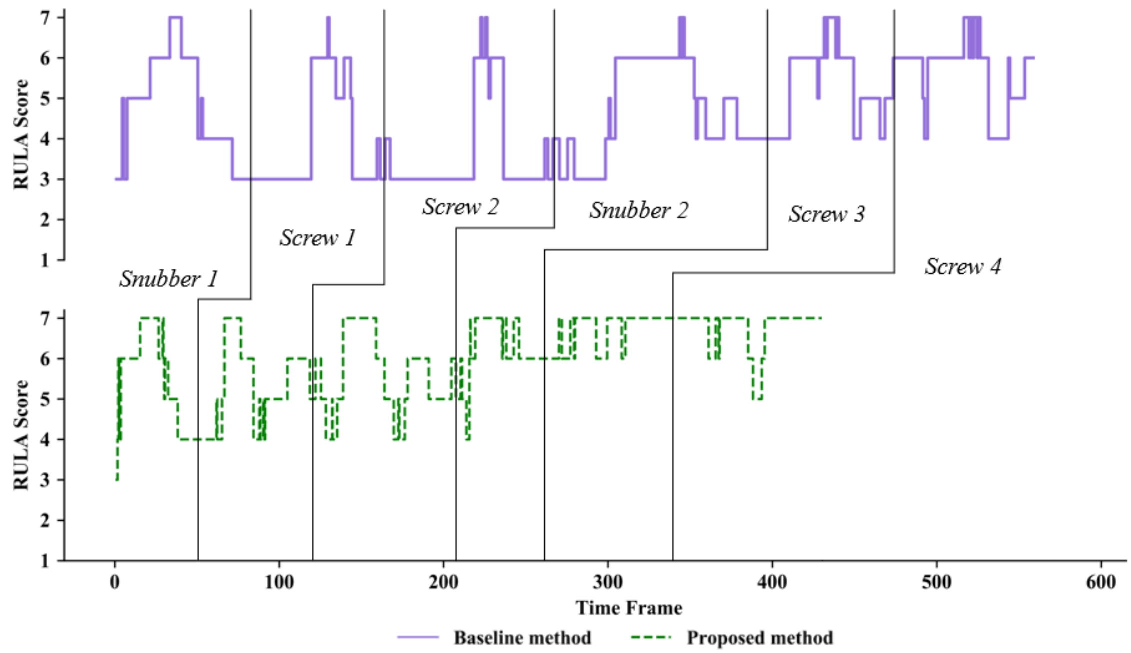

(b)

Figure 5-12. REBA and RULA total risk rating comparison for Case 2: (a) REBA score; (b) RULA score

Results obtained from the posture risk assessment show that the average risk ratings of two cases from REBA are 5.77 and 5.30, respectively, which both correspond to a medium risk level. As for RULA, the average risk ratings of the two cases are 5.21 and 4.60, respectively, and workers exposed to a medium risk level for Case 1 and a low risk level for Case 2. However, the posture risk ratings are mapped with the standard motion time duration in the proposed method, which are resulted in average risk ratings of 6.10 and 6.64 from REBA and 5.43 and 6.10 from RULA for Case 1 and Case 2, respectively. The average risk levels are all corresponding to the medium risk level using the proposed method. By comparing the average risk ratings between two design alternatives, Case 2 yields the lower risk in the baseline method, which should be adopted for the workstation design, while Case 1 obtaining the lower risk in the proposed method is the better solution. Thus, the standard motion time can affect the decision making of workplace design.

In Case 1, the average risk ratings from the proposed method are approximately 5.59% and 4.22% increases in REBA and RULA, respectively. The slight increases in the average risk ratings result from the minor decrease in the standard motion time durations with the proposed method. In Case 2, the average risk ratings are approximately 25.38% increases in REBA and 32.50% increases in RULA. The possible reasons for the greater increases in average risk ratings include: (1) the 23.3% decrease in motion time durations with the proposed method; and (2) the increases in the risk ratings of the adjusted activity scores caused by the high degree of repetitiveness for the motions in Case 2. As mentioned above, the activity condition is evaluated by the degree of repetitiveness, which corresponds to the motion time. Thus, the average risk ratings of Case 2 are increased more after the standard motion time integration. Table 5-4 summarizes the REBA and RULA risk ratings and risk levels with average, maximum, and minimum factors, for Case 1 and Case 2, respectively.

Table 5-4. REBA and RULA results from two cases for baseline method and proposed method

	Design Factors	Case 1 REBA	Case 1 RULA	Case 2 REBA	Case 2 RULA
3D	Mean	5.77	5.21	5.30	4.60
	Max	9	7	9	7
	Min	1	3	1	3
	Risk level	3.07	2.86	3.09	2.54
3D-MEC	Mean	6.10	5.43	6.64	6.10
	Max	9	7	10	7
	Min	1	3	2	3
	Risk level	3.18	2.98	3.26	3.36

In terms of the maximum and minimum risk ratings, they remain the same since the postures are the same, as indicated in Case 1. However, if the standard motion time integration affects the activity condition, the increase in the degree of repetitiveness may increase the maximum and minimum risk scores, vice versa (Wang et al. 2021b). In addition, the detailed risk rating results of each body segment from both two cases are comparable between the baseline method and the proposed method, as summarized in Table 5-5. The risk ratings of the upper arms and wrists are slightly increased in the proposed method; the risk ratings of the neck are slightly decreased in the proposed method. Thus, the average risk ratings of each body segment are slightly affected by the standard motion time integration when the motion time durations are comparable.

Table 5-5. REBA and RULA risk ratings of each body segment

	Case 1				Case 2			
	REBA		RULA		REBA		RULA	
	3D	3D-MEC	3D	3D-MEC	3D	3D-MEC	3D	3D-MEC
Neck	1.05	1.03	1.19	1.13	1.38	1.33	2.17	2.02
Trunk	4.08	4.19	4.08	4.19	3.66	3.64	3.66	3.64
Legs	1.65	1.67	1.00	1.00	1.90	1.93	1.00	1.00
Upper Arm	3.05	3.15	3.05	3.15	2.28	2.55	2.28	2.55
Lower Arm	1.88	1.87	1.88	1.87	1.84	1.90	1.84	1.90
Wrist	2.62	2.68	3.62	3.68	2.50	2.64	3.50	3.64

The proportion of motions at each risk level for two cases is varied between the baseline method and the proposed method, as shown in Table 5-6. Throughout the collective motions, no motions are exposed to the risk level of 5 in REBA and the risk level of 1 in RULA for two cases with two methods. Based on the 3D method, Case 1 exposes workers to the highest risk with approximately 22.09% and 11.13% in REBA and RULA, respectively, which are higher than those of Case 2 (approximately 11.55% and 4.69%). Thus, the optimum choice of completing this task is Case 2 in the 3D method. However, with the proposed method, the proportion of motions that are exposed to the risk level of 4 is slightly increased for Case 1, approximately 7.89% and 5.82% in REBA and RULA, respectively. For Case 2, the proportion of motions at the risk level of 4 is highly raised by 14.57% and 41.66% in REBA and RULA, respectively. Thus, with the standard motion time integration, Case 1 is the optimum choice of completing this task in the proposed method.

Table 5-6. REBA and RULA risk level comparison for the baseline method and proposed method

		Case 1			Case 2		
Method	Risk level	3D	3D-MEC	Difference	3D	3D-MEC	Difference
REBA	1	0.70%	0.37%	−0.32%	0.54%	0.00%	−0.54%
	2	13.57%	10.80%	−2.76%	1.62%	0.47%	−1.15%
	3	63.65%	58.85%	−4.81%	86.28%	73.41%	−12.87%
	4	22.09%	29.98%	7.89%	11.55%	26.12%	14.57%
	5	0.00%	0.00%	0.00%	0.00%	0.00%	0.00%
RULA	1	0.00%	0.00%	0.00%	0.00%	0.00%	0.00%
	2	24.70%	19.37%	−5.33%	50.54%	10.35%	−40.19%
	3	64.17%	63.69%	−0.49%	44.77%	43.29%	−1.47%
	4	11.13%	16.95%	5.82%	4.69%	46.35%	41.66%

5.3 Discussion

Based on the task movement analysis results, the case study underscores the importance of integrating standard motion time into the framework for evaluating design alternatives and comparing ergonomic risk ratings to support decision making prior to implementation of the workstation design. Based on the case study, it is recommended to have the working table tilted to 20° for the task of hardware installation as a workstation design modification, as presented in Case 1. The worker in the Case 1 workstation design scenario is exposed to a lower risk rating compared to the worker in Case 2, meaning that Case 1 is the optimum choice for completing this task. In contrast, when applying the previously developed 3D method, the optimum choice is Case 2. Thus, integrating the motion time information into the 3D model can highly influence the ergonomic risk results and decision making with respect to selecting the optimum workplace design alternative. In other words, the incorporation of standard motion time information is essential for 3D-based ergonomic analysis of continuous motions for workplace design.

The results also indicate that the proposed 3D-MEC method can consistently generate the standard motion times for ergonomic risk ratings of continuous motions, even though the detailed animations may obtain more time frames, or the rapid animation may contain fewer time frames in the 3D model. The proposed method ensures consistency by providing the standard motion time and objective and reliable risk ratings of continuous motions for the purpose of evaluating workplace design alternatives. The existing 3D-based method mainly relies on manual observation and user experience for the collection of motion time data, meaning that the accuracy is generally low. Moreover, the traditional method fails to capture standard motion time, which defines the speed of motion and the degree of repetitiveness in continuous motions; this deficiency of the traditional 3D-based method also hampers the accuracy and utility of the resulting ergonomic risk ratings. By improving the accuracy of the ergonomic risk scores, standard motion time information greatly improves decision making with respect to workplace design in modular construction. In addition, the proposed method eliminates the reliance on time studies and on the designer's experience, thereby expediting the workplace design process.

To summarize, the research described in this chapter offers four contributions to the body of knowledge. (1) The research improves the level of automation and the accuracy of risk rating results in 3D-based ergonomic risk assessment by integrating the standard motion time determination algorithm. (2) The standard motion time determination algorithm outputs the motion time data in a standard manner, as an alternative to time studies, which are subject to human perception errors and other issues that compromise their accuracy and usefulness. In addition, the consistency of the results is ensured as a by-product of the automation aspect of the proposed ergonomic risk assessment system incorporating standard motion time. To be specific, the standard cycle time in a normal production performance is objective data, making it more accurate, consistent, efficient, and cost-effective for workplace design. (3) The proposed 3D-MEC method collects posture data from 3D human models and automatically determines the standard motion time, which makes the process of comparing and editing the various design alternatives at the design stage easier and more convenient, without having to physically imitate the tasks, and even if the workplace itself is still at the design stage and has not yet been implemented. (4) The proposed 3D-MEC method is also highly efficient since it can reduce the time required for motion data collection in real-world observation. The proposed method also circumvents potential production interruptions for motion data collection or workplace reconstruction for the purpose of implementing ergonomic improvements to the existing workplace.

The research has some limitations that need to be resolved in future research. In the present research, the arm and hand motions are automatically identified and analyzed as part of the standard motion time determination, and this information is integrated with the ergonomic risk assessment for the purpose of evaluating design alternatives. However, these arm and hand motions are not sufficient to represent 100% of all manual construction operations (e.g., walking between workstations, lifting objects from the floor to the working surface, etc.). Nevertheless, arm and hand motions are the primary motions in manual assembly tasks at workstations in modular construction, and these motions are characterized in detail in MTM-1, whereas full body motions, such as walking, bending, and stooping, are not described in detail in MTM-1. Moreover, eye motions and force-related motions (i.e., apply pressure and disengage) are excluded due to the limitations of 3D modelling. The proposed method applies MTM-1 for the integration of standard motion time with ergonomic risk assessment since it is the most detailed PMTS approach currently available. Other PMTSs, such as MOST and MODAPTS, can also be implemented to investigate they might achieve better performance with respect to integrating standard motion time with ergonomic risk assessment. Other promising avenues of future research include: (1) developing a standard motion time determination algorithm for full body motions to supplement the MTM-1 body motion categorization; (2) incorporating full body motion assessment into the evaluation of workplace design, and considering multiple workstations rather than limiting the scope of the evaluation to single workstations; and (3) incorporating productivity analysis in order to improve both ergonomic performance and efficiency through workplace design.

5.4 Summary

In this chapter, a predetermined motion time system is integrated with ergonomic posture risk assessment methods to automatically determine the motion time and compile the ergonomic risk results in terms of the standard motion time feature for ergonomic-centric workplace design. The rule-based motion recognition algorithm could determine the standard motion time of the continuous motions in the completion of construction tasks based on the MTM-1 system in this research. The mapping process of risk ratings and standard motion time generates the standard motion time-based ergonomic risk ratings for continuous motions, which improves the accuracy and reliability of risk assessments for continuous motions. Furthermore, the proposed 3D-MEC method provides a more reliable, less time-consuming, easy to apply, and cost-effective method to assess multiple workplace design alternatives, since no requirement of physically imitating tasks and motion data collection for design alternatives in the real-world implementation.

CHAPTER 6: POSTURAL SWAY ANALYSIS FOR THE LIMITS OF AUTOMATED ERGONOMIC RISK ASSESSMENT OF DYNAMIC MOTIONS IN MODULAR CONSTRUCTION

Various observation-based ergonomic risk assessment methods are widely used to automatically evaluate ergonomic risks of continuous motions. However, discrepancy of assessment results is identified and the limits of automated ergonomic risk assessments for continuous motions involving postural sway have not yet been examined. This chapter discusses the investigation of the postural sway effects on the automated ergonomic risk assessments of dynamic motions in the optical marker-based motion capture system. In this study, twenty-three participants were recruited to perform three construction tasks to identify the minor movement of body joints naturally occurring due to posture sway during continuous motions. These minor movements of body joints are used to determine the posture categories in the adjustment risk rating process. Posture sway-incorporated ergonomic risk assessment method is proposed to eliminate the overestimations and fluctuations in risk results, which overcomes the limits of automated ergonomic risk assessment and improves its accuracy and reliability in evaluation of dynamic and continuous motions. A case study of two workplace designs for manual assembly tasks is presented to validate the effectiveness of the proposed method.

6.1 Methodology for Posture Sway-incorporated Assessment

The presented research employs motion capture measures that aim to identify the acceptable magnitudes of body joint angles naturally occurring due to the body sway that affects the results of ergonomic posture risk assessments for the continuous motions. The investigation was conducted in an optical marker-based motion capture laboratory at the University of Alberta in

Edmonton, Canada. The overview of the proposed methodology is presented in Figure 6-1. The inputs include the plant observations of the dynamic motions in the completion of operational tasks, experiment design based on the observations and task maneuver, and the subjects' anthropometry information for the motion capture experiment. The main processes are divided into five steps: (1) conduct the experiments to acquire information on the human body motions; (2) analyze the captured body joint angles for posture sway analysis; (3) determine the posture sway magnitudes for the posture categories in the adjustment risk rating process in REBA and RULA; (4) assess ergonomic risks by using the captured body joint angles and the identified posture categories for adjustment; and (5) compare the risk ratings obtained using the original method and the proposed method to verify the posture sway effect on the ergonomic risk ratings.

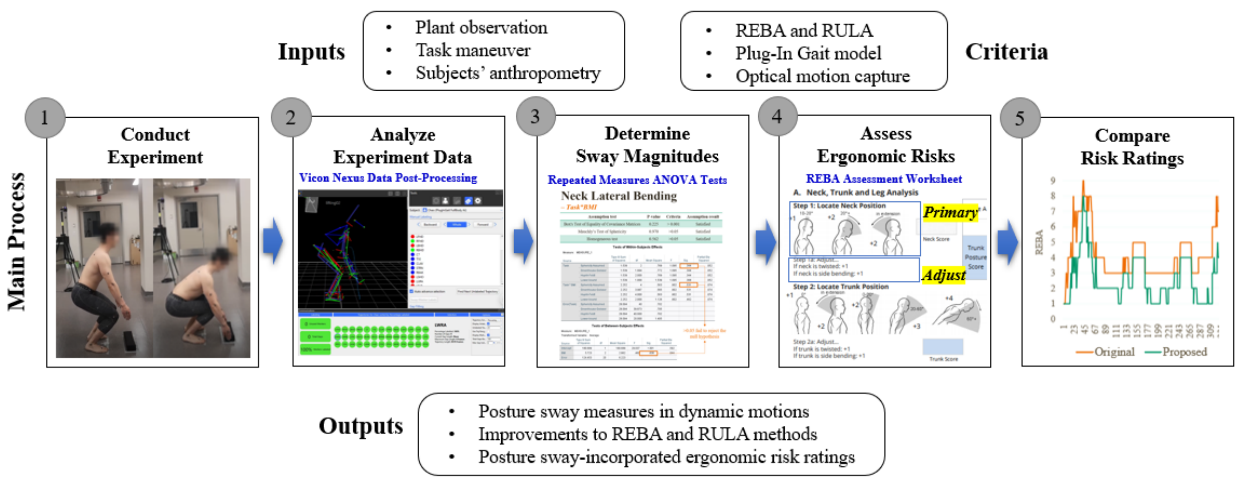

Figure 6-1. Overview of the proposed methodology

6.1.1 Participants

With the ethical approval, a total of 23 right-handed adults participated in the experiment, including 13 male subjects and 10 female subjects with no history of injury. Their heights ranged from 160 to 189 cm, body weights varied from 45 to 105 kg, and ages varied from 20 to 49 years.

The summary of participant characteristics information is presented in Table 6-1. All participants were the university students, and none of them presented any physical condition that could affect their posture and motion. Before recruiting participants, the present study received the ethical approval from the research ethics committee at the University of Alberta in Edmonton, Canada. The purpose and procedure of this experimental study were explained to all participants in detail before the experiment. All participants signed an informed consent form prior to the participation in this experimental study. The participation in this study is voluntary, confidential, and anonymous. In addition, there is no potential harm to the human body in the experiment. The consent form used for the study (and approved by the research ethics board) is presented in Appendix A.

Table 6-1. Participant characteristics information (n = 23)

Group	Number of participants	Age (year)		Height (cm)		Weight (kg)		BMI (kg/m^2)	
		Mean	SD	Mean	SD	Mean	SD	Mean	SD
Male	13	29.0	7.6	177.3	6.5	78.6	17.3	24.8	4.4
Female	10	27.7	2.8	166.4	5.0	58.6	9.0	21.1	2.7
Total	23	28.4	5.9	172.6	8.0	69.9	17.3	23.2	4.1

6.1.2 Experimental Instrument

Optical marker-based motion capture is a widely used measure to capture human motions because of its high accuracy. In this experiment, the Vicon Nexus system (Version 2.12) was used to capture and record the kinematics of body segments while performing the operational tasks. Eight high-speed digital cameras of type Vero v2.2 were positioned all over the workspace at the University of Alberta's occupational ergonomics laboratory. The participants were equipped with the spherical self-adhesive reflective markers of a diameter of 9.5 mm. The markers methods used are from the Vicon Plug-In Gait (PiG) full body marker placement recommendations (Vicon 2021). In addition, the motion data collection was recorded with two video cameras at 30 frame per second (fps). The positions of the cameras are presented in Figure 6-2.

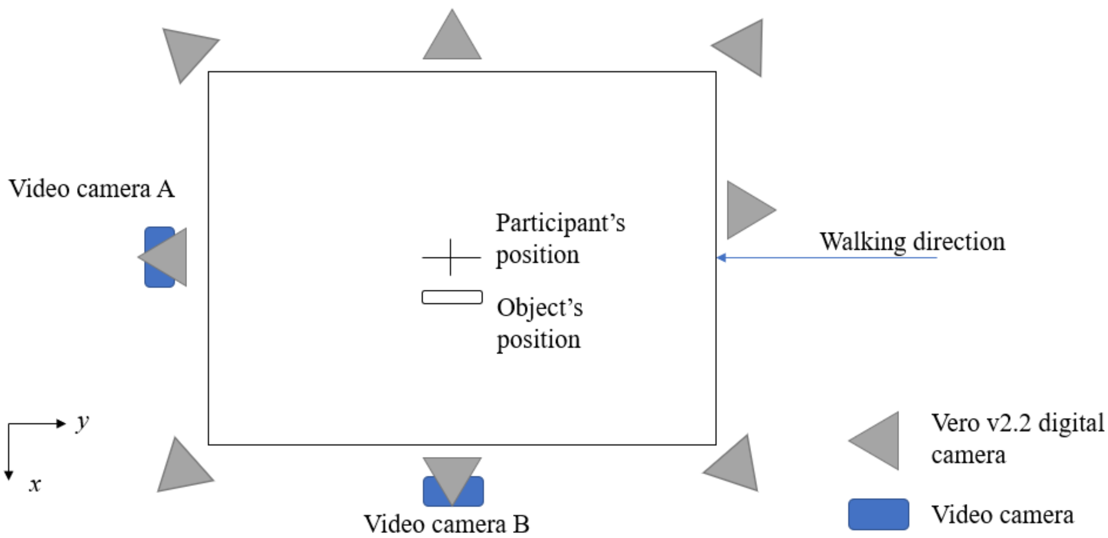

Figure 6-2. Spatial organization of cameras

6.1.3 Evaluation Parameters

The evaluation parameters are determined by the investigation on the ergonomic posture assessment methods (i.e., REBA and RULA) in the present study, which are objectively captured by the optical maker-based motion capture system. Based on the observations, these parameters are expected to be evaluated in different working conditions. The descriptions of the evaluation parameters in REBA and RULA and the associated angles in the PiG model are shown in Table 6-2.

Table 6-2. Summary of evaluation parameters

Body segment	Description in REBA and RULA	Angles in PiG Model
Neck	Twisted	Neck rotation
	Side bending	Neck lateral bend
Trunk	Twisted	Trunk rotation
	Side bending	Trunk lateral bend
Upper arm	Abducted	Shoulder lateral bend
Wrist	Twisted	Wrist rotation
	Side bending	Wrist lateral bend

6.1.4 Experimental Design

The aim of these experiments is to identify the acceptable magnitudes of body joints in the body sway for the qualitatively categorized adjustment factors in REBA and RULA, including the side bending and twisted of neck, the side bending and twisted of trunk, the side bending and twisted of wrists, and abducted arms. To effectively identify these parameters, three manual tasks commonly occur in the plant are imitated in the motion capture system, including Task #1: walking scenario that workers are walking between different workstations; Task #2: moving scenario that workers are moving the tools or work elements (i.e., panels) from shelves to working area; and Task #3: lifting scenario that workers are lifting the work elements from the floor to the working table. These tasks are designed based on the observations in the modular construction facilities. In addition, the designed tasks cover most of the basic motions and thus are enough to identify the adjustment factors in the rule-based assessment methods.

In this experiment, the participants were positioned barefoot in a comfortable position. All participants were instructed to remain as still as possible in neutral quite standing posture for 30 s with arms besides the body, eyes looking straight ahead, and the body weight evenly distributed on both feet. A lightweight bar was used as an object to keep the distance between arms and hands the same as the shoulder width during the experiments. The participants were also instructed to maintain a 0° neck rotation angle, a 0° neck lateral bending angle, a 0° trunk rotation angle, a 0° trunk lateral bending angle, a 0° shoulder abduction angle, and 0° of wrist rotation and lateral bending angle during the performance of all tasks. The experimenter observed the participants' body postures and angle data from the markers to ensure that participants maintained stable body sway conditions and body postures during the performance of all tasks.

The detailed requirements of three tasks are described as follows. In Task #1, the participants were required to walk naturally with a control of the head, neck, and torso. The participants were walking along a straight line indicated on the ground. To avoid inconsistencies, the participants were required to walk from the outside of the capture volume. Most of the participants have 4 or 5 steps captured due to the space limit. Thus, the data of 4 steps for each subject is used for data analysis. In Task #2, the participants used both hands to hold the lightweight bar with straight arms. The bar is moved from the belly to the arm length away at the shoulder height. The subject is required to complete the moving task without raising up the shoulders. In Task #3, the participants were lifting the lightweight bar that initially placed on the ground at 20 cm in front of the participants. The participants were required to pick up the bar to the pelvis front by lowering the center of mass and reaching it with straight arms. It should be noted that the wrists are under control to avoid any movements in all tasks except walking condition in Task #1. All the participants performed 10 trials in each Experiment. A break of 30 seconds between trials was used to avoid the muscle fatigue in completing the tasks. The graphical displays of three tasks are shown in Figure 6-3.

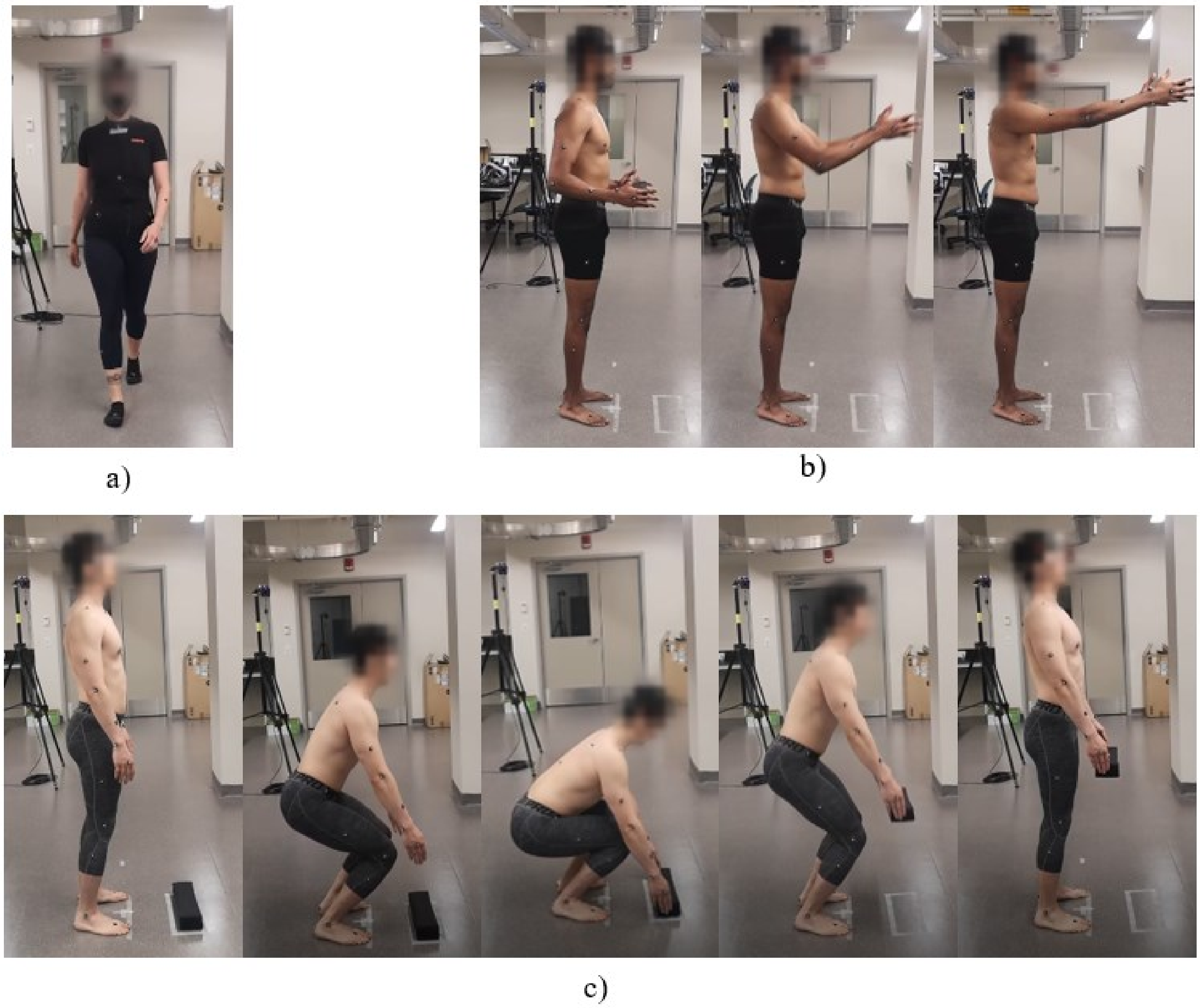

a) b) c)

Figure 6-3. Graphic displays of three tasks: (a) Task #1, (b) Task #2, and (c) Task #3

6.1.5 Data Collection and Data Processing

Since the Vicon PiG full body model was used in this experiment, a total of 39 markers were attached to the participant's skin at specific joints according to the PiG full body labeling configuration, which defines the following body segments: head, torso, upper arms, forearms, hands, upper legs, lower legs, and feet. The anatomical positions of the reflective markers during performing the tasks and the instruction of marker placement are illustrated in Figure 6-3 and Table 6-4. The asymmetry of the marker placement is desirable as it helps the auto labeling routine distinguish right from left. The PiG model calculates joint kinematics and kinetics from the 3D coordinates of markers and specific anthropometric measurements of each participant. The anthropometric measurements of each participant include the body mass, height, leg length, knee width, ankle width, shoulder offset, elbow width, wrist width, and hand thickness for the left and right side of the body. According to the approved ethics, the faces of participants were blurred after video recordings of the motions, and the video recordings were synchronized in the post-processing phase.

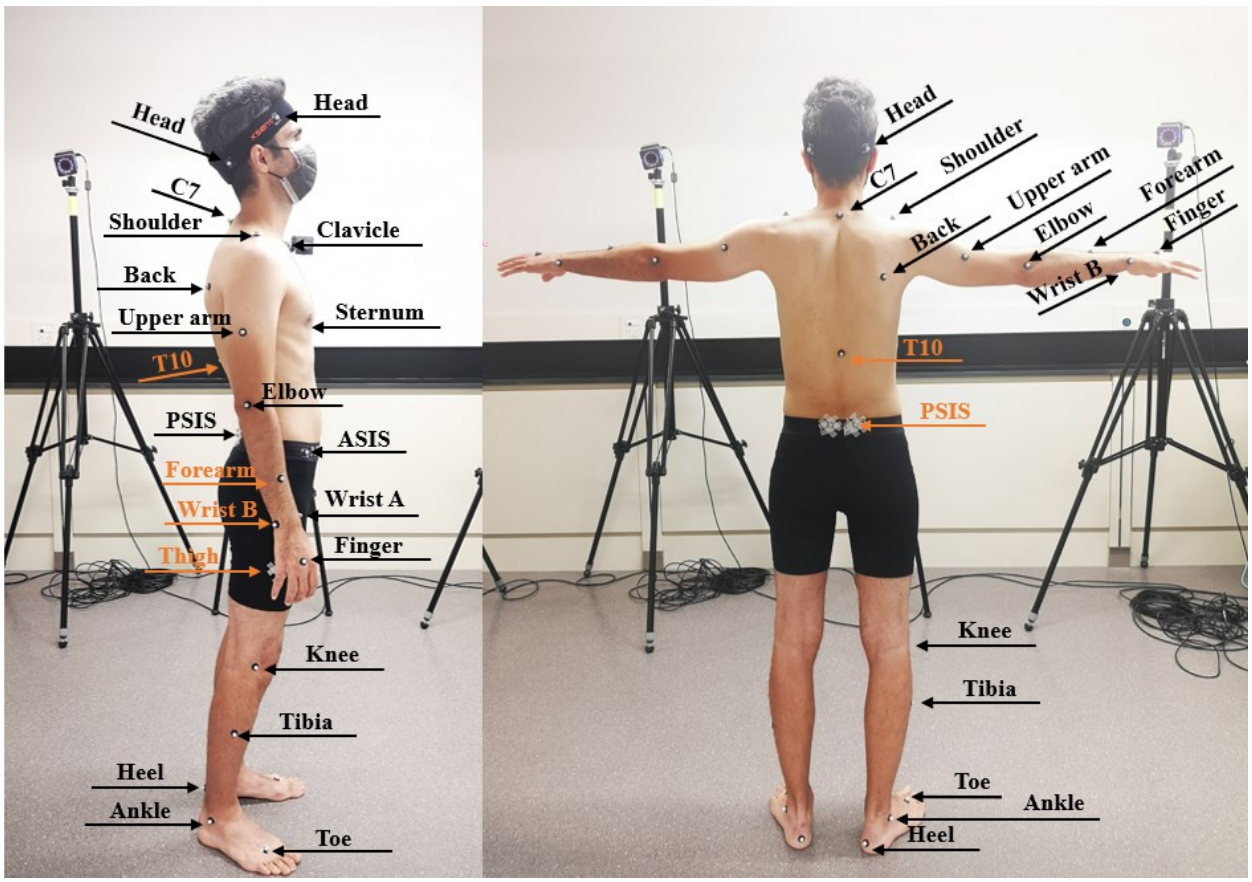

Figure 6-4. Positions of 39 reflective markers in the experiment

Table 6-3. Description of 39 reflective markers positions and marker names in the PiG model

Marker positions	Marker position descriptions	PiG marker names
Head	On the left and right temples On the left and right backs of head	LFHD, RFHD, LBHD, RBHD
Clavicle	On the jugular notch (between the two collar bones)	CLAV
Sternum	On the xiphoid process of the sternum	STRN
Cervical vertebra 7	On the spinous process of the 7th cervical vertebra where the back of the neck ends	C7
Thoracic vertebra 10	On the spinous process of the 10th thoracic vertebra (count 10 vertebrae down from C7 when the subject bends forward)	T10
Right back	Anywhere over the right scapula that helps to distinguish the right from left on the subject	RBAK
Pelvis-anterior superior iliac (ASIS)	On the left and right anterior superior iliac spine where the hip bones protruding laterally	LASI, RASI
Pelvis-posterior superior iliac (PSIS)	On the left and right posterior superior iliac spine (immediately below the sacroiliac joints, at the point where the spine joins the pelvis)	LPSI, RPSI
Shoulder	On the left and right acromion-clavicular joint	LSHO, RSHO
Upper arm	On the middle of the line that connects the shoulder marker and elbow marker (asymmetrically between left and right) for each arm	LUPA, RUPA
Elbow	On the lateral epicondyle for each arm	LELB, RELB
Forearm	On the middle of the line that connects the elbow marker and the midpoint of wrist markers (asymmetrically between left and right) for each arm	LFRM, RFRM

Wrist	On the radial styloid process of the ulna (thumb side) and the styloid process of the radius (little finger side), respectively, for each wrist.	LWRA, RWRA, LWRB, RWRB
Finger	On the proximal phalanx of the middle knuckle for each hand	LFIN, RFIN
Thigh	On the middle of the line that connects the ASIS marker and knee marker (asymmetrically between left and right) for each leg	LTHI, RTHI
Knee	On the flexion-extension axis of the left and right knees, respectively	LKNE, RKNE
Tibia	On the outer edge of the fibula bone at the middle of the line that connects the ankle marker and knee marker for each leg	LTIB, RTIB
Ankle	On the lateral malleolus along a line that connects the opposite side of the malleolus for each ankle	LANK, RANK
Heel	On the calcaneus at the same height as the toe marker	LHEE, RHEE
Toe	Over the second metatarsal head, on the mid-foot side of the equinus break between forefoot and mid-foot	LTOE, RTOE

All raw motion data were recorded at 120 Hz with the Vicon Nexus software (version 2.12). A calibration of the Vicon motion capture system was conducted at the beginning of the recording session for each participant. Calibration results indicate that the image error of maximum 0.2 pixels is acceptable for the motion capture experiment in the present study. The marker trajectory processing operations in the Vicon Nexus system include 3D reconstruction, trajectory smoothing, gap filling, and data exporting. In this experiment, the rigid body method was used for the trunk and the kinematic method was used for the limb for the missing markers and gap filling operations.

The 3D coordinates and the joint angles were exported from the Vicon Nexus system for the data post-processing.

In this experiment, the body joint angles are expressed in the three anatomical planes, which are the sagittal, frontal, and coronal planes. These joint angles were calculated using YXZ Cardan rotation sequences, where Y represents the flexion or extension, X represents the abduction or adduction, and Z represents the internal or external rotation. The mean curve of the 10 trials per participant was calculated, and from that, the mean value of all the adjustment factors were obtained over the all the participants.

6.1.6 Statistical Analysis and Determination of Acceptable Magnitude

The statistical analysis was accomplished using IBM SPSS Statistic software (version 28.0.1.0) and the significance level was maintained at $\alpha = 0.05$ for all tests. The repeated measures Analysis of Variance (ANOVA) was conducted to evaluate the effect of tasks, gender, and BMI conditions on the body sway during the continuous motions. Before carrying out the statistical analyses of the targeted factors, Mauchly's test of sphericity was tested. The Greenhouse-Geisser adjustment was applied when the sphericity assumption was not met. The post-hoc analysis was conducted using Tukey's test with Bonferroni adjustments when a significant effect was found.

The determination of the acceptable magnitude of the natural posture sway is based on the repeated measures ANOVA results. The average value is used in the determination when there is no significant difference among three tasks. The ceiling value, meanwhile, is used in the determination when different values are outputted for the same evaluation parameter. The ceiling value is the least nearest successive integer of a specified value, whish is calculated using Equation 6-1.

$$\lceil \delta \rceil = min\{ n \in \mathbb{Z} \mid n \geq \delta \} \qquad \text{Equation 6-1}$$

where δ is a real number representing the body joint angles, n is an integer, and $\mathbb{Z}$ is the set of integers.

6.2 Results

The one-way repeated measures ANOVA was conducted with the tasks as the independent variables, and each evaluation parameter as the dependent variable. For each dependent variable, the average value over 10 trials was obtained for the following analyses. Appendix B shows an example output of the statistical analysis. As summarized in Table 6-4, the one-way repeated measures ANOVA results demonstrated that there were no significant differences of angular displacement among three tasks for the neck side bending ($p = 0.505$) and neck twisted ($p = 0.086$); moreover, there were significant differences among three tasks for trunk side bending, trunk twisted, shoulder abducted, wrist side bending, and wrist twisted (all $p < 0.05$).

Tukey post-hoc tests were conducted and the pairwise compassion indicated that there were no significant differences between walking and lifting for trunk side bending ($p = 0.051$), between moving and lifting for trunk twisted ($p = 0.378$), and between walking and moving/lifting for wrist twisted ($p = 1$; $p = 0.053$); however, there were significant differences for the rest of the pairwise comparison (all $p < 0.05$).

Table 6-4. One-way repeated measures ANOVA results on task effects

Factor	Tasks (Mean ± SD) Walking	Moving	Lifting	F	p-value	Tukey post-hoc test Pairwise comparison	p-value
Neck side bending	2.416 ± 0.298	2.303 ± 0.387	2.590 ± 0.280	0.695	0.505	–	
Neck twisted	3.165 ± 0.392	2.720 ± 0.377	3.517 ± 0.392	2.598	0.086	–	
Trunk side bending	3.127 ± 0.231	1.449 ± 0.208	2.354 ± 0.237	19.108	<0.001	W-M W-L M-L	<0.001 0.051 0.004
Trunk twisted	4.004 ± 0.210	2.141 ± 0.247	2.578 ± 0.210	26.833	<0.001	W-M W-L M-L	<0.001 <0.001 0.378
Shoulder abducted	18.075 ± 1.083	32.959 ± 1.244	25.357 ± 2.090	49.523	<0.001	W-M W-L M-L	<0.001 <0.001 0.001
Wrist side bending	5.164 ± 0.858	13.482 ± 1.900	9.344 ± 1.667	13.015	<0.001	W-M W-L M-L	<0.001 0.039 0.015
Wrist twisted	19.280 ± 2.583	17.243 ± 1.615	9.646 ± 1.682	5.224	0.023	W-M W-L M-L	1 0.053 <0.001

Note: W-M = walking vs. moving; W-L = walking vs. lifting; M-L = moving vs. lifting.

The acceptable posture sway magnitudes of the evaluation parameters are listed in Table 6-5. For the neck aside bending and neck twisted, the acceptable magnitudes of neck side bending and neck twisted are 3° and 4°, respectively. The average values of three tasks are used to determine the boundaries since there were no significant differences among three tasks. And the ceiling values were then selected to set the boundaries. According to the results in the pairwise comparison, the acceptable magnitudes of trunk side bending and trunk twisted are 2° and 3°, respectively, which were determined by the ceiling value of the average value from the moving task and the ceiling value of the average value from the moving and lifting tasks. The acceptable magnitude of shoulder abducted parameter is 19°, which was determined by the ceiling value of the average value from the walking task. For the wrist, the side bending and twisted parameters are 6° and 10°, respectively, which were calculated based on the walking task and lifting task, respectively. The posture category and the corresponding risk scores are summarized in Table 6-5.

Table 6-5. Acceptable posture sway magnitudes of evaluation parameters

	Acceptable magnitude	Posture category	Risk score
Neck side bending	3°	$-3° \leq \gamma \leq 3°$	0
		$\gamma > 3°$ or $\gamma < -3°$	+1
Neck twisted	4°	$-4° \leq \beta \leq 4°$	0
		$\beta > 4°$ or $\beta < -4°$	+1
Trunk side bending	2°	$-2° \leq \gamma \leq 2°$	0
		$\gamma > 2°$ or $\gamma < -2°$	+1
Trunk twisted	3°	$-3° \leq \beta \leq 3°$	0
		$\beta > 3°$ or $\beta < -3°$	+1
Shoulder abducted	19°	$-19° \leq \gamma \leq 19°$	0
		$\gamma > 19°$ or $\gamma < -19°$	+1
Wrist side bending	6°	$-6° \leq \gamma \leq 6°$	0
		$\gamma > 6°$ or $\gamma < -6°$	+1
Wrist twisted	10°	$-10° \leq \beta \leq 10°$	0
		$\beta > 10°$ or $\beta < -10°$	+1

Note: β = rotation; γ = lateral bending.

The posture sway-incorporated ergonomic risk assessment methods are developed based on the REBA and RULA assessment methods and the acceptable posture sway magnitudes of evaluation parameters in Table 6-5. The posture sway-incorporated REBA system is presented in Figure 6-5. The proposed system consists of four main sections: (1) a primary risk rating section for positions in the sagittal plane, (2) an adjustment risk rating section for positions in other two planes, (3) a rule-based scoring system with force/load and coupling scores, and (4) an adjustment risk rating of activity score for repetitive motions. The posture sway-incorporated RULA system is presented in Figure 6-6. Three main sections are developed in the proposed system, which are (1) primary risk rating section, (2) adjustment risk rating section, and (3) the rule-based scoring system with muscle use and force/load scores. It should be noted that the section of adjustment risk ratings is achieved by using the proposed method in this study. With the adoption of acceptable magnitudes of evaluation parameters, the ergonomic risk ratings resulted from the body sway are eliminated, which overcomes the overestimations and fluctuations in the assessment results.

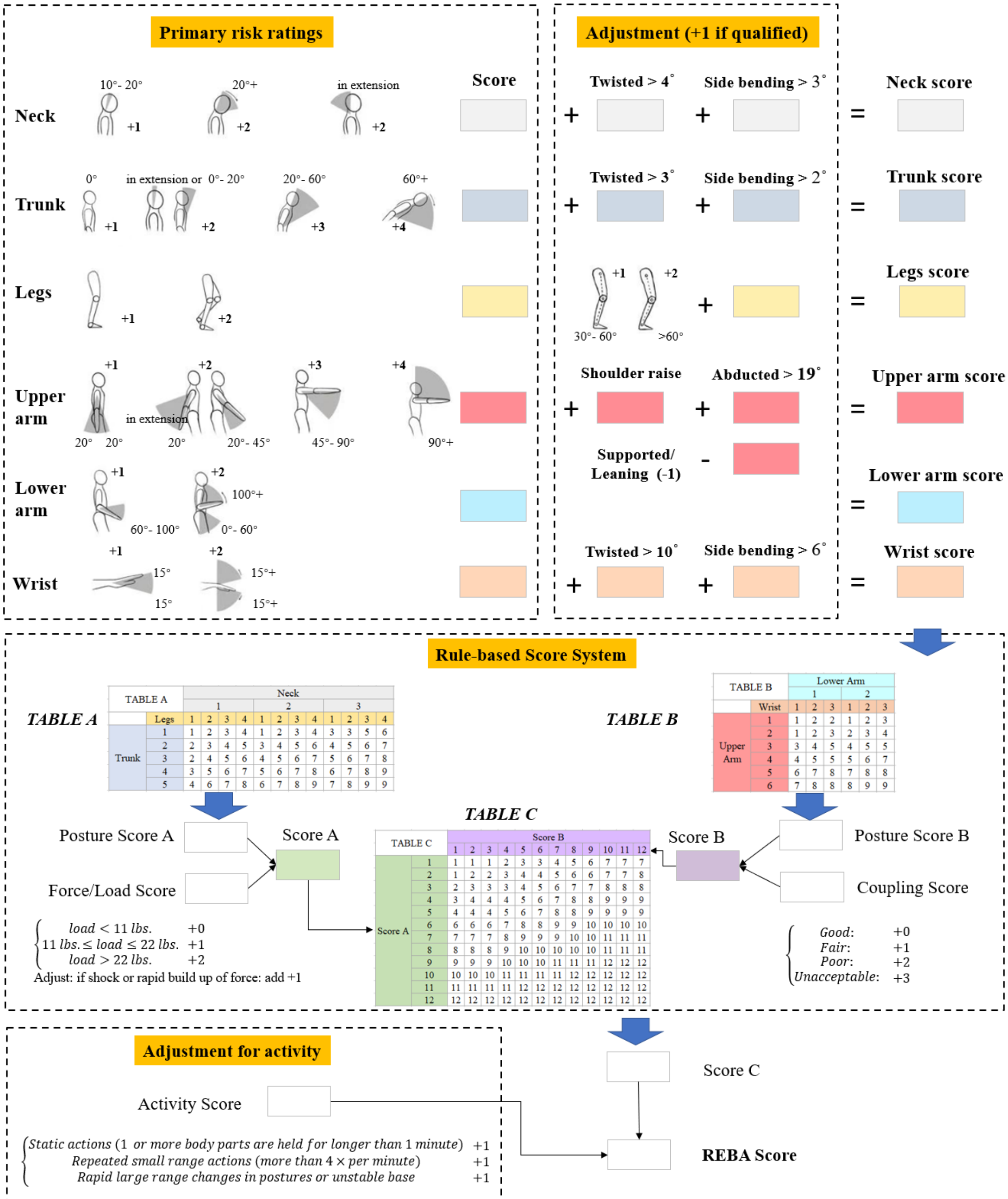

Figure 6-5. Posture sway-incorporated REBA system

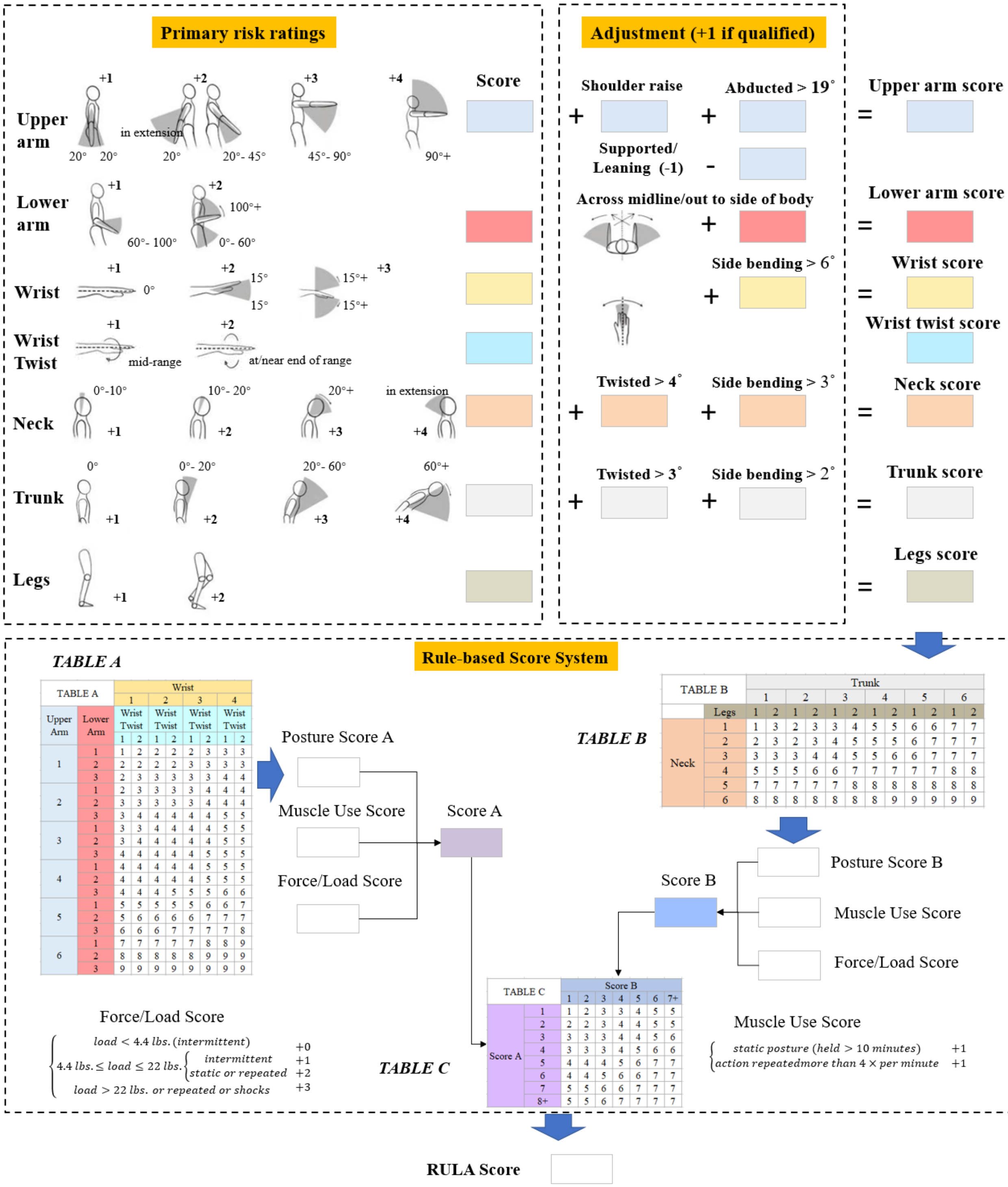

TABLE A		Wrist 1		Wrist 2		Wrist 3		Wrist 4	
		Wrist Twist		Wrist Twist		Wrist Twist		Wrist Twist	
Upper Arm	Lower Arm	1	2	1	2	1	2	1	2
1	1	1	2	2	2	2	3	3	3
	2	2	2	2	2	3	3	3	3
	3	2	3	3	3	3	3	4	4
2	1	2	3	3	3	3	4	4	4
	2	3	3	3	3	3	4	4	4
	3	3	4	4	4	4	4	5	5
3	1	3	3	4	4	4	4	5	5
	2	3	4	4	4	4	4	5	5
	3	4	4	4	4	4	5	5	5
4	1	4	4	4	4	4	5	5	5
	2	4	4	4	4	4	5	5	5
	3	4	4	4	5	5	5	6	6
5	1	5	5	5	5	5	6	6	7
	2	5	6	6	6	6	7	7	7
	3	6	6	6	7	7	7	7	8
6	1	7	7	7	7	7	8	8	9
	2	8	8	8	8	8	9	9	9
	3	9	9	9	9	9	9	9	9

TABLE B		Trunk 1		Trunk 2		Trunk 3		Trunk 4		Trunk 5		Trunk 6	
	Legs	1	2	1	2	1	2	1	2	1	2	1	2
Neck	1	1	3	2	3	3	4	5	5	6	6	7	7
	2	2	3	2	3	4	5	5	5	6	7	7	7
	3	3	3	3	4	4	5	5	6	6	7	7	7
	4	5	5	5	6	6	7	7	7	7	7	8	8
	5	7	7	7	7	7	8	8	8	8	8	8	8
	6	8	8	8	8	8	8	8	9	9	9	9	9

TABLE C		Score B 1	2	3	4	5	6	7+
Score A	1	1	2	3	3	4	5	5
	2	2	2	3	4	4	5	5
	3	3	3	3	4	4	5	6
	4	3	3	3	4	5	6	6
	5	4	4	4	5	6	7	7
	6	4	4	5	6	6	7	7
	7	5	5	6	6	7	7	7
	8+	5	5	6	7	7	7	7

Figure 6-6. Posture sway-incorporated RULA system

6.3 Case Study

The proposed method is implemented in a case study of workstation design in the window manufacturing facility. This section focuses on the evaluation of two workstation design alternatives as an example and further explains the implementation of the proposed method. The workstation is designed for the manual operations of the hardware installation on the window frames, including picking up hardware from the shelves, placing hardware in the target position on the window frame, attaching hardware to the window frame using screws and a screwdriver. For a typical window frame, there are usually hinges, a snubber, an operator, a tie bar, and a handle to be installed at the workstation. Lifting and rotating the window frame may be required due to the target positions of these hardware items on the window frame.

In this case, two design alternatives and the corresponding prototypes are shown in Table 6-6. These two prototypes are built according to the design specifications in the modular construction lab at the University of Alberta, Edmonton, Canada. The wearable motion capture suit, Xsens MVN Awinda (Xsens 2021), is used to collect whole-body motion data based on a total of 17 inertial measurement units (IMU). The IMUs are firmly attached to the head, back, shoulders, upper and lower arms, hands, upper and lower legs, and feet using elastic straps. The IMU sensor is composed of a three-axis accelerometer, a three-axis gyroscope, and a three-axis magnetometer. The experiment was conducted using the prototypes and a 1.62 kg, 35 cm × 40 cm rectangular window frame. Five participants without any history of WMSDs performed the continuous motions in the operational task, and their motions were captured and recorded using the wireless IMU-based motion capture system (Dias Barkokebas et al. 2021). All participants reported that the motion capture suit was comfortable to work with. Each participant was required to perform a calibration procedure to determine the sensor-to-segment alignment before the experiment. The

Xsens MVN Analyze 2020.0 software is used to analyze the motion data. In addition, video cameras are used to record videos of continuous motions in the experiment as a way of checking for inconsistencies.

Table 6-6. Two workstation design alternatives and corresponding prototypes

Workstation design	Design A	Design B
Shop drawing	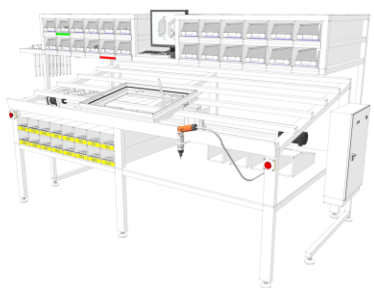	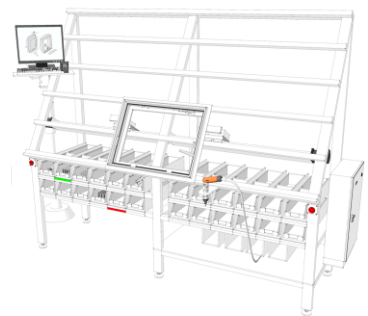
Prototypes		
Table slope	20°	60°
Table dimensions	Length (x) = 2,800 mm Height (y) = 850 mm Width (z) = 1,500 mm	Length (x) = 2,800 mm Height (y) = 850 mm Width (z) = 800 mm
Shelf dimensions	Length (x) = 3,000 mm Height (y) = 1,800 mm Width (z) = 1,000 mm	Length (x) = 2,800 mm Height (y) = 1,000 mm Width (z) = 800 mm

The posture sway-incorporated REBA and RULA assessment methods from the proposed methodology are used to calculate the risk scores in the hardware installation operations associated with the design alternatives. The REBA and RULA risk ratings from the original method and proposed method are compared for each subject, as summarized in Table 6-7. For the REBA assessment, the mean risk ratings are varied from 7.61 to 8.59 for Design A and from 6.79 to 8.26 for Design B in the original method. With the proposed method, the mean risk ratings are varied from 4.95 to 5.94 for Design A and from 4.75 to 5.82 for Design B. Different magnitudes of posture sway are identified among five subjects. Thus, the reductions of risk ratings are varied among five subjects. In terms of the maximum risk ratings, all the subjects obtain a score of 10 for the REBA assessment in the original method except for Subject 1 in Design A and Subject 2 in Design B. In the proposed method, a maximum risk of 9 for the REBA assessment is captured expect for Subject 2 in Design B. Compared to the original method, the minimum risk ratings are also reduced in the proposed method. Similar results can be identified for the RULA assessment. However, the reductions of risk ratings in RULA are less then those in REBA.

Table 6-7. REBA and RULA risks from the original and proposed methods for each subject

			Design A					Design B				
		Subject	S-1	S-2	S-3	S-4	S-5	S-1	S-2	S-3	S-4	S-5
REBA	Original	Mean	7.86	8.52	8.42	7.61	8.59	6.79	8.23	8.21	7.33	8.26
		Max	11	10	10	10	10	10	11	10	10	10
		Min	4	3	4	3	4	4	4	4	3	4
	Proposed	Mean	5.36	5.32	4.95	5.68	5.94	4.90	4.92	4.75	5.02	5.82
		Max	9	9	9	9	9	9	8	9	9	9
		Min	2	1	1	2	2	2	1	3	2	2
RULA	Original	Mean	6.30	6.59	6.40	6.09	6.55	5.94	6.60	6.48	5.88	6.40
		Max	7	7	7	7	7	7	7	7	7	7
		Min	3	3	3	3	3	3	3	3	3	3
	Proposed	Mean	5.23	5.34	4.72	5.15	5.41	4.87	5.12	5.07	4.51	5.03
		Max	7	7	7	7	7	7	7	7	7	7
		Min	2	2	3	2	2	2	2	3	2	2

Table 6-8 summarizes the average REBA and RULA risk scores with the mean, maximum, and minimum risks and risk level for all subjects, for Design A and Design B, respectively. In terms of mean risk ratings, the average REBA risk scores are decreased from 8.20 and 7.76 in the original method to 5.49 and 5.08 in the proposed method for Design A and Design B, respectively. The risk level changes from high risk level to medium risk level for Design A when using the proposed method. However, the risk level remains the same for Design B at a medium risk level. In terms of maximum and minimum risk scores, both Design A and Design B obtain a maximum risk of 10 and a minimum risk of 4 in the original method and that of 9 and 2 in the proposed method, respectively.

Table 6-8. Average REBA and RULA risks from the original and proposed methods for all subjects

		REBA		RULA	
	Factor	Design A	Design B	Design A	Design B
Original method	Mean	8.20	7.76	6.39	6.26
	Max	10	10	7	7
	Min	4	4	3	3
	Risk level	High risk	Medium risk	High risk	High risk
Proposed method	Mean	5.45	5.08	5.17	4.92
	Max	9	9	7	7
	Min	2	2	2	2
	Risk level	Medium risk	Medium risk	Medium risk	Medium risk

Similar to REBA results, the average RULA risk scores are 6.39 and 6.26 resulting in the high risk level in the original method and 5.17 and 4.92 in the medium risk level in the proposed method, for Design A and Design B, respectively. The maximum RULA risk scores among all subjects remain the same. However, the minimum RULA risks drop from 3 to 2 when using the proposed method. The risk comparison indicates that posture sway is being identified in the continuous motions. Using the proposed method, approximately 33.5% and 34.5% reductions in the average REBA risk scores and approximately 19% and 21.4% reductions in the average RULA risk scores are identified for Design A and Design B, respectively. Significant reductions in the risk ratings using the proposed method indicate that posture sway is commonly occurred in the dynamic motions for completing the physical operational tasks. Thus, the proposed method is effective to eliminate the overestimations in ergonomic risk ratings due to the posture sway.

The time frames in percentage of having the adjustment within the tolerance of posture sway are computed for the comparison between the original method and the proposed method. There are approximately 18.5% and 22.7% of time that the subject's neck twisted and side bending within the tolerances, respectively. Similarly, approximately 18.0% and 20.3% of time that the subject's trunk twisted and side bending within the tolerances. The upper arm had approximately 34.9% of time identified as abducted condition within the tolerance. Moreover, there are approximately 89.1% of time the wrist twisted and approximately 24.1% of time the wrist bended to the side. The wrists are naturally more flexible than other body segments such as neck, trunk, and upper arms. Thus, it is difficult for the wrists to keep stable at 0° all the time in the dynamic motions.

The REBA and RULA risk ratings in the original method and the proposed method for Design A and Design B are plotted in Figure 6-7 and Figure 6-8, respectively. For both REBA and RULA assessments, the risk ratings in the original method are higher than those in the proposed method for most of the time frames in the continuous motions for both design alternatives. However, the changes of REBA risk ratings are larger than the changes of RULA risk ratings for the same design. Thus, the effect of posture sway on REBA is greater than that on RULA.

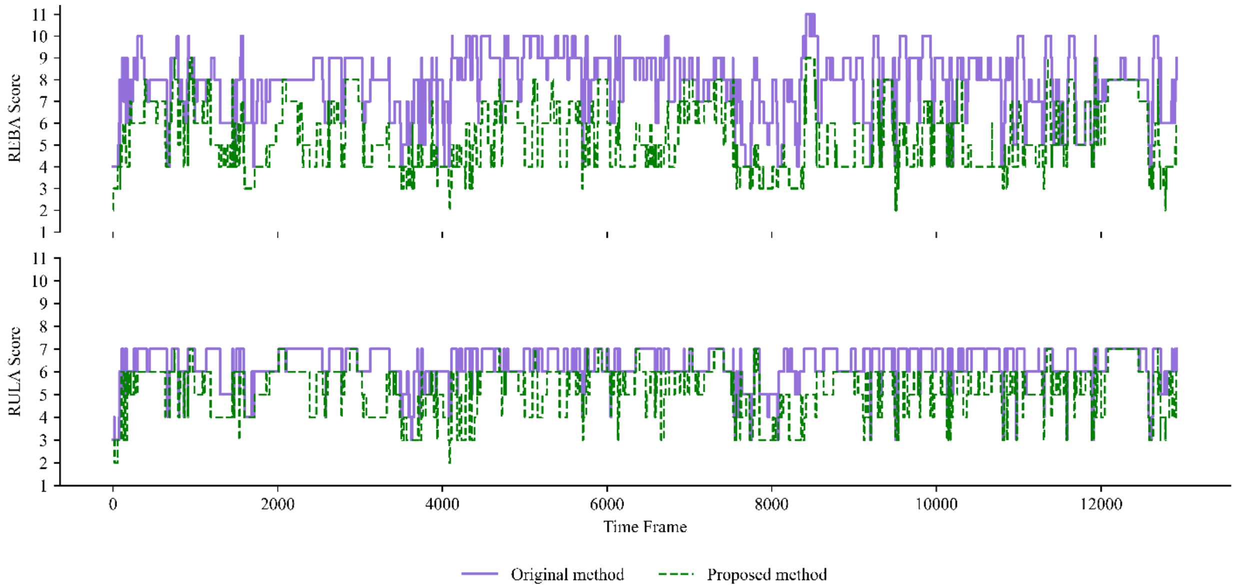

Figure 6-7. REBA and RULA risk ratings for Design A in the original method and proposed method

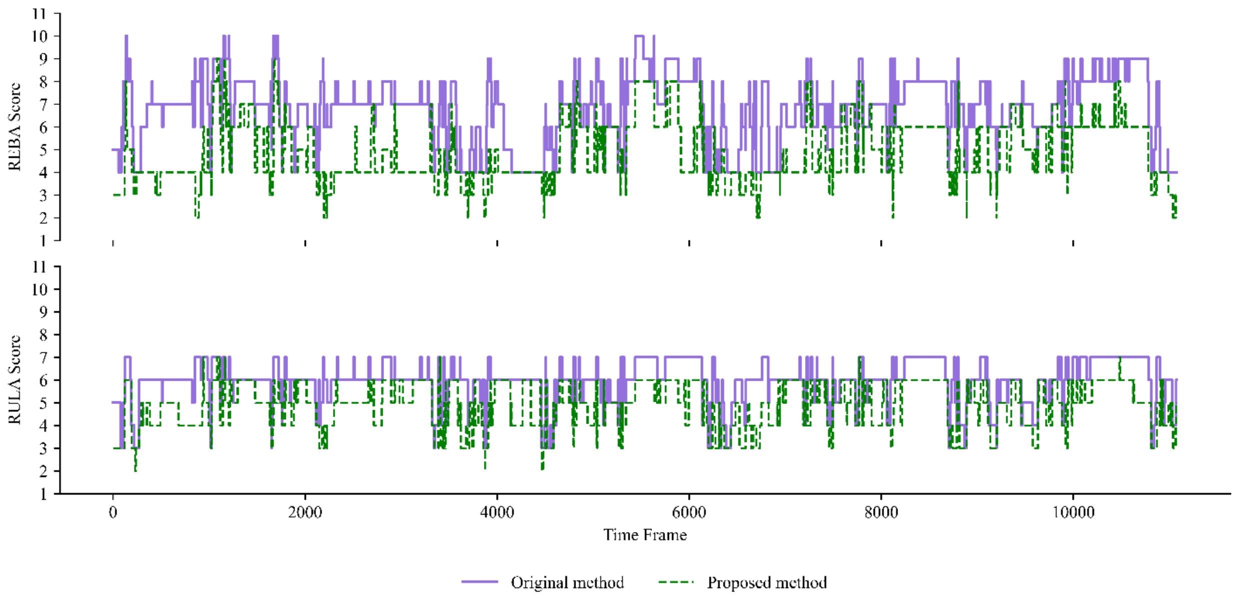

Figure 6-8. REBA and RULA risk ratings for Design B in the original method and proposed method

Accurate ergonomic risk assessments are crucial for the workplace design and modification in industrialized construction. Due to the lack of body joint allowance settings in the current rule-based ergonomic risk assessment methods, ergonomic risk rating results of the continuous motions tend to be overestimated. In this study, the acceptable posture sway magnitudes of 7 evaluation parameters are determined in the experiment. However, the shoulder raise score in the adjustment risk rating process is not involved in this study. The shoulder is a complex system composed of the humerus, clavicle, scapula, glenoid, acromion, and surrounding soft tissue structures. The normal shoulder range of motion include the flexion and extension, the abduction and adduction, and the internal and external rotations of the shoulder. Thus, the shoulder raise defined in REBA and RULA cannot be simply determined by the joint angles of the related bones, which is not examined in the present research.

6.4 Summary

In this chapter, an experimental study of posture sway in continuous motions was conducted in the optical marker-based motion capture system. A total of 23 participants are involved in this posture sway analysis. Three common operational tasks were performed in the experiment. The minor movements of body joints due to the posture sway that naturally occurring are identified. After the experiment, the repeated measures ANOVA was conducted to evaluate the effect of tasks, gender, and BMI conditions on the posture sway during the continuous motions. In this study, the acceptable magnitudes of body joints in the body sway for the qualitatively categorized adjustment factors in REBA and RULA include the side bending and twisted of neck, the side bending and twisted of trunk, the side bending and twisted of wrists, and abducted arms. According to the identified acceptable posture sway magnitudes, the posture sway-incorporated ergonomic risk assessment methods (posture sway-incorporated REBA and RULA) are proposed. A case study of two workplace designs in industrialized construction were used to validate the effectiveness of the proposed method. The issues of overestimations and fluctuations in the ergonomic risk ratings are solved by using the proposed method. In summary, the proposed method is effective to overcome the overestimations and fluctuations in the ergonomic assessment results, which facilitates the consistency and reliability of automated ergonomic risk assessments of continuous motions.

CHAPTER 7: CONCLUSIONS

7.1 Research Conclusions

As a labour-intensive industry, construction is, in terms of its occupational health and safety performance, largely dependent on workers' ergonomic performance. Accurate ergonomic risk assessments of working postures and motions are thus an essential component of workplace design and modification, which, in turn, are beneficial to construction in terms of proactively mitigating the potential risks of WMSDs and improving productivity. However, the current practice of using ergonomic risk assessment for automated evaluation of continuous motions is challenged in three notable respects: (1) inaccuracy of the ergonomic risk assessment as a result of human perception errors and subjectivity during observations—and as a result of measurement errors and instrument limitations when using vision-based approaches—to estimate body joint angles; (2) lack of consideration of standard motion time when analyzing the ergonomic risks of continuous motions in operational tasks; and (3) overestimation of risks in existing methods for ergonomic risk assessment of continuous motions due to a failure to account for the effect of natural posture sway, and due to the ambiguous descriptions of posture categories in the adjustment risk rating in REBA and RULA.

This research proposes an ergonomic-centric framework for automated ergonomic risk assessments of continuous motions in the completion of manual tasks that seeks to fill the aforementioned research gaps to support rapid workplace design and work modification in industrialized construction. The main idea here is to automatically evaluate the ergonomic performance of the workplace design and modifications by using the dynamic and continuous motions for the completion of operational tasks with respect to workplace design. In this research, 3D modelling is used as an example to demonstrate the development and implementation of the proposed framework. In this way, existing ergonomic risk assessment methods can be improved with respect to the three main objectives discussed in Chapters 4–6.

- Chapter 4 proposes a 3D fuzzy logic-based solution to estimate ergonomic risk for rapid workplace design in construction. A specialized fuzzy expert system is developed that can be integrated with existing ergonomic risk assessment methods such as REBA and RULA in the 3D visualization. This ensures more accurate and reliable assessment results of ergonomic risks by addressing the human perception issues that, in current practice, hamper the estimation of body joint angles in continuous motions. A laboratory experiment of a repetitive lifting task conducted using a motion capture system is presented to demonstrate the feasibility and applicability of the proposed framework, demonstrating the improved accuracy and reliability of the proposed framework for ergonomic risk assessment.
- Chapter 5 develops a standard motion time-based method that allows for the ergonomic risk rating results of continuous motions to be adjusted using the standard motion times obtained from the predetermined motion time system. The proposed method implements a standard motion time determination algorithm to automatically identify the motions and realign the ergonomic risks with standard motion times that have been systematically and objectively generated. An industrial case study of a window manufacturing company in Alberta, Canada, is presented to demonstrate the applicability of the proposed 3D standard motion time-based ergonomic risk analysis framework.
- Chapter 6 proposes two novel posture sway-incorporated ergonomic risk assessment systems (posture sway-incorporated REBA and posture sway-incorporated RULA) for the

evaluation of dynamic and continuous motions. An experimental study conducted in an optical marker-based motion capture system to quantitatively analyze human body motions is presented. In the experiment, the minor movements of body joints that naturally occur due to posture sway are identified in three different working conditions: a walking scenario, a moving scenario, and a lifting scenario. A case study of two workstation designs and corresponding prototypes are presented to validate the effectiveness of the proposed posture sway-incorporated ergonomic risk assessment systems.

7.2 Research Contributions

The research outcomes have resulted in several academic contributions:

- A novel 3D fuzzy logic-based method of ergonomic risk assessment has been proposed. The proposed method increases the accuracy and reliability of ergonomic risk rating results compared to the current 3D-based ergonomic risk assessment for rapid workplace design in construction.
- A specialized rule-based fuzzy inference algorithm is integrated with 3D automated posture-based ergonomic risk assessments to better capture the gradual transitions characteristic of continuous human motion without abrupt changes in risk ratings.
- A novel standard motion time-based method for assessment the ergonomic risk of continuous motions is achieved by integrating the predetermined motion time system with ergonomic risk assessment methods. The proposed method is capable of adjusting the motion times in the simulated tasks in order to increase the accuracy of ergonomic risk assessment at the motion level.

- A rule-based motion recognition algorithm is proposed to automatically recognize all the motions in the 3D model. Standard motion time durations of the recognized motions can be automatically generated based on the interpretation of the predetermined motion time system.

- The posture sway-incorporated ergonomic risk assessment systems (posture sway-incorporated REBA and RULA) are developed based on the identified minor movements of body joints in the posture sway experiment. The proposed method overcomes the overestimation and fluctuations of ergonomic risk rating results.

7.3 Future Works

The developed ergonomic-centric methods of automated assessment of continuous motions for workplace design can help construction workers work better and safer. The scope of this study was limited to the investigation of ergonomic risk evaluation in the 3D visualization for workplace design in industrialized construction. The challenges may face when implementing the developed methods to assess whole-body movements in more complex operations in construction since the whole-body motions in the MTM-1 are not fully described. In addition, the implementation with the computer vision and virtual reality technologies are also recommended to test the effectiveness of the developed methods for real-time assessment.

Although the research findings support the proposed frameworks, certain future works should be noted and explored.

- The accuracy and reliability of the developed simulation model in Chapter 4 still largely depend on the quality of the developed 3D human model and the availability of the observational data and recorded images and videos from the construction industry.

- The posture categories of the adjustment risk rating process are determined based on the posture sway experiment of 23 participants with normal BMI in the motion capture laboratory. The experiment of participants with a range of BMI and construction workers in the field with different levels of experience are recommended be conducted to accurately determine the posture categories.
- The posture categories of the adjustment risk rating for shoulder raise are not investigated in this research, which should be examined and determined in other experimental study.
- With the standard motion time durations, an automated productivity analysis can be proposed to provide the labour productivity and overall work efficiency in order to obtain more comprehensive performance assessments as the ergonomic-centric workplace design and modification framework is further developed.
- An optimization study can be performed for automatically analyzing the optimal trade-off between ergonomic risk and labour productivity for manual construction tasks.

REFERENCES

Allin, S. J., Beach, C., Mitz, A., and Mihailidis, A. (2008). Video based analysis of standing balance in a community center. *Proceedings, 30th Annual International Conference of the IEEE Engineering in Medicine and Biology Society*. 4531–4534). IEEE. https://doi.org/10.1109/IEMBS.2008.4650220.

Arfken, G., and Weber, H. J. (2000). *Mathematical Methods for Physicists*, 5th ed., Boston, MA, USA: Academic Press. pp. 14–15, (ISBN-10: 0120598256; ISBN-13: 978-0120598250).

Autodesk Inc. (2021). Create amazing worlds in 3ds Max, https://www.autodesk.com/products/3ds-max/overview?s_tnt=69291:1:0. Accessed May, 2021.

Berg, K., Wood-Dauphine, S., Williams, J. I., and Gayton, D. (1989). Measuring balance in the elderly: Preliminary development of an instrument. *Physiotherapy Canada*, 41(6), 304–311. https://doi.org/10.3138/ptc.41.6.304

Borg, G. (1970). Perceived exertion as an indicator of somatic stress. *Scandinavian Journal of Rehabilitation Medicine*, 2(2), 92–98. https://doi.org/10.2340/1650197719702239298.

Boschman, J. S., van der Molen, H. F., Sluiter, J. K., and Frings-Dresen, M. H. (2012). Musculoskeletal disorders among construction workers: A one-year follow-up study. *BMC Musculoskeletal Disorders*, 13, 196. https://doi.org/10.1186/1471-2474-13-196.

Brilakis, I., Park, M. W., and Jog, G. (2011). Automated vision tracking of project related entities. *Advanced Engineering Informatics*, 25(4), 713–724. https://doi.org/10.1186/1471-2474-13-196.

Build Force Canada (2021). Construction industry key indicators. https://www.buildforce.ca/en/key-indicators. Accessed December, 2021.

Burdorf, A. (2010). The role of assessment of biomechanical exposure at the workplace in the prevention of musculoskeletal disorders. *Scandinavian Journal of Work, Environment and Health*, 36(1), 1–2. https://doi.org/10.5271/sjweh.2882.

Bureau of Labor Statistics (2016). Nonfatal occupational injuries and illnesses requiring days away from work, 2015. U.S. Department of Labor. https://www.bls.gov/news.release/pdf/osh2.pdf. Accessed May, 2021.

Canadian Centre for Occupational Health and Safety (CCOHS) (2022). Work-related Musculoskeletal Disorders (WMSDs), https://www.ccohs.ca/oshanswers/diseases/rmirsi.html. Accessed March, 2022.

Chang, H., and Krebs, D. E. (1999). Dynamic balance control in elders: Gait initiation assessment as a screening tool. *Archives of Physical Medicine and Rehabilitation*, 80(5), 490–494. https://doi.org/10.1016/S0003-9993(99)90187-9.

Chen, J. G., Jung, H. S., and Peacock, B. J. (1994). A fuzzy sets modelling approach for ergonomic workload stress analysis. *International Journal of Industrial Ergonomics*, 13(3), 189–216. https://doi.org/10.1016/0169-8141(94)90068-X.

Chen, J. Y., Qiu, J., and Ahn, C. B. (2017). Construction worker's awkward posture recognition through supervised motion tensor decomposition. *Automation in Construction*, 77, 67–81. https://doi.org/10.1016/j.autcon.2017.01.020.

CPWR (2019). Trends of musculoskeletal disorders and interventions in the construction industry (quarterly data report). https://www.cpwr.com/wp-content/uploads/2020/06/Quarter3-QDR-2019.pdf. Accessed December, 2021.

Dane, D., Feuerstein, M., Huang, G. D., Dimberg, L., Ali, D., and Lincoln, A. (2002). Measurement properties of a self-report index of ergonomic exposures for use in an office work environment. *Journal of Occupational and Environmental Medicine*, 44(1), 73–81.

David, G. C. (2005). Ergonomic methods for assessing exposure to risk factors for work-related musculoskeletal disorders. *Occupational Medicine*, 55(3), 190–199. https://doi.org/10.1093/occmed/kqi082.

de Ru, W.G. and Eloff, J.H.P. (1996). Risk analysis modelling with the use of fuzzy logic. *Computers and Security*, 15(3), 239–248. https://doi.org/10.1016/0167-4048(96)00008-9.

Dias Barkokebas, R., Al-Hussein, M., and Li, X. (2021). Virtual reality–motion capture-based ergonomic risk assessment of workstation designs of construction manufacturing facilities. *Proceedings, CSCE Construction Specialty Conference*, Niagara Falls, ON, Canada (virtual conference), May 26–29.

Eichelberger, P., Ferraro, M., Minder, U., Denton, T., Blasimann, A., Krause, F., and Baur, H. (2016). Analysis of accuracy in optical motion capture – A protocol for laboratory setup evaluation. *Journal of Biomechanics*, 49(10), 2085–2088. https://doi.org/10.1016/j.jbiomech.2016.05.007.

Ergonomics Plus (2021a). REBA employee assessment worksheet. https://ergo-plus.com/wp-content/uploads/REBA.pdf. Accessed December, 2021.

Ergonomics Plus (2021b). RULA employee assessment worksheet. https://ergo-plus.com/wp-content/uploads/RULA.pdf. Accessed December, 2021.

Escorcia, V., Davila, M. A., Golparvar-Fard, M., and Niebles, J. C. (2012). Automated vision-based recognition of construction worker actions for building interior 124 construction operations using RGBD cameras. *Proceedings, Construction Research Congress, ASCE*, West Lafayette, IN, USA. May 21–23. http://ascelibrary.org/doi/10.1061/9780784412329.089.

Freivalds, A., and Niebel, B. (2013). *Niebel's Methods, Standards, and Work Design*. McGraw Hill, New York, NY, USA, (ISBN-10: 0073376361; ISBN-13: 978-0073376363).

Fung, I. W. H., Tam, V. W. Y., Tam, C. M., and Wang, K. (2008). Frequency and continuity of work-related musculoskeletal symptoms for construction workers. *Journal of Civil Engineering and Management*, 14(3), 183–187. https://doi.org/10.3846/1392-3730.2008.14.15

Genaidy, A. M., Mital, A., and Obeidat, M. (1989). The validity of predetermined motion time systems in setting production standards for industrial tasks. *International Journal of Industrial Ergonomics*, 3(3), 249–263. https://doi.org/10.1016/0169-8141(89)90025-5.

Goffredo, M., Schmid, M., Conforto, S., and D'Alessio, T. (2006). A markerless sub-pixel motion estimation technique to reconstruct kinematics and estimate the centre of mass in posturography. *Medical Engineering and Physics*, 28(7), 719–726. https://doi.org/10.1016/j.medengphy.2005.10.007.

Golabchi, A., Guo, X., Liu, M., Han, S., and Lee, S. (2018). An integrated ergonomics framework for evaluation and design of construction operations. *Automation in Construction*, 95, 72–85. https://doi.org/10.1016/j.autcon.2018.08.003.

Golabchi, A., Han, S., AbouRizk, S., and Kanerva, J. (2016a). Micro-motion level simulation for efficiency analysis and duration estimation of manual operations. *Automation in Construction*, 71, 443–452. https://doi.org/10.1016/j.autcon.2016.08.028.

Golabchi, A., Han, S., and Fayek, A. R. (2016b). A fuzzy logic approach to posture-based ergonomic analysis for field observation and assessment of construction manual operations. *Canadian Journal of Civil Engineering*, 43(4), 294–303. https://doi.org/10.1139/cjce-2015-0143.

Golabchi, A., Han, S., Fayek, A. R., and AbouRizk, S. (2017). Stochastic modeling for assessment of human perception and motion sensing errors in ergonomic analysis. *Journal of Computing in Civil Engineering*, 31(4), 04017010. https://doi.org/10.1061/(ASCE)CP.1943-5487.0000655.

Golabchi, A., Han, S., Seo, J., Han, S., Lee, S., and Al-Hussein, M. (2015). An automated biomechanical simulation approach to ergonomic job analysis for workplace design. *Journal of Construction Engineering and Management*, 141(8), 04015020. https://doi.org/10.1061/(ASCE)CO.1943-7862.0000998.

Groover, M. P. (2013). *Work Systems: The Methods, Measurement and Management of Work*. Pearson Higher Education, (ISBN-10: 1292027053; ISBN-13: 9781292027050).

Han, S., Lee, S., and Peña-Mora, F. (2013). Vision-based detection of unsafe actions of a construction worker: Case study of ladder climbing. *Journal of Computing in Civil Engineering*, 27(6), 635–644. https://doi.org/10.1061/(ASCE)CP.1943-5487.0000279.

Hebert, J.S., and Lewicke, J. (2012). Case report of modified box and blocks test with motion capture to measure prosthetic function. *Journal of Rehabilitation Research and Development*, 49(8), 1163–1174. http://doi.org/10.1682/JRRD.2011.10.0207.

Hebert, J.S., Lewicke, J., Williams, T. R., and Vette, A. H. (2014). Normative data for modified box and blocks test measuring upper-limb function via motion capture. *Journal of Rehabilitation Research and Development*, 51(6), 919–932. http://doi.org/10.1682/JRRD.2013.10.0228.

Heyde, G.C. (1983). *Modapts Plus*. Heyde Dynamics, Sydney, Australia, (ISBN-10: 0959659730; ISBN-13: 9780959659733).

Hignett, S., and McAtamney, L. (2000). Rapid entire body assessment (REBA). *Applied Ergonomics*, 31(2), 201–205. https://doi.org/10.1016/S0003-6870(99)00039-3.

Hinkle, D. E., Wiersma, W., and Jurs, S. G. (2003). *Applied Statistics for the Behavioral Sciences*, 5th edition. Boston, MA, USA: Houghton Mifflin, (ISBN 9780618124053).

Inyang, N., Al-Hussein, M., El-Rich, M., and Al-Jibouri, S. (2012). Ergonomic analysis and the need for its integration for planning and assessing construction tasks. *Journal of Construction Engineering and Management*, 138(12), 1370–1376. https://doi.org/10.1061/(ASCE)CO.1943-7862.0000556.

Janowitz, I. L., Gillen, M., Ryan, G., Rempel, D., Trupin, L., Swig, L., Mullen, K., Rugulies, R., and Blanc, P. D. (2006). Measuring the physical demands of work in hospital settings: Design and implementation of an ergonomics assessment. *Applied Ergonomics*, 37(5), 641–658. https://doi.org/10.1016/j.apergo.2005.08.004.

Kamali, M., and Hewage, K. (2016). Life cycle performance of modular buildings: A critical review. *Renewable and Sustainable Energy Reviews*, 62, 1171–1183. https://doi.org/10.1016/j.rser.2016.05.031

Karhu, O., Härkönen, R., Sorvali, P., and Vepsäläinen, P. (1981). Observing working postures in industry: Examples of OWAS application. *Applied Ergonomics*, 12(1), 13–17. https://doi.org/10.1016/0003-6870(81)90088-0.

Karhu, O., Kansi, P., and Kuorinka, I. (1977). Correcting working postures in industry: A practical method for analysis. *Applied Ergonomics*, 8(4), 199–201. https://doi.org/10.1016/0003-6870(77)90164-8.

Karwowski, W., Gaweda, A., Marras, W. S., Davis, K., Zurada, J. M., and Rodrick, D. (2006). A fuzzy relational rule network modeling of electromyographical activity of trunk muscles in manual lifting based on trunk angles, moments, pelvic tilt and rotation angles. *International Journal of Industrial Ergonomics*, 36(10), 847–859. https://doi.org/10.1016/j.ergon.2006.06.006.

Karwowski, W., Mulholland, N. O., Ward, T. L., and Jagannathan, V. (1987). A fuzzy knowledge base of an expert system for analysis of manual lifting tasks. *Fuzzy Sets and Systems*, 21(3), 363–374. https://doi.org/10.1016/0165-0114(87)90136-9.

Kim, S., and Nussbaum, M. A. (2013). Performance evaluation of a wearable inertial motion capture system for capturing physical exposures during manual material handling tasks. *Ergonomics*, 56(2), 314–326. https://doi.org/10.1080/00140139.2012.742932.

Kivi, P., and Mattila, M. (1991). Analysis and improvement of work postures in the building industry: Application of the computerised OWAS method. *Applied Ergonomics*, 22(1), 43–48. https://doi.org/10.1016/0003-6870(91)90009-7.

Klir, G. J., and Yuan, B. (1995). *Fuzzy Sets and Fuzzy Logic: Theory and Applications*. Prentice Hall, Upper Saddle River, NJ, USA, (ISBN 0-13-101171-5).

Kuorinka, I., Jonsson, B., Kilbom, A., Vinterberg, H., Biering-Sørensen, F., Andersson, G., and Jørgensen, K. (1987). Standardised Nordic questionnaires for the analysis of musculoskeletal symptoms. *Applied Ergonomics*, 18(3), 233–237. https://doi.org/10.1016/0003-6870(87)90010-X.

Labour and Immigration (2019). Workplace injury, disease and fatality statistics, provincial summary 2018, Labour and Immigration, Government of Alberta. https://open.alberta.ca/dataset/c1c1b935-a5d5-456a-b86c-c9986fa5542d/resource/70c3df37-5a76-4f98-804a-0aef1cd39f1a/download/lbr-workplace-injury-disease-fatality-statistics-provincial-summary-2018.pdf. Accessed May, 2021.

Li, G., and Buckle, P. (1998). A practical method for the assessment of work-related musculoskeletal risks – quick exposure check (QEC). *Proceedings, The Human Factors and Ergonomics Society, 42nd Annual Meeting*, Chicago, IL, USA, Oct. 5–9. https://doi.org/10.1177/154193129804201905.

Li, G., and Buckle, P. (1999). Current techniques for assessing physical exposure to work-related musculoskeletal risks, with emphasis on posture-based methods. *Ergonomics*, 42(5), 674–695. https://doi.org/10.1080/001401399185388.

Li, K.W., and Yu, R. (2011). Assessment of grip force and subjective hand force exertion under handedness and postural conditions. *Applied Ergonomics*, 42(6), 929–933. https://doi.org/10.1016/j.apergo.2011.03.001.

Li, X., Gül, M., and Al-Hussein, M. (2019a). An improved physical demand analysis framework based on ergonomic risk assessment tools for the manufacturing industry. *International Journal of Industrial Ergonomics*, 70, 58–69. https://doi.org/10.1016/j.ergon.2019.01.004.

Li, X., Han, S., Gül, M., Al-Hussein, M., and El-Rich, M. (2018). 3D visualization-based ergonomic risk assessment and work modification framework and its validation for a lifting task, *Journal of Construction Engineering and Management*, 144(1), 04017093. https://doi.org/10.1061/(ASCE)CO.1943-7862.0001412.

Li, X., Han, S., Gül, M., and Al-Hussein, M. (2019b). Automated post-3D visualization ergonomic analysis system for rapid workplace design in modular construction. *Automation in Construction*, 98, 160–174. https://doi.org/10.1016/j.autcon.2018.11.012.

Li, X., Komeili, A., Gül, M., and El-Rich, M. (2017). A framework for evaluating muscle activity during repetitive manual material handling in construction manufacturing. *Automation in Construction*, 79, 39–48. https://doi.org/10.1016/j.autcon.2017.01.005.

Lord, S. R., Clark, R. D., and Webster, I. W. (1991). Postural stability and associated physiological factors in a population of aged persons. *Journal of Gerontology*, 46(3), M69–M76. https://doi.org/10.1093/geronj/46.3.M69.

Mattila, M., Karwowski, W., and Vilkki, M. (1993). Analysis of working postures in hammering tasks on building construction sites using the computerized OWAS method. *Applied Ergonomics*, 24(6), 405–412. https://doi.org/10.1016/0003-6870(93)90172-6.

Maynard, H. B., Stegmerten, G. J., and Schwab, J. L. (1948). *Methods-Time Measurement*. McGraw Hill, New York, NY, USA, (ISBN-10: 111420286X; ISBN-13: 9781114202863).

McAtamney, L., and Corlett, E. N. (1993). RULA: A survey method for the investigation of work-related upper limb disorders. *Applied Ergonomics*, 24(2), 91–99. https://doi.org/10.1016/0003-6870(93)90080-S.

McCauley-Bell, P., and Badiru, A. B. (1996). Fuzzy modeling and analytic hierarchy processing–means to quantify risk levels associated with occupational injuries–part II: The development of a fuzzy rule-based model for the prediction of injury. *IEEE Transactions on Fuzzy Systems*, 4(2), 132–138. https://doi.org/10.1109/91.493907.

Meredith, M., and S. Maddock, S. (2001). Motion capture file formats explained. Department of Computer Science, University of Sheffield, http://www.dcs.shef.ac.uk/intranet/research/public/resmes/CS0111.pdf. Accessed January, 2020.

Merlino, L. A., Rosecrance, J. C., Anton, D., and Cook, T. M. (2003). Symptoms of musculoskeletal disorders among apprentice construction workers. *Applied Occupational and Environmental Hygiene*, 18(1), 57–64. https://doi.org/10.1080/10473220301391.

Moynihan, G. P., Fonseca, D. J., Merritt, T. W., and Ray, P. S. (1995). An object-oriented system for ergonomic risk assessment. *Expert Systems*, 12(2), 149–156. https://doi.org/10.1111/j.1468-0394.1995.tb00047.x.

Nayak, U. S. L. (1987). Comparison of the Wright ataxiameter and the Kistler force platform in the measurement of sway. *Journal of Biomedical Engineering*, 9(4), 302–304. https://doi.org/10.1016/0141-5425(87)90077-X.

NIOSH. (2014). Observation-based posture assessment: Review of current practice and recommendations for improvement. By Lowe, B. D., Weir, P. L., and Andrews, D.M., Cincinnati, OH, USA: U.S. Department of Health and Human Services, Centers for Disease Control and Prevention, National Institute for Occupational Safety and Health, *DHHS (NIOSH)* publication No. 2014–13.

Nunes, I. L. (2006). ERGO_X – The model of a fuzzy expert system for workstation ergonomic analysis, in: W. Karwowski (Ed.). *International Encyclopedia of Ergonomics and Human Factors - 3 Volume Set*, CRC Press, pp. 3114–3121, (ISBN 041530430X).

Nunes, I. L. (2009). FAST ERGO_X – A tool for ergonomic auditing and work-related musculoskeletal disorders prevention. *Work*, 34(2), 133–148. https://doi.org/10.3233/WOR-2009-0912.

Occhipiniti, E. (1998). OCRA: A concise index for the assessment of exposure to repetitive movements of the upper limbs. *Ergonomics*, 41, 1290–1311. https://doi.org/10.1080/001401398186315.

Occupational Safety and Health Administration (2022). Ergonomics, https://www.osha.gov/ergonomics. Accessed March, 2022.

Pavlovic-Veselinovic, S., Hedge, A., and Veselinovic, M. (2016). An ergonomic expert system for risk assessment of work-related musculo-skeletal disorders. *International Journal of Industrial Ergonomics*, 53, 130–139. https://doi.org/10.1016/j.ergon.2015.11.008.

Poveda, C. A., and Fayek, A. R. (2009). Predicting and evaluating construction trades foremen performance: Fuzzy logic approach. *Journal of Construction Engineering and Management*, 135(9), 920–929. https://doi.org/10.1061/(ASCE)CO.1943-7862.0000061.

Punnett, L., and Wegman, D. H. (2004). Work-related musculoskeletal disorders: The epidemiologic evidence and the debate. *Journal of Electromyography and Kinesiology*, 14(1), 13–23. https://doi.org/10.1016/j.jelekin.2003.09.015

Razmi, J., and Shakhs-Niyaee, M. (2008). Developing a specific predetermined time study approach: An empirical study in a car industry. *Production Planning and Control*, 19(5), 454–460. https://doi.org/10.1080/09537280802052028.

Rey, M. I., Galende, M., Fuente, M. J., and Sainz-Palmero, G.I. (2017). Multi-objective based Fuzzy Rule Based Systems (FRBSs) for trade-off improvement in accuracy and interpretability: A rule relevance point of view. *Knowledge-Based Systems*, 127, 67–84. https://doi.org/10.1016/j.knosys.2016.12.028.

Rinder, M. M., Genaidy, A., Salem, S., Shell, R., and Karwowski, W. (2008). Interventions in the construction industry: A systematic review and critical appraisal. *Human Factors and Ergonomics in Manufacturing*, 18(2), 212–229. https://doi.org/10.1002/hfm.20109.

Rodgers, J. L., and Nicewander, W. A. (1988). Thirteen ways to look at the correlation coefficient. *The American Statistician*, 42(1), 59–66. https://doi.org/10.1080/00031305.1988.10475524.

Runkler, T. A. (1996). Extended defuzzification methods and their properties. *Proceedings, IEEE 5th International Fuzzy Systems*, New Orleans, LA, USA, 694–700. https://doi.org/10.1109/FUZZY.1996.551822.

Ryu, J., Diraneyya, M. M., Haas, C. T., and Abdel-Rahman, E. (2021). Analysis of the limits of automated rule-based ergonomic assessment in bricklaying. *Journal of Construction Engineering and Management*, 147(2), 04020163. https://doi.org/10.1061/(ASCE)CO.1943-7862.0001978.

Schneider, S. P. (2001). Musculoskeletal injuries in construction: A review of the literature. *Applied Occupational and Environmental Hygiene*, 16(11), 1056–1064. https://doi.org/10.1080/104732201753214161.

Schofield, J. S., Parent, E., Lewicke, J., Carey, J. P., El-Rich, M., and Adeeb, S. (2014). Leg dominance may not be a predictor of asymmetry in peak joint moments and ground reaction forces during sit-to-stand movements. *Journal of Applied Biomechanics*, 30(1), 179–183. http://doi.org/10.1123/jab.2013-0108.

Seo, J., Han, S., Lee, S., and Kim, H. (2015). Computer vision techniques for construction safety and health monitoring. *Advanced Engineering Informatics*, 29(2), 239–251. https://doi.org/10.1016/j.aei.2015.02.001.

Spirduso, W. W. (1995). *Physical Dimensions of Aging*. Human Kinetics. Champaign, IL, USA, (ISBN-10: 0873223233; ISBN-13: 9780873223232).

Statistics Canada (2021). Table 36-10-0434-03 Gross domestic product (GDP) at basic prices, by industry, annual average (x1,000,000). https://www150.statcan.gc.ca/t1/tbl1/en/tv.action?pid=3610043403. Accessed December, 2021.

Taneja, S., Akinci, B., Garrett, J. H., Soibelman, L., Ergen, E., Pradhan, A., and Anil, E. B. (2011). Sensing and field data capture for construction and facility operations. *Journal of Construction Engineering and Management*, 137(10), 870–881. https://doi.org/10.1061/(Asce)Co.1943-7862.0000332.

Thomas, H.R., Maloney, W.F., Horner, R.M.W., Smith, G.R., Handa, V.K., and Sanders, S.R. (1990). Modeling construction labor productivity. *Journal of Construction Engineering and Management*, 116(4), 705–726. https://doi.org/10.1061/(ASCE)0733–9364(1990)116:4(705).

Tuan, S.T., Karim, A.N.M., Kays, H.M.E., Amin, A.K.M.N., and Hasan, M.H. (2014). Improvement of workflow and productivity through application of Maynard Operation Sequence Technique (MOST). *Proceedings, 2014 International Conference on Industrial Engineering and Operations Management*, Bali, Indonesia, 2162–2171.

Umer, W., Antwi-Afari, M.F., Li, H., Szeto, G.P., and Wong, A.Y. (2018). The prevalence of musculoskeletal disorders in the construction industry: A systematic review and meta-analysis. *International Archives of Occupational and Environmental Health*, 91, 125–144. https://doi.org/10.1007/s00420-017-1273-4.

University of Michigan (2017). Center for Ergonomics, 3D Static Strength Prediction Program, https://c4e.engin.umich.edu/assets/3DSSPP-Version-7.0.0-Manual.pdf. Accessed January, 2020.

Valero, E., Sivanathan, A., Bosche, F., and Abdel-Wahab, M. (2016). Musculoskeletal disorders in construction: A review and a novel system for activity tracking with body area network. *Applied Ergonomics*, 54, 120–130. https://doi.org/10.1016/j.apergo.2015.11.020.

Vena, A., Budney, D., Forest, T., and Carey, J. P. (2011a). Three-dimensional kinematic analysis of the golf swing using instantaneous screw axis theory, part 1: Methodology and verification. *Sports Engineering*, 13(3), 105–123. http://doi.org/10.1007/s12283-010-0058-8.

Vena, A., Budney, D., Forest, T., and Carey, J. P. (2011b). Three-dimensional kinematic analysis of the golf swing using instantaneous screw axis theory, part 2: Golf swing kinematic sequence. *Sports Engineering*, 13(3), 125–133. http://doi.org/10.1007/s12283-010-0059-7.

Vicon. (2021). Plug-in Gait reference guide. https://docs.vicon.com/display/Nexus212/Plug-in+Gait+Reference+Guide. Accessed May, 2021.

Vignais, N., Bernard, F., Touvenot, G., and Sagot, J. C. (2017). Physical risk factors identification based on body sensor network combined to videotaping. *Applied Ergonomics*, 65, 410–417. https://doi.org/10.1016/j.apergo.2017.05.003.

Vignais, N., Miezal, M., Bleser, G., Mura, K., Gorecky, D., and Marin, F. (2013). Innovative system for real-time ergonomic feedback in industrial manufacturing. *Applied Ergonomics*, 44(4), 566–574. https://doi.org/10.1016/j.apergo.2012.11.008.

Wang, D., Dai, F., and Ning, X. (2015). Risk assessment of work-related musculoskeletal disorders in construction: State-of-the-art review. *Journal of Construction Engineering and Management*, 141(6), 04015008. https://doi.org/10.1061/(ASCE)CO.1943-7862.0000979.

Wang, F., Skubic, M., Abbott, C., and Keller, J. M. (2010). Body sway measurement for fall risk assessment using inexpensive webcams. *Proceedings, 2010 Annual International Conference of the IEEE Engineering in Medicine and Biology*, 2225–2229, IEEE. https://doi.org/10.1109/IEMBS.2010.5626100.

Wang, J., Han, S., and Li, X. (2021a). 3D fuzzy ergonomic analysis for rapid workplace design and modification in construction. *Automation in Construction*, 123, 103521. https://doi.org/10.1016/j.autcon.2020.103521.

Wang, J., Li, X., Han, S. and Al-Hussein, M. (2020). Construction workers' behaviors assessment using 3d visualization and fuzzy logic method. *Proceedings, International Conference on Construction and Real Estate Management (ICCREM) 2020: Intelligent Construction and Sustainable Buildings*, Stockholm, Sweden, ASCE, 47–54.

Wang, J., Mohamed, Y., Han, S., Li, X., and Al-Hussein, M. (2021b). Automated ergonomics-based productivity analysis for intelligent manufacturing in industrialized construction. *Proceedings, CSCE Construction Specialty Conference*, Niagara Falls, ON, Canada (virtual conference), May 26–29.

Waters, T. R., Putz-Anderson, V., Garg, A., and Fine, L. J. (1993). Revised NIOSH equation for the design and evaluation of manual lifting tasks. *Ergonomics*, 36, 749–776. https://doi.org/10.1080/00140139308967940.

Wing, A. M., Clapp, S., and Burgess-Limerick, R. (1995). Standing stability in the frontal plane determined by lateral forces applied to the hip. *Gait and Posture*, 3(1), 38–42. https://doi.org/10.1016/0966-6362(95)90807-5.

Xsens (2021). Xsens MVN user manual. https://www.xsens.com/hubfs/Downloads/usermanual/MVN_User_Manual.pdf. Accessed November, 2021.

Yeung, S. S., Genaidy, A. M., Huston, R., and Karwowski, W. (2002). An expert cognitive approach to evaluate physical effort and injury risk in manual lifting – A brief report of a pilot study. *Human Factors and Ergonomics in Manufacturing*, 12(2), 227–234. https://doi.org/10.1002/hfm.10010.

Yin, X., Liu, H., Chen, Y., and Al-Hussein, M. (2019). Building information modelling for off-site construction: Review and future directions. *Automation in Construction*, 101, 72–91. https://doi.org/10.1016/j.autcon.2019.01.010.

Yu, Y., Yang, X., Li, H., Luo, X., Guo, H., and Fang, Q. (2019). Joint-level vision-based ergonomic assessment tool for construction workers. *Journal of Construction Engineering and Management*, 145(5), 04019025. https://doi.org/10.1061/(ASCE)CO.1943-7862.0001647.

Zadeh, L. A. (1965). Fuzzy sets. *Information and Control*, 8(3), 338–353. https://doi.org/10.1016/S0019-9958(65)90241-X.

Zadeh, L. A. (1975a). The concept of a linguistic variable and its application to approximate reasoning–I. *Information Sciences*, 8(3), 199–249. https://doi.org/10.1016/0020-0255(75)90036-5.

Zadeh, L. A. (1975b). The concept of a linguistic variable and its application to approximate reasoning–II. *Information Sciences*, 8(4), 301–357. https://doi.org/10.1016/0020-0255(75)90046-8.

Zadeh, L. A. (1975c). The concept of a linguistic variable and its application to approximate reasoning–III. *Information Sciences*, 9(1), 43–80. https://doi.org/10.1016/0020-0255(75)90017-1.

Zandin, K.B. (1980). *MOST Work Measurement Systems*. Marcel Dekker, New York, NY, USA, (ISBN-10: 082476899X; ISBN-13: 9780824768997).

APPENDIX A

Information Letter and Consent Form

Study Title: Ergonomics and workplace design for industrialized construction

Research Investigator:
Jingwen Wang
PhD student
jingwen.wang@ualberta.ca

Supervisor:
Xinming Li
Assistant Professor
Department of Mechanical Engineering
University of Alberta
10-365 Donadeo Innovation Centre for Engineering, 9211 116 street NW
Edmonton, AB, Canada T6G 1H9

Background

The construction manufacturing industry in North America has a disproportionately high number of lost-time injuries due to the higher physical demand of labour-intensive tasks. It is thus essential to investigate the physical demands of body movement in order to proactively identify ergonomic risk in the workplace.

Purpose

The purpose of this research is to assist the industrialized construction industry in reducing ergonomic risks of manufacturing operations. The risk assessment will enable the health and safety department to better assess job requirements, ensure that the workload is within workers' capacity, identify and evaluate the ergonomic risks posed by various tasks after completing ergonomic analysis, and eventually provide recommendations to improve work processes by mitigating the risks associated with tasks in the manufacturing plant. In the long term, this project could reduce work-related fatigue and potential injury.

Study Procedures

The study procedures of this project are listed as follows (only steps 2 require your involvement):

1. Carry out observations (data collection and time study) of production line tasks and design for the task imitation experiment.
2. Imitate the motions that was performed by the workers in the lab, capture the motion by using the wearable motion capture suit.
3. Analyze the body posture through the collected data and identify the awkward body postures and propose corrective measures.

The types of data to be collected are described in greater detail below:

- **Motion capture**: the motion for the entire body will be collected through the wearable motion capture devices. You have to wear the straps and/or suit on the top of your regular but tight clothes.
- **Video recording**: video recordings will be collected from a distance and from different directions. Although the video images will include recognizable human subjects, in any publications arising from this research, faces of human subjects appearing in photographs will be obscured.

Benefits

- The student volunteer may benefit from the research experience on using motion capture system and they can have access to know how graduate students conduct research projects.

- If by any chance the research is approved to be failure, there may be no direct benefits to the participants.

Risk

- There are no foreseeable risks to you during the study procedure.
- The student may perform physical postures that is similar to the occupational task from a worker in the industry facility, however without the similar load that you have the handle. Thus, no physical stress or injury will be placed.
- If any unforeseen risk emerges that may affect your willingness to continue participation in the study, you will be informed immediately.

Voluntary Participation

- You are under no obligation to participate in this study. The participation is completely voluntary.
- You retain the right not to answer specific questions, even if participating in the study.
- You have the right to end your participation in the study at any time. You can withdraw at any time before the final publication of the research by informing the PI in a written format (e.g., email, letter, etc.).

Confidentiality & Anonymity

- Any information collected will be kept confidential, with hard copies to be stored in a secure location and any digital data (e.g., digital photos/video) to be stored on a password-protected server. These documents will not be used for other purposes and will be permanently deleted after five years.

- Findings arising from this study will be disseminated in the Research Investigator's dissertation, as well as in research articles, such as conference papers and journal papers, which will be made publicly available. No study participants will be personally identified in any of the aforementioned publications.

Further Information

If you have any further questions regarding this study, please do not hesitate to contact the Research Investigator or his/her supervisor, Xinming (Sherry) Li (xinming.li@ualberta.ca). The plan for this study has been reviewed by the University of Alberta's Research Ethics Board to ensure its adherence to ethical guidelines. For questions regarding participant rights and ethical conduct of research, contact the Research Ethics Office at (780) 492-0459.

Consent Statement

I have read this form and the research study has been explained to me. I have been given the opportunity to ask questions and my questions have been answered. If I have additional questions, I have been told whom to contact. I agree to participate in the research study as indicated below and will receive a copy of this consent form upon signing:

[Check all that apply]

- ☐ I consent to participate in the motion capture experiment in the lab on campus.
- ☐ I consent for my image (including face) to appear in video data collected as part of this research project.

____ _______________

Participant’s Name (printed) and Signature Date

____ _______________

Name (printed) and Signature of Person Obtaining Consent Date

APPENDIX B

Example Output of ANOVA

Within-Subjects Factors

Measure: MEASURE_1

Tasks	Dependent Variable
1	NeckLTask1
2	NeckLTask2
3	NeckLTask3

Descriptive Statistics

	Mean	Std. Deviation	N
Neck Lateral Walking	2.4161	1.42826	23
Neck Lateral Moving	2.3030	1.85769	23
Neck Lateral Lifting	2.5896	1.34371	23

Multivariate Tests[a]

Effect		Value	F	Hypothesis df	Error df	Sig.	Partial Eta Squared
Tasks	Pillai's Trace	.059	.662[b]	2.000	21.000	.526	.059
	Wilks' Lambda	.941	.662[b]	2.000	21.000	.526	.059
	Hotelling's Trace	.063	.662[b]	2.000	21.000	.526	.059
	Roy's Largest Root	.063	.662[b]	2.000	21.000	.526	.059

a. Design: Intercept

Within Subjects Design: Tasks

b. Exact statistic

Mauchly's Test of Sphericity[a]

Measure: MEASURE_1

Within Subjects Effect	Mauchly's W	Approx. Chi-Square	df	Sig.	Epsilon[b] Greenhouse-Geisser	Huynh-Feldt	Lower-bound
Tasks	.998	.035	2	.982	.998	1.000	.500

Tests the null hypothesis that the error covariance matrix of the orthonormalized transformed dependent variables is proportional to an identity matrix.[a]

a. Design: Intercept

Within Subjects Design: Tasks

b. May be used to adjust the degrees of freedom for the averaged tests of significance. Corrected tests are displayed in the Tests of Within-Subjects Effects table.

Tests of Within-Subjects Effects

Measure: MEASURE_1

Source		Type III Sum of Squares	df	Mean Square	F	Sig.	Partial Eta Squared
Tasks	Sphericity Assumed	.958	2	.479	.695	.505	.031
	Greenhouse-Geisser	.958	1.997	.480	.695	.504	.031
	Huynh-Feldt	.958	2.000	.479	.695	.505	.031
	Lower-bound	.958	1.000	.958	.695	.414	.031
Error (Tasks)	Sphericity Assumed	30.347	44	.690			
	Greenhouse-Geisser	30.347	43.926	.691			

	Huynh-Feldt	30.347	44.000	.690			
	Lower-bound	30.347	22.000	1.379			

Tests of Within-Subjects Contrasts

Measure: MEASURE_1

Source	Tasks	Type III Sum of Squares	df	Mean Square	F	Sig.	Partial Eta Squared
Tasks	Linear	.346	1	.346	.483	.494	.021
	Quadratic	.612	1	.612	.923	.347	.040
Error (Tasks)	Linear	15.752	22	.716			
	Quadratic	14.594	22	.663			

Tests of Between-Subjects Effects

Measure: MEASURE_1

Transformed Variable: Average

Source	Type III Sum of Squares	df	Mean Square	F	Sig.	Partial Eta Squared
Intercept	409.531	1	409.531	69.211	<.001	.759
Error	130.176	22	5.917			

Estimated Marginal Means

1. Grand Mean

Measure: MEASURE_1

		95% Confidence Interval	
Mean	Std. Error	Lower Bound	Upper Bound
2.436	.293	1.829	3.044

2. Tasks

Estimates

Measure: MEASURE_1

			95% Confidence Interval	
Tasks	Mean	Std. Error	Lower Bound	Upper Bound
1	2.416	.298	1.798	3.034
2	2.303	.387	1.500	3.106
3	2.590	.280	2.009	3.171

Pairwise Comparisons

Measure: MEASURE_1

					95% Confidence Interval for Difference[a]	
(I) Tasks	(J) Tasks	Mean Difference (I-J)	Std. Error	Sig.[a]	Lower Bound	Upper Bound
1	2	.113	.241	1.000	–.511	.737
	3	–.173	.250	1.000	–.820	.473
2	1	–.113	.241	1.000	–.737	.511
	3	–.287	.244	.759	–.919	.346
3	1	.173	.250	1.000	–.473	.820
	2	.287	.244	.759	–.346	.919

Based on estimated marginal means
a. Adjustment for multiple comparisons: Bonferroni.

Multivariate Tests

	Value	F	Hypothesis df	Error df	Sig.	Partial Eta Squared
Pillai's trace	.059	.662[a]	2.000	21.000	.526	.059
Wilks' lambda	.941	.662[a]	2.000	21.000	.526	.059
Hotelling's trace	.063	.662[a]	2.000	21.000	.526	.059
Roy's largest root	.063	.662[a]	2.000	21.000	.526	.059

Each F tests the multivariate effect of Tasks. These tests are based on the linearly independent pairwise comparisons among the estimated marginal means.
a. Exact statistic

Profile Plots